Targeting and Elimination of T Cell Subpopulations by Chimeric Antigen Receptor-modified T Cells

Dissertation

for the award of the degree

"*Doctor rerum naturalium*"

of the Georg-August-Universität Göttingen

within the doctoral program "Molecular Medicine"

of the Georg-August University School of Science (GAUSS)

submitted by

Stela Nikolaeva Petkova

born in Sliven, Bulgaria

Göttingen, 2021

This thesis was conducted at the Institute of Cellular and Molecular Immunology at the Georg-August University of Göttingen from April 2017 until March 2021 under the supervision of Dr. Niklas Engels and Prof. Dr. Jürgen Wienands.

Thesis Committee

Prof. Dr. Jürgen Wienands, Institute for Cellular and Molecular Immunology, University Medical Center Göttingen

Prof. Dr. Alexander Flügel, Institute for Neuroimmunology and Multiple Sclerosis Research, University Medical Center Göttingen

Prof. Dr. Michael Schön, Department of Dermatology, Venereology and Allergology, University Medical Center Göttingen

Members of the Examination Board

Referee: Prof. Dr. Jürgen Wienands, Institute for Cellular and Molecular Immunology, University Medical Center, Göttingen

2nd Referee: Prof. Dr. Alexander Flügel, Institute for Neuroimmunology and Multiple Sclerosis Research, University Medical Center Göttingen

Further members of the Examination Board

Prof. Dr. Michael Schön, Department of Dermatology, Venereology and Allergology, University Medical Center Göttingen

Prof. Dr. Heidy Hahn, Department of Human Genetics, University Medical Center Göttingen

Prof. Dr. Dieter Kube, Department of Haematology and Oncology, University Medical Center Göttingen

Prof. Dr. Lutz Walter, Department of Primate Genetics, German Primate Center, Göttingen

Date of oral examination: June 1st, 2021

Affidavit

I hereby declare that the submitted thesis “Targeting and Elimination of T Cell Subpopulations by Chimeric Antigen Receptor-modified T Cells” is my own work. All sources and aids are acknowledged as references.

Stela Petkova

Göttingen, 2021

Table of content

1. Abstract

Chimeric antigen receptors (CARs) demonstrated a high potential for the elimination of tumor cells in cancer immunotherapy. The first successful application of CAR-expressing T cells aimed at the elimination of B cells in hematological malignancies. However, despite being a breakthrough, which highlighted the potential of the CAR T cell technology, its application in targeting T cells currently has limitations. On the one hand, it is the limited choice of target molecules that are presented on malignant cells, but not on healthy cells. On the other hand, the design of the signaling components included into CAR constructs needs to be 'fine-tuned' to provide higher efficiency and persistence of the CAR-modified T cells.

Adapting the CAR T cell platform to treat T cell malignancies poses challenges in terms of the targeting approach. Redirecting the CAR-expressing T cells requires a careful selection of the target antigen, because unlike for B cells, the elimination of the entire T cell population is not a feasible strategy. Therefore, for selective elimination of defined subpopulations, I explored the possibility to redirect CAR-expressing cells against TCR Vβ clonotypes. As a model and proof of principle, I used TCR Vβ 5.3$^+$ subpopulation. To this end, I generated an anti-Vβ 5.3 CAR in a dual chain format (anti-Vβ 5.3 dcCAR). In this study, I could show that the dcCAR T cells selectively eliminate TCR Vβ 5.3$^+$ T cell line *in vitro*. Moreover, co-culture experiments with isolated primary human T cells showed specific recognition of the target subpopulation. Taken together, these findings demonstrate the potential of this targeting approach to specifically eliminate defined T cells subpopulations.

Since the cytoplasmic domains in currently used CAR molecules have an impact on the functionality and efficiency of the CAR-expressing T cells, the effect of the immunoglobulin tail tyrosine (ITT) motif in the anti-Vβ 5.3 dcCAR was assessed. For this purpose, the CD28-derived ITT motif included in most conventional CAR backbones was exchanged with the ITT motif from the lymphoid and myeloid co-receptor DAP10. The modified costimulatory domain of the anti-Vβ 5.3 dcCAR showed increased signaling capacity in comparison to the conventional CD28 ITT-containing domain, but similar cytotoxic efficiency exerted by both dcCAR-expressing Bw58 cells.

The findings of this study provide a groundwork for further investigation of CAR molecules intended to target selectively defined TCR Vβ-specific subpopulations, by utilizing other Vβ-specific monoclonal antibodies as variable domains of CARs. Moreover, the improved signaling potential as a result of the ITT exchange in the CARs, provides a basis for expanding the current knowledge about the potential role of additional signaling elements in CAR activity-modulating co-receptors. Altogether, these findings could contribute to the improvement of the CAR T cell platform in the future.

2. Introduction

2.1 The immune system – a brief overview

The main function of the human immune system is to provide a defense against pathogens invading the body[1,2]. Another important role is to recognize and eliminate malignant cells, which is of critical importance to prevent the development of cancer[3]. In order to provide protection, the immune system is equipped with a diverse arsenal of strictly coordinated ´players´ that orchestrate cell-mediated and humoral defense mechanisms. They are classified into two branches – an innate and an adaptive system that have distinct but also overlapping functions to ensure protective immunity.

Once the primary physical barriers of the body, such as epithelial or mucosal tissues, are breached by microorganisms, the first line of defense is provided by the cells of the innate immune system. These include functionally diverse cell types like macrophages, granulocytes, natural killer (NK) cells and dendritic cells (DC). They represent the ´fast-acting´ units of the cellular immune system that provide rapid recognition and quick elimination of pathogens. Each of these types of immune cells is equipped with receptors whose specificities are germline-encoded and recognize groups of foreign molecules expressed by many pathogens[4].

The NK cell subset of the innate immune system has also an important role in providing an early anti-tumor response[5]. NK cells are constantly patrolling the body and interact with host cells, which express major histocompatibility complex (MHC) class I molecules[6]. These molecules present short peptides, which are derived from intracellular proteins. Downregulation of MHC class I expression on malignant cells and upregulation of ligands for activating receptors on NK cells triggers tumor cell lysis by secretion of perforin and granzymes[7,8]. The anti-tumor role of NK cells is further complemented by specific cells of the adaptive immune system – the cytotoxic T cells. A key difference to those, however, is that NK cells do not require previous antigen encounter and priming by professional antigen-presenting cells (pAPCs) to be able to exert their cytotoxic response[9,10].

The DCs represent a bridge between the cellular compartment of the innate and adaptive immune system. They are considered to be the most efficient pAPCs among others (i.e macrophages and B-cells), which makes them ´key players´ in the activation process of adaptive immune responses[11]. DCs have an essential role in the primary immune response by presenting internally processed antigenic peptides to naïve T cells of the adaptive immune system[12–14].

The cellular compartment of the adaptive immune system is comprised of B and T lymphocytes, which originate from common lymphoid progenitor cells in the bone marrow[15,16]. The generated B and T lymphocytes represent the ´highly-specialized´ antigen-recognition division of the immune system. In comparison to the innate immune cells, they are equipped with a diverse repertoire of antigen-specific receptors. Each B and T cell have a unique B cell antigen receptor (BCR) or T cell antigen receptor (TCR), respectively which share a certain homology in structure. They are generated by somatic recombination events during development which is

their unique property to generate an enormous diversity of antigen specificities and contribute to more efficient pathogen clearance[17,18].

2.2 The antigen receptors on B and T cells

The antigen receptors on B and T cells each have unique, clonotypic specificities and furthermore share some structural as well as functional characteristics. The BCR contains two immunoglobulin heavy chains (IgH) and two immunoglobulin light chains (IgL) that together form a membrane-bound immunoglobulin (mIg) molecule, which represents the antigen recognition moiety of the BCR. The mIg is non-covalently associated with a heterodimer of transmembrane proteins, composed of immunoglobulin-associated alpha and beta chains (Igα/β or CD79 a/b)[19,20], which carry the immunoreceptor tyrosine-based activation motif (ITAM) required for triggering of intracellular signaling events upon antigen recognition[21] (Figure 2.1). The BCR can bind to different classes of molecules like proteins, carbohydrate ligands, or even nucleic acids. Antigen recognition is provided by the so-called variable domains (VH or VL) of the mIg molecule, which together provide the unique antigen specificity. The vast diversity of unique specificities is achieved by a process, called V(D)J recombination or somatic recombination, where individual germline-encoded gene segments designated as variable (V), joining (J) and diversity (D-for the heavy chain) are assembled to give rise to the variable regions of the mIg during B cell development. The constant domains of the mIgH chain (CH) exist in different isotypes referred to as mIgM, mIgD, mIgG, mIgE and mIgA. Also, the IgL chains have distinct constant domains (CL), called kappa and lambda in mice and humans[22]. Upon antigen recognition, the immuno-competent B cells, which can recognize native proteins, can differentiate either into plasma cells that secrete antibodies or into memory B cells that provide long-term protection upon re-encounter with the same antigen[23].

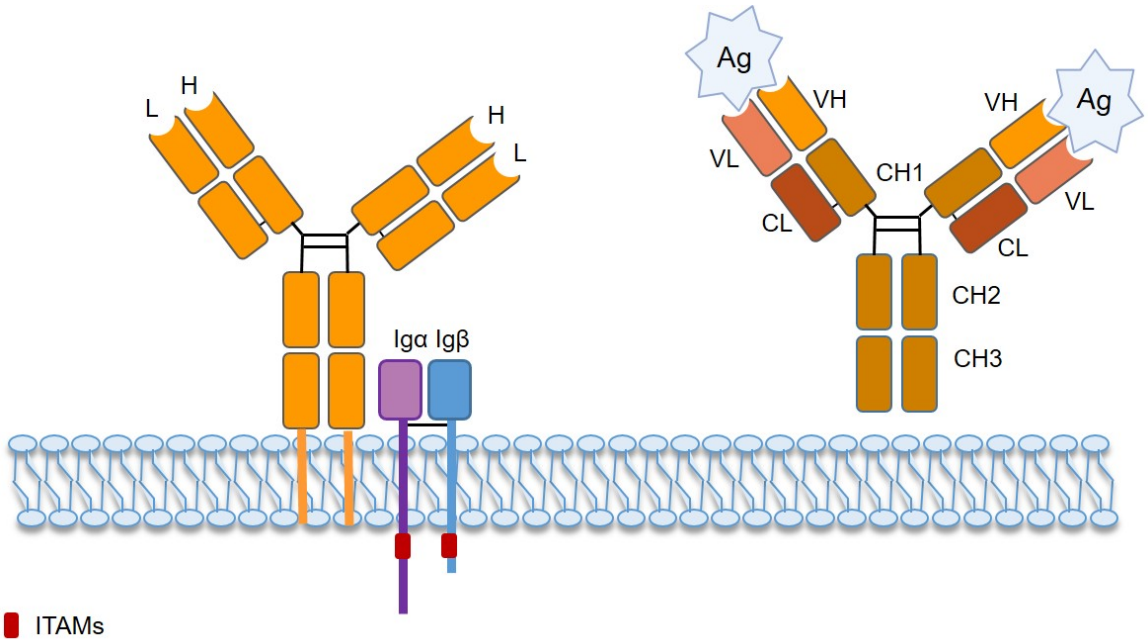

Figure 2.1. Schematic depictions of a BCR and a soluble immunoglobulin molecule (antibody). All BCR isotypes contain two identical immunoglobulin heavy chains as well as two identical Ig light chains (IgH and IgL). The immunoglobulin molecule is anchored to the plasma membrane by transmembrane domains in the IgH chains. The immunoglobulin molecules are non-covalently associated with a heterodimer of Igα and Igβ subunits that carry ITAM motifs in their intracellular domains, which are required to initiate intracellular signaling upon antigen binding. The soluble form of the mIg, commonly referred to as antibody, contains the same extracellular domains of the IgH and IgL chains. The antibody represented here is an IgG isotype. H – heavy chain, L – light chain, Igα - immunoglobulin-associated alpha chain, Igβ - immunoglobulin-associated beta chain, Ag – antigen, VH – variable domain of the heavy chain, VL – variable domain of the light chain, CH – constant domains of the heavy chain, CL – constant domains of the light chain, ITAMs - immunoreceptor tyrosine-based activation motifs.

In T cells, the antigen receptor contains the TCR alpha (α) and beta chains (β) in the majority of cells (TCR α/β T cells) or gamma and delta in TCR γ/δ T cells. TCR α and β chains lack intracellular signaling motifs and – like the mIg in B cells – are non-covalently associated with an additional protein complex, which in T cells is termed CD3. The CD3 protein complex contains several molecules such as CD3 gamma (CD3γ), delta (CD3δ) and epsilon (CD3ε) which are associated with a homodimer of two CD3 zeta (CD3ζ) molecules. Like the Ig α/β complex, the CD3 carries intracellular ITAM motifs, required for triggering of signaling events upon antigen recognition[24](Figure 2.2). In contrary to B cells, T cells can only recognize internally processed short peptides that are presented on MHC class I or II molecules on the cell surface of other cells. This recognition can have two consequences, depending on the sub-type that a T cell belongs to. Either it triggers direct cytotoxicity towards infected cells, which is predominantly mediated by cytotoxic T cells (CTLs), or it enhances the immune response by secretion of pro-inflammatory cytokines. The latter is predominantly mediated by T helper cells (Th)[25–27].

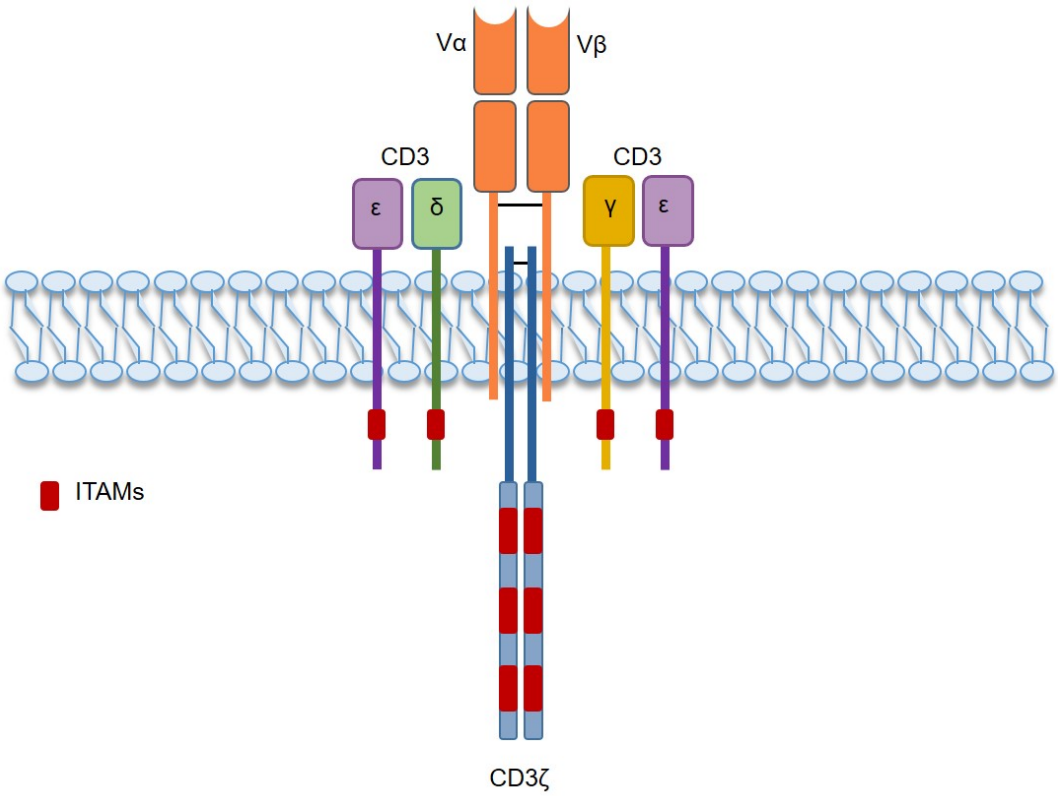

Figure 2.2 Schematic depiction of a TCR. The TCR contains α and β chain heterodimer in the majority of T cells, which is non-covalently associated with a CD3 protein complex. The complex consists of two CD3ε subunits, each associated with either CD3γ or CD3δ chain. The TCR α/β subunit is furthermore associated with a homodimer of two CD3ζ chains. Each of the CD3 chains contains intracellular ITAM motifs that initiate intracellular signaling upon antigen recognition. Vα – variable domain of alpha chain, Vβ – variable domain of beta chain, CD3 – cluster of differentiation 3, ITAMs - immunoreceptor tyrosine-based activation motifs.

The genes encoding the TCR α and β chains are rearranged on the DNA level in the process of random recombination of gene segments (V(D)J recombination) that occurs during T cell development[28,29]. This recombination mechanism leads to the generation of an enormously diverse repertoire of unique TCR specificities[30].

In the formation of the TCR α chain, V and J gene segments are being re-arranged to give rise to a functional variable region. The gene locus encoding the α chain of the TCR contains approximately 70 different V and 61 J segments to be chosen from in the recombination event, thereby providing the basis for the vast TCR α chain diversity[31]. These recombinations lead to the formation of the most diverse region of each TCR chain - the complementarity-determination region 3 (CDR3) that is involved in the antigen binding of the TCR.

In the assembly of the TCR β chain, besides the V and J regions, an additional D gene segment is being re-arranged. In the first step, random D and J segments recombine, followed by the

recombination of one of the more than 50 V gene segments (Figure 2.3). The junction between V and D/J gene segments gives rise to the CDR3 region in the TCR Vβ chain. Following the re-arrangement of the V-D-J regions, the functional V-region exon is transcribed and spliced to the constant domain-encoding segment (C) to form the transcript encoding the TCR β chain. The productive assembly of the recombined TCR α and β chains and their association with the CD3 complex leads to the surface expression of a functional TCR with unique specificity[32].

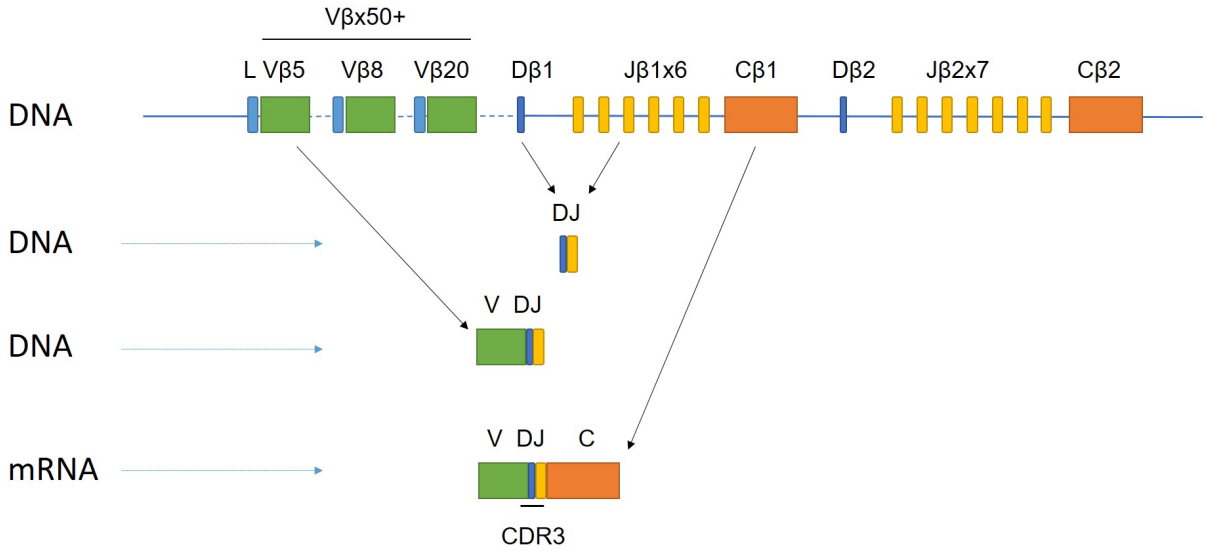

Figure 2.3 Schematic representation of the human TCR β chain-encoding locus. The TCR β chain-encoding gene segments are randomly re-arranged by joining one of the germline-encoded D (dark blue) and J (yellow) gene segments and subsequently joining of one of the >50 Vβ-encoding gene segments (green), which determine the TCR Vβ-chain clonotype of the T cells. Each Vβ gene segment is preceded by a leader sequence (light blue). Assembly of the V, D and J segments forms the complementarity-determining region 3 (CDR3), which defines the antigen-specificity of the TCR. Following the re-arrangement of the V-D-J regions, the functional V-region exon is transcribed and spliced to the constant domain-encoding segment (C) to form the transcript encoding the TCR β chain.

There are more than 50 different germline-encoded TCR β chain V gene segments in the human genome that can be selected in the process of V(D)J recombination. Although the recombined V-gene segments are assigned in a random manner, there is a preferential usage of some among others in the assembly of the Vβ chain[33]. Based on the similarities of the nucleotide sequences of the utilized V gene segments, T cells are classified into different subpopulations (i.e TCR Vβ 20, Vβ 8, Vβ 5.3, etc.). The individual TCR Vβ subpopulations have different distribution ratios in the T cell population in humans[34–36]. Recognition of peptides from the TCR Vβ-expressing T cells leads to clonal expansion of the respective subpopulations[37,38]. Recently, many efforts have been directed towards sequencing of the TCR Vβ repertoire both in healthy individuals and in patients with cancer or autoimmune diseases[36, 39,40]. Several studies have reported a clonotypic expansion of particular TCR Vβ families in T and B cell malignancies

in comparison to their distribution in peripheral blood of healthy individuals[37,41–43]. Furthermore, clonotypic expansion of certain T cell subpopulations was reported in autoimmune diseases as well[44,45]. Thus, characterization of the human TCR Vβ repertoire has a significant impact on the diagnostic but also on the development of future immunotherapies to treat T-cell mediated diseases.

The mechanisms of the immune system to provide protection have been investigated in great detail. The acquired knowledge about the immunological processes has been used to develop therapeutic strategies in clinical settings[46,47]. The understanding of the fundamental similarities and differences between the BCR and TCR has led to the generation of chimeric antigen receptors (CARs), which combine properties of each and could provide enhanced immune response against tumor cells that have escaped the intrinsic immune surveillance.

2.3 Chimeric Antigen Receptors (CARs)

2.3.1 Structural aspects of CARs

The knowledge about the immune system's functional principles has been used to develop novel clinical applications, collectively termed immunotherapies. Examples of such an approach are the genetically engineered CARs[48–50]. They are synthetic receptors that combine the extracellular antigen recognition properties of an immunoglobulin with the intracellular signaling motifs of T cell-activating receptors (Figure 2.4). Specifically, the VH and VL domains of a monoclonal antibody are converted into a single chain format called single chain variable fragment (scFv)[51]. The scFv is then coupled to an extracellular spacer domain, followed by a transmembrane region and intracellular signaling motifs derived from different T cell-expressed receptors. When expressed in (polyclonal) T cells, the genetically engineered CAR sensitizes the transfected cells against a target that display the cognate extracellular CAR antigen[52].

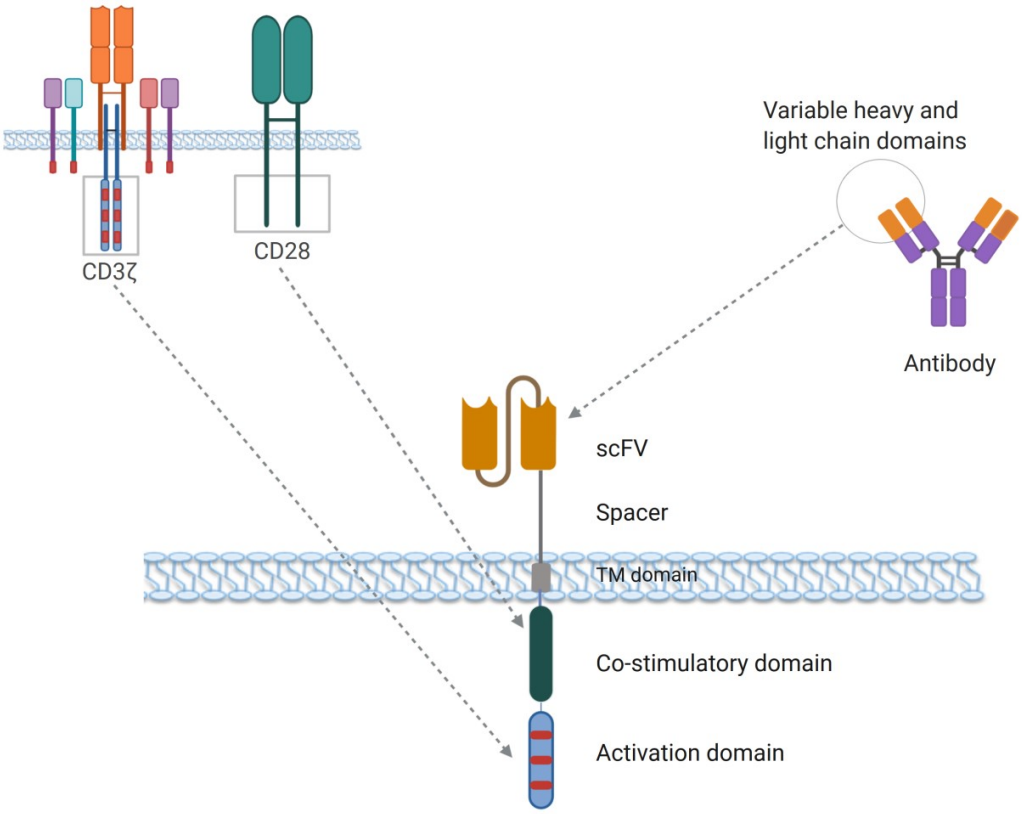

Figure 2.4 Schematic representation of a scCAR. The conventional design of a second generation CAR includes the antigen-specific variable domains of a monoclonal antibody, connected by a linker in an scFv format (yellow), which is followed by a spacer region. These elements form the ectodomain expressed on the cell surface, which is followed by a transmembrane domain (TM domain). In second generation CARs, the endodomain usually contains the ITAMs of CD3ζ (Activation domain, blue, ITAMs in red) and additional signaling domains from T cell co-receptors (here CD28, green).

2.3.1.1 The ectodomains of CARs

The first successful design of a chimeric antigen receptor was described in 1989 by the group of Zelig Eshhar. They generated and expressed a chimeric TCR, by creating a genetic construct where the V regions were substituted with those of an IgH and IgL chain in an open reading frame with either one of the constant domains of TCR α and β chain[53]. Upon transfection of a cytotoxic T cell line, they observed the expression of a functional antigen receptor that had acquired the respective immunoglobulin specificity. Subsequently, it was shown that the newly generated chimeric antigen receptor could trigger activation of the cells without the need for MHC-restricted antigen presentation[53]. A few years later, this approach was developed further from the same group by generating antigen-binding antibody domains in the format of scFv coupled to CD3ζ signaling domains. Cells that expressed the scFv-based CAR were shown to lyse target cells in a non-MHC restricted manner as well[54].

Following these pioneering experiments, the design of CAR molecules was further refined and the technology was significantly improved. Not only in terms of expanding the variety of antigen specificities but also in terms of improving the CAR backbones[50]. In the majority of CARs the antigen recognition part consists of immunoglobulin-derived VH and VL domains, which are connected with a synthetic linker that sustains the antigen-binding region[55]. The benefit of using such scFv modules is that the entire receptor is encoded within one open reading frame and thus can be transfected into T cells using a single expression vector.

However, this conventional design also has its limitations. In many cases the conversion of VH and VL domains into an scFv format results in either lower affinity or complete loss of binding[56]. This impedes the applicability of some antibodies in the context of CARs[57]. Furthermore, the artificial linkers included in scFvs, which are usually comprised of several repeats of glycine and serine amino acid residues, are reported to trigger host immune responses against the CAR-modified T cells, thus leading to their low persistence after infusion to the patient[58]. Besides the reported immunogenicity, recently obtained data shows another limitation of scFv-based CAR designs that is caused by aggregation of single chain CARs (scCARs) on the T cell surface and subsequent triggering of so-called ”chronic signaling”[59]. This effect leads to an antigen-independent constitutive low level of intracellular signaling that appears to cause ”exhaustion” of the CAR-expressing T cells *in vivo*[59–61].

Another important component in the design of CARs is the extracellular spacer region. The majority of CAR designs utilizes two Ig-like domains of the heavy chain (CH2-CH3) domains of an IgG1, IgG2 or IgG4 antibody. Other widely used spacer regions are derived from the extracellular parts of CD28 or CD8 costimulatory receptors [49,62,63]. The spacer region provides a distance of the scFV from the membrane of CAR-expressing cells to the target epitope. Thus, its length might need to be ´fine-tuned´ depending on the particular target antigen to ensure optimal cell-to-cell interaction between the CAR-expressing cells and target cells.

To circumvent the aforementioned limitations of the conventional scFv CARs, a new design of the ectodomains has been proposed recently[64]. The dual chain CAR (dcCAR) format includes antigen-binding domains in a native IgG-like format instead of scFv conversion. In the dcCAR design (Figure 2.6) the extracellular parts of IgH and IgL chains are coupled to intracellular T cell signaling domains, similar to the scCARs[64]. This design circumvents the limitations that come along with scFv conversion and furthermore bypass the usage of an artificial linker. In addition, the incorporation of the respective heavy chain constant domains of the native antibody format might circumvent the need for further adjustment of the spacer length.

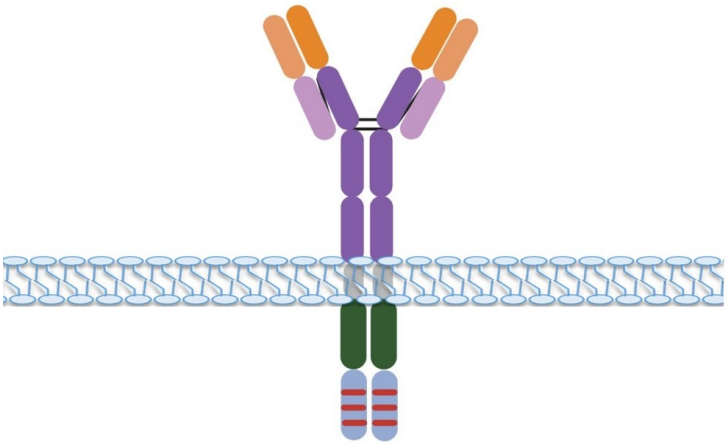

Figure 2.5 Schematic representation of a second generation dcCAR. In this CAR design, the ectodomain consists of the antigen-specific IgH and IgL chain domains in a native IgG-like format, which are anchored to the plasma membrane via transmembrane domains (grey). The intracellular signaling motifs shown here are the same as in the second generation scCARs – CD28 (green) and CD3ζ (blue) with the ITAM motifs (red). Variable domains of the heavy chain (dark orange), Variable domains of the light chain (light orange), kappa/lambda light chain constant domains (light purple) and constant domains from 1 to 3 of an IgG heavy chain (dark purple).

2.3.1.2 The intracellular domains of CARs

The currently used intracellular signaling domains in CARs have a role not only in triggering activation of the CAR-expressing T cells, but also regulate their effector cytokine profile, metabolism and survival[49]. The first described designs of CAR molecules, the so-called first generation CARs (Figure 2.6), contained only the CD3ζ ITAMs as intracellular activation domain[65]. However, T cells expressing these CARs were shown to be less efficient in terms of persistence[66–68]. This problem was solved in the so-called second generation CARs by the addition of intracellular signaling domains from co-receptor molecules (Figure 2.6). The majority of second generation CARs contain the cytoplasmic domains from either CD28 or TNF receptor family members such as e.g. 4-1BB, which are also found in the first clinically approved CARs directed against CD19-expressing B cells (Yescarta™ and Kymriah™). The 4-1BB signaling domain contributes to improved persistence of the CAR T cells *in vivo* but induces slower effector response, whereas the CD28-mediated co-stimulatory domain provides very rapid activation, proliferation, and target cell lysis by the CAR-expressing cells[69,70].

Although CD28 and 4-1 BB are the most widely used co-stimulatory domains in CARs and have proven to be effective in clinical settings, other cytoplasmic domains have also been investigated. Among these are ICOS, CD27, OX40 and DNAX-activating protein 10 (DAP10) cytoplasmic domains, which have been evaluated for their impact on the effector functions and persistence of the modified CAR-expressing cells[71–73,74]. Programmed cell death protein 1-directed CAR T cells which employed DAP10 co-stimulatory domain instead of CD28 have been shown to induce long-term tumor-free survival in mouse model of lymphoma[75]. Furthermore, the CAR-modified T cells showed preferential cytokine profile and differentiation to a memory phenotype mediated by the DAP10 co-stimulatory domain[75,76].

Second generation CARs were further modified to improve their functional properties, which gave rise to the so-called third and fourth generation of CARs (Figure 2.6). The third-generation of CARs includes two different cytoplasmic co-stimulatory domains (i.e. CD28 and 4-1BB) adjacent to the CD3ζ activation domain. The fourth generation contains a second generation CAR molecule, which upon antigen recognition leads to inducible expression of a recombinant protein, i.e. a cytokine or a co-stimulatory ligand to enhance the activation of the CAR-expressing cells. This fourth-generation is also referred to as 'T cells redirected for universal cytokine-mediated killing' (TRUCKs)[77,78].

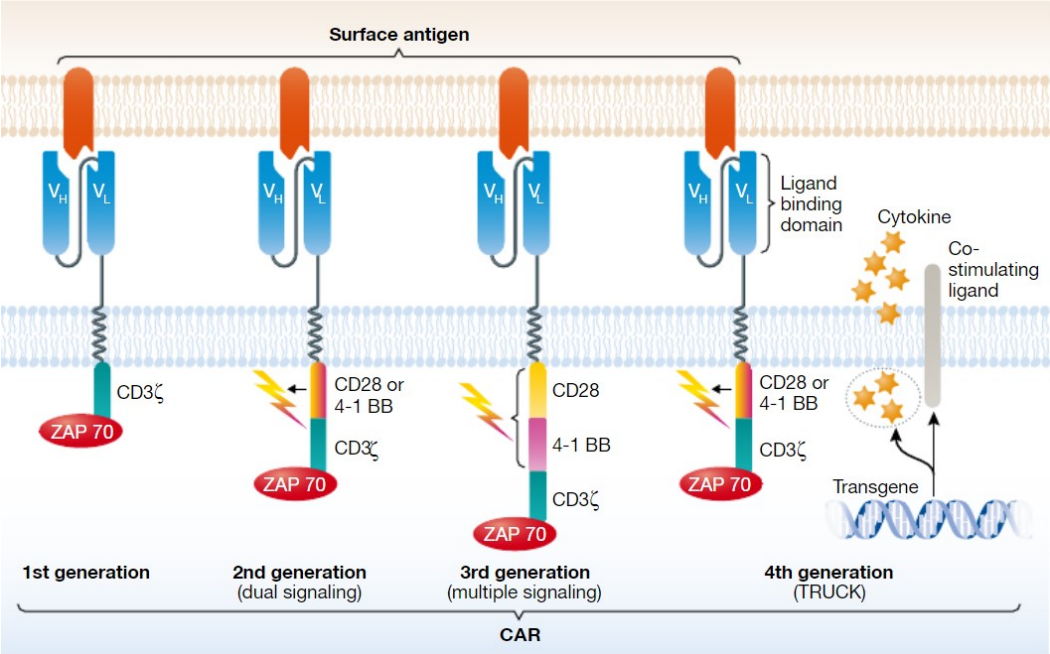

Figure 2.6 Schematic representations of the different CAR generations. The first generation CARs contain only the CD3ζ cytoplasmic activation domain, whereas the second generation CARs contain an additional cytoplasmic domain from a co-stimulatory receptor (in this case either CD28 or 4-1BB). Third generation CARs contain two different co-stimulatory domains (in this case both CD28 and 4-1BB). Fourth generation CARs (TRUCKs) usually contain second generation CAR genetic constructs and in addition a gene cassette for expression of recombinant protein (i.e. cytokine or co-stimulatory ligand) upon activation of the CAR-modified cells. The figure is modified from J. Hartmann, J et al.[50].

To improve the efficacy and the safety of CAR T cell therapies, several other CAR designs were investigated such as CARs with dual specificity and suicidal CARs (equipped with a suicidal gene that can be triggered for the elimination of the CAR T cells)[79,80]. The application of CARs is further expanded by modification of other immune cells used for expression of the respective CAR molecules. Currently investigated are CAR-modified γ/δ T cells, NK cells[81–83] and DCs[84]. So far, however, the most utilized CAR applications are based on the modification of T cells.

2.4 CAR-redirected T cells

2.4.1 CARs exploit the TCR signaling network

Intracellular signaling in T lymphocytes is a strictly orchestrated process triggering intracellular cascades of biochemical interactions, mediated by an assembly of protein complexes (signalosomes)85. Early in the development of T cells, intracellular signaling events occur after assembly and surface expression of a functional TCR. Engagement of the TCR with peptides presented on MHC molecules can induce T cell activation by phosphorylation of the ITAM motifs in the cytoplasmic part of the CD3 complex. Signaling cascades triggered by the interaction of activating co-stimulatory receptors complement the process in naïve T cells and promote proliferation, cytotoxic response or cytokine secretion by the T cell86.

An important difference between antigen recognition by a TCR and a CAR molecule is that the modified CAR-expressing T cells bypass the need for peptide presentation by MHC molecules for antigen recognition. This allows the triggering of T cell effector functions not only against processed peptides but against native antigens as well. Furthermore, CAR backbones containing the intracellular signaling domains of co-receptors bypass the need for co-stimulation to promote effector functions in the transfected cells. Up to date, it is considered that CARs trigger similar signal transduction pathways to the TCR-driven ones[87]. The signal transduction mechanisms utilized by the TCR and CARs after antigen recognition involve the phosphorylation of the ITAM motifs in the intracellular CD3ζ domains by lymphocyte-specific protein tyrosine kinase (Lck), which leads to an assembly of signalosome complex, composed of additional signaling molecules and adaptor proteins[87]. Lck-mediated phosphorylation of Itk leads to activation of phospholipase Cγ1 (PLCγ1) and a catalytic cleavage of phosphatidylinositol (4, 5)-bisphosphate, resulting in the generation of second messengers such as diacylglycerol and inositol (1, 4, 5)-trisphosphate, which leads to an increase of the intracellular level of Ca^{2+} ions[88,89]. Hence, the decrease of the Ca^{2+} ions levels in the endoplasmic reticulum leads to influx of ions from the extracellular space. Furthermore, these processes activate additional signaling pathways including mitogen-activated protein kinases (MAPK), nuclear factor of activated T cells (NF-AT) and nuclear factor of κb (NF-κb)[85]. By regulating the transcription of genes, the respective transcription factors induce T cell responses such as proliferation, cytokine production and effector functions.

Besides the ITAM-driven signaling, an important role in enhancing the signaling events upon activation has the interaction of co-receptors with their respective ligands. CD28 and DAP10 co-receptors have a copy of an evolutionarily conserved stretch of amino acids known as immunoglobulin tail tyrosine (ITT) phosphorylation motif[90,91]. ITT-like motifs have the consensus sequence YxNM (single letter code for amino acid where ‘Y’ stands for tyrosine and ‘x’ stands for any residue). ITT motifs incorporated in the cytoplasmic region of co-receptor molecules have a role in enhancing the downstream signaling events by providing docking sites for the recruitment of additional signaling molecules[21,23,91,92].

2.4.2 The role of the ITT motif in signaling of co-stimulatory domains

In the so-called second generation CAR constructs, the membrane-proximal cytoplasmic co-stimulatory region enhances the activation of the T cell responses. In comparison to 4-1BB, the cytoplasmic domain of CD28 is known to provide a rapid and enhanced activation of CAR T cells. The cytoplasmic domain of CD28 contains a copy of an ITT motif (Figure 2.7)[90]. Phosphorylation of this tyrosine residue allows for the recruitment of the adaptor protein Growth factor receptor-bound 2 (Grb2) and/or PI3K kinase, which complements and enhances the ITAM-induced activation signal, thus enhancing IL-2 production by the activated T cells[93,94]. CD28-mediated signaling is further complemented by the presence of two proline-rich binding motifs which also recruit Grb2, Lck, filamin-A (FII A), and Itk and further enhance the signaling[94,95].

DAP10 in NK and cytotoxic T cells is a small type 1 transmembrane protein, which contributes to signal transduction through the Natural killer (NK) group 2 member D (NKG2D) receptor[91]. The latter is a strong activating receptor for NK cells and a co-stimulatory receptor for $CD8^+$ T cells[96,97,98]. The cytoplasmic part of DAP10 has a certain homology to CD28 co-stimulatory domain as they both contain the consensus ITT motif sequence (YxMN) and can potentiate downstream signaling by providing a binding site for the Grb2/Vav complex and PI3K upon tyrosine phosphorylation[91,99].

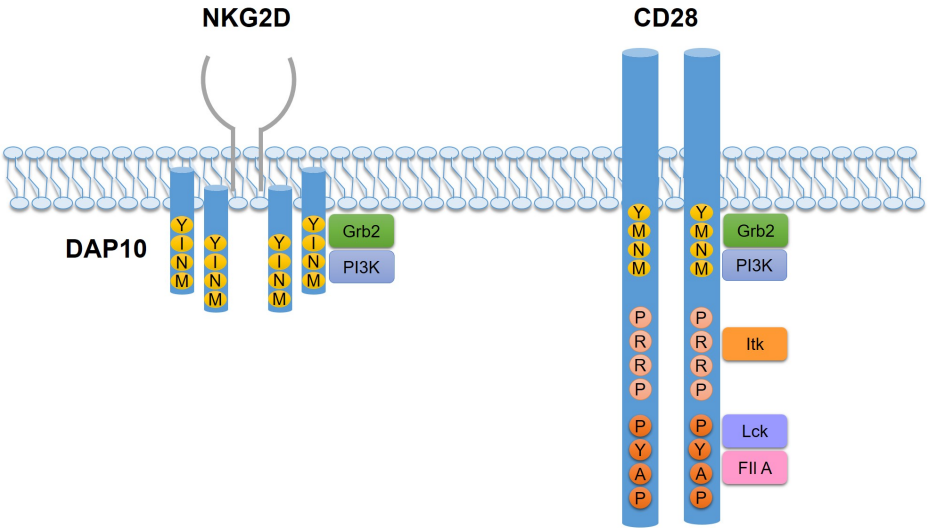

Figure 2.7 Schematic depiction of CD28 and DAP10 cytoplasmic domains. The evolutionary conserved ITT motif is marked in yellow. It allows binding of the SH2-domains of Grb2 and PI3K. The CD28 cytoplasmic tail contains two proline-rich motifs in addition to the ITT motif. The proximal proline-rich motif (in pink) recruits Itk, whereas the distal one (red) provides binding sites for Lck, Grb2, FII A.

The DAP10 has been shown as capable to initiate cytotoxic response in NK cells partially independent from ITAM-driven signaling[100]. Reports about the utilization of DAP10 as a co-stimulatory domain in CAR constructs show that it significantly increases the anti-tumor

properties both in CAR NK and cytotoxic CAR T cells[74,98,101–103]. It also contributes to the differentiation of the T cells towards memory effector phenotype, which might provide an enhanced persistence of the CAR-modified T cells[74].

Despite the findings of the role of DAP10 when included as a co-stimulatory domain in second and third generation CAR constructs, little is known about the contribution of the ITT motif on signaling in CAR-expressing T cells. CD28 and DAP10 share partial homology and initiate similar downstream signaling events. However, whether a second generation CAR backbone containing the DAP10 ITT-like motif instead of CD28ITT would affect the activation and effector response of the CAR-expressing T cells needs further investigation.

2.4.3 Cytotoxic effector functions of CAR T cells

Transfection of phenotypically distinct T cells (i.e. $CD4^+$ or $CD8^+$ T cells) with CARs sensitizes the cells to exert either direct cytotoxicity against target cells or leads to the secretion of pro-inflammatory cytokines that further enhance the immune response[104]. CD8-expressing T cells exert cytotoxic responses by utilizing two major mechanisms: i) by releasing cytotoxic granules or ii) by inducing apoptosis via triggering of death-domain receptors[105,106]. The conventional CTLs recognize and eliminate their target cells by release of lytic granules, which are rich in perforin and granzymes and can trigger apoptosis[107]. Upon degranulation, perforin forms pores in the target cell membrane that allows entry of granzymes. The latter are then triggering programmed cell death of the target cells by activating various caspase enzymes or via caspase-independent mechanisms[108].

Another mechanism by which cytotoxic T cells can eliminate antigen-expressing cells is by death receptor-mediated apoptosis[109]. This mechanism of killing usually occurs later than exocytosis of perforin and granzymes. A major and well-characterized driver of death receptor-mediated apoptosis is Fas ligand (FasL), a member of the tumor necrosis factor (TNF) family. After antigen recognition and activation, cytotoxic T cells can upregulate the expression of FasL on their cell surface. This process leads to binding to its receptor Fas on target cells, clustering of molecules and triggering programmed cell death of the target cell via proteolytic activation of caspases[110–112].

Both cytotoxic mechanisms of CTLs, secretory and death receptor-mediated, could potentially have a synergistic or additive effect on target-cell elimination by CAR T cells[7]. Although the secretory cytotoxic pathway acts faster in comparison to the FasL-mediated response, both mechanisms might complement each other in serial killing events of activated T cells[7].

2.5 Application of CAR-T cells in immunotherapies

The application of the CAR T cell platform was a breakthrough in the treatment of B cell malignancies[113]. The first successful demonstrations of its clinical application were reported in 2013 when patient-derived T cells were modified with an anti-CD19 CAR-encoding genetic construct and infused back to the patient in an autologous adoptive T cell transfer[114]. This approach has shown remarkable clinical outcome[114,115]. However, CD19-redirected CAR T cells

do not provide selective elimination of only malignant cells, since the CD19 is a pan-B cell marker. In clinical settings, the immune suppression as a result of B cell depletion by CD19 CAR T cells can be at least partially overcome by a routine infusion of immunoglobulins[116].

Up to date, the available immunotherapies for treatment of T cell malignancies are rather limited. In most of the cases T cell leukemia and lymphomas are treated with chemotherapy regimens, which are often not sufficient to achieve stable remission without relapses[117]. As a consequence, for some patients, an allogeneic stem cell transplantation is required, which possess a risk of development of graft-versus-host disease[118]. A number of other therapeutic agents have been explored for the depletion of T cells, among which are immunotherapies with monoclonal antibodies such as anti-CD3 (OKT3), or polyclonal anti-thymocyte globulins (ATG). However, the application of these was limited due to not sufficient efficacy and severe side effects that were associated with cytokine-release syndrome or broad immunosupression[119].

The general applicability of the CAR T cell platform to target T cells is also currently limited. One reason for this is the choice of a suitable target to redirect the CAR-expressing T cells. In the last years, several antigens have been investigated for application of the CAR T cell platform against T cell malignancies. These include the pan-T cell markers such as CD5, CD7 or CD3, which have been reported to have higher expression levels on T cells in certain leukemia and lymphoma conditions[120–125]. However, the results indicate that the respective T cell-redirected CAR T cells showed high rates of fratricide, which caused poor persistence and limited efficacy of such approaches in mice[126]. Therefore, in most cases, gene editing or blocking of cell surface expression of the respective antigens on the CAR-modified T cells was required to prevent fratricide and to induce an effective anti-tumor response[122].

Another T cell-specific target structure that has been evaluated for selective targeting is the constant domain 1 of the human TCR β chain (TCR VβC1). In this approach, an scFv from monoclonal antibody, specific for the TCR VβC1, was used to design a T cell redirected CAR. However, this targeting approach is based on the mutually exclusive re-arrangement of the TCR VβC1 and TCR VβC2 during TCR assembly in T cell development and would lead to sparing of approximately half of the T cell population[127]. Thus, identifying other suitable markers for redirecting CARs is of great importance to improve the selectivity and eliminate only defined subpopulations in order to preserve T cell immunity. Another potential marker to redirect CAR T cells is the Vβ domain of the TCR. Since there are monoclonal antibodies that recognize individual subpopulations of Vβ-expressing T cells, utilizing them to design CARs have a potential for selective elimination and sparing the majority of T cells. This strategy may circumvent the problems that arise when CAR T cells are directed against large subpopulations of T cells.

2.6 Aims of this thesis

Despite the progress in exploring possible T cell surface markers to redirect CARs against T cells, there is an urgent need for improvement of the selectivity and efficacy of these approaches. Therefore, to evaluate the potential for selective targeting of T cells via the CAR platform, I investigated the possibility to sensitize the CAR-expressing T cells against individual TCR Vβ subpopulations. To this end, I generated and functionally characterized a CAR against the Vβ 5.3 domain of the TCR. This approach limits the fratricide only to the defined Vβ-expressing T cells, which can be beneficial for the overall efficiency of the modified CAR T cells and their application in future immunotherapies. During my PhD project, I focused on the following aims:

1. Generation of a prototypic Vβ 5.3-specific CAR construct

   Using a second generation CAR backbone, I generated CAR constructs (both in scCAR and dcCAR format) that possess the specificity to recognize Vβ 5.3-expressing T cell subpopulations. This was achieved by using the variable regions from the TCR Vβ 5.3-specific monoclonal antibody.

2. Functional characterization of TCR Vβ 5.3-specific CAR-T cells

   To test the functionality of the anti-Vβ 5.3 CARs, I generated a cell culture-based system consisting of CAR-expressing Bw58 T cells and TCR Vβ 5.3^{+} Jurkat cells. Furthermore, I evaluated the selective recognition of the cognate antigen on human primary T cells by Bw58 dcCAR T cells.

3. Evaluation of the effect of the ITT-motif exchange on the second generation anti-Vβ 5.3 dcCAR

   To explore the effect of ITT-mediated signal amplification on the CAR-expressing T cells, I exchanged the ITT-like motif of CD28 with the one from DAP10, which in previous experiments proved to be a more effective signal amplifier. I evaluated the signaling potential of the modified CAR backbone and compared the cytotoxic activity of the respective CAR-expressing T cells.

3. Materials and Methods

3.1 Materials

3.1.1 Buffers and Solutions

Table 1: List of buffers and solutions with their respective composition.

Name	Composition
Krebs-Ringer buffer	140 mM NaCl
	10 mM HEPES (pH 7.4)
	10 mM D-glucose
	4 mMKCl
	1 mM $MgCl_2$
	1 mM $CaCl_2$
	in ddH_2O
Lysogeny broth (LB) medium	10 g/l Tryptone
	5 g/l Yeast Extract
	5 g/l NaCl (pH 7.0)
	in ddH_2O
Phosphate buffered saline (PBS)	137 mM NaCl
	4.3 mM Na_2HPO_4
	2.7 mM KCl
	1.4 mM KH_2PO_4 (pH 6.6)
	in ddH_2O
RPMI media with 10% FCS (R10)	10% (v/v) heat-inactivated FCS
	1x PenStrep
	1 mM sodium pyruvate
	1 mM L-glutamine
	50 µM β-mercaptoethanol
	in RPMI-1640 medium
RPMI media without FCS (R0)	1x PenStrep
	1 mM sodium pyruvate
	1 mM L-glutamine
	50 µM β-mercaptoethanol

3.1.2 Chemicals and reagents

Table 2: Chemicals and reagents used in this study.

Name	Manufacturer
5-Bromo-4-chloro-3-indolyl β-D-galactopyranoside (X-Gal)	Roth
7-Aminoactinomycin D (7-AAD)	BD Biosciences
Agarose	Peqlab
Annexin V APC	BioLegend
Annexin V Binding Buffer	BD Biosciences
Annexin V Brilliant Violet 421	BD Biosciences
BD Golgi STOP Protein Transport inhibitor	BD Biosciences
dATPs	Invitrogen
DNA Ladder GeneRuler 1 kb	Fermentas
dNTPs Mix	NEB
Fetal Calf Serum (FCS)	Anprotec
Gel Loading Dye (6x), purple	NEB
Hexadimethrine Bromide (Polybrene)	Sigma
Indo-1 AM	Life Technologies
Isopropyl-β-D-thiogalactopyranosid (IPTG)	Sigma
L-Glutamine (200 mM)	Gibco
NEB buffer 1.1, 2.1, 3.1 & CutSmart	NEB
Penicillin/Streptomycin (100x)	Gibco
Pluronic F-127	Life Technologies
Puromycin	Invivogen
Roswell Park Memorial Institute (RPMI) 1640 Medium	Gibco
Sodium Pyruvate (100 mM)	Gibco
T4 Ligase Buffer	NEB
TransIT-293 Transfection Reagent	Mirus
Trypsin/EDTA (0.05%)	Gibco

3.1.3 Consumables

Table 3: Consumables used in this study.

Consumables	Manufacturer
Cell Culture plastic ware	Greiner Bio-One
FACS tubes	Sarstedt
Filter tips	Greiner Bio-One
LS columns	Miltenyi Biotec
Parafilm	Bemis
PCR tubes	Sarstedt
Pipette tips	Greiner Bio-One
Polypropylene tubes	Greiner Bio-One
Reaction tubes	Greiner Bio-One
Sterile filters	Sarstedt

3.1.4 Databases

Table 4: Online databases.

Application	Source
Sequence data blast	http://www.ncbi.nlm.nih.gov/
Sequence data alignment	http://multalin.toulouse.inra.fr/multalin/
Protein information	http://www.uniprot.org/

3.1.5 Enzymes

Enzymes were used according to manufacturer's recommendations.

Table 5: Enzymes and manufacturers.

Enzymes	Manufacturer
Calf Intestine Phosphatase (CIP)	NEB
Pfu Polymerase™	Promega
Restriction Endonucleases	NEB
Taq Polymerase	NEB
T4 DNA Ligase	NEB

3.1.6 Genetic constructs

Table 6: Genetic constructs used in this study.

Name	Source	Application
pMSCV puro II	this study	Contains additional NotI and BamHI sites in the multiple cloning site
pMSCV puro II HPB #4	this study	Encoding TCR Vβ 5.3 chain
pCR2.1/MEM262 XbaI	this study	Cloning of anti-Vβ 5.3-reactive variable heavy (VH) and light (VL) domains
pUC57-O-CARMEM	this study	Cloning of anti-Vβ 5.3-reactive scFV in a second generation CAR backbone
pMSCV puro II – O-CARMEM	this study	Expression of anti-Vβ5.3 scFV CAR
pCR2.1 VJMEM kappa light chain #1	this study	Cloning of anti-Vβ 5.3 -reactive kappa light chain
MIRFP VJMEM kappa Light chain #5	this study	Expression of anti-Vβ 5.3 kappa light chain
pCR2.1 VJMEM Lambda light chain #2	this study	Cloning of anti-Vβ 5.3 lambda light chain
MIRFP VJMEM lambda Light chain #4	this study	Expression of anti-Vβ 5.3 lambda light chain
pBUD human IgG1	N. Engels	Overlap-extension PCR to fuse human IgG1 spacer to the CAR construct
hPOS CAR	N. Engels	Overlap-extension PCR to fuse CD28 TM, CD28 and CD3ζintracellular CAR backbone to the CAR
hPB2 CAR	N. Engels	Overlap-extension PCR to fuse CD28 TM, CD28 and CD3ζ intracellular CAR backbone to the CAR
pCR2.1VHdcCAR CD28TM	this study	Cloning of anti-Vβ5.3 heavy chain CAR construct
pMSCVpuroII VHdcCAR CD28TM	this study	Expression of anti-Vβ 5.3 heavy chain CAR construct
pCR2.1 VHDAP10-1	this study	Site-directed mutagenesis for substitution of amino acid sequences D-V in CD28 ITT motif
pCR2.1 VHDAP10-3	this study	Site-directed mutagenesis for substitution of amino acid LL-ED in CD28 ITT motif
pCR2.1 VHDAP10 (G-K)	this study	Site-directed mutagenesis for substitution of amino acid HS-GK in CD28 ITT motif

pCR2.1 VHDAP10 (I-P)	this study	Site-directed mutagenesis for substitution of amino acid MT-IP in CD28 ITT motif
pMSCVpuro II VHDAP10	this study	Expression of anti-Vβ 5.3 heavy chain DAP10 ITT CAR construct

3.1.7 Laboratory equipment

Table 7: Laboratory equipment.

Instruments	**Manufacturer**
Agarose Gel Electrophoresis	Peqlab
Analytical balance MC1	Sartorius
Bacteria incubator Heraeus Kelvitron®t	Heraeus
Bacterial Shaking Incubator	Infors
Balance BP 61	Sartorius
Balance TF 612	Sartorius
Cell culture incubator HeraCell 150	Heraeus
Cell culture safety cabinet Herasafe	Heraeus
Centrifuge 5415D	Eppendorf
Centrifuge 5417R	Eppendorf
Centrifuge Multifuge 3 S-R	Heraeus
Centrifuge RC 3B Plus	Sorvall
Electrophoresis Power Supply	Amersham Biosciences
Flow cytometer BD FACSCalibur	BD Biosciences
Flow cytometer BD LSR II	BD Biosciences
Freezer HERAfreeze	Heraeus
Inverted microscope Axiovert 35	Zeiss
MidiMACS™ Separator	Miltenyi Biotec
Mastercycler EP gradient	Eppendorf
NanoDrop 2000 Spectrophotometer	NanoDrop 2000 Spectrophotometer
Neubauer improved Counting Chamber	Brand
pH meter InoLab	WTW
Pipettes	Eppendorf
Sprout® Mini centrifuge	Heathrow Scientific
ThermoMixer®C	Eppendorf
Ultra-low Temperature Freezer (-150 °C)	Panasonic
UV illuminator	Intas
Water purification system Arium®Pro	Sartorius

3.1.8 Antibodies

Monoclonal and polyclonal antibodies were used for cell surface staining or blocking. The respective concentrations were kept either according to the manufacturer's recommendations or were titrated for optimal staining as indicated in the respective method part.

Table 8: Antibodies used in this study.

Name	Clone	Isotype	Supplier
anti-human CD2 APC	RPA-2.10	Mouse IgG1, kappa	BioLegend
anti-human CD38 Brilliant Violet 421 (BV421)	HB-7	Mouse IgG1, kappa	BioLegend
anti-human CD5 APC	UHT2	Mouse IgG1 kappa	BioLegend
anti-human IgG Alexa Fluor 647 (AF647)	polyclonal	Goat IgG	Southern Biotech
anti-human Kappa LC FITC	A8B5	Mouse IgG1	ImmunoTools
anti-human Lambda LC FITC	4C2	Mouse IgG1	ImmunoTools
Mouse IgG2b Kappa Isotype Control	eBMG2b	Mouse IgG2b, kappa	Invitrogen
Purified anti–mouse CD178 (FasL)	MFL3	Armenian Hamster IgG	BioLegend
anti-human TCR Vβ5 FITC	MEM-262	Mouse IgG2a, κappa	BioLegend
anti-human TCR Vβ8 eFluor 450	JR-2	Mouse IgG2b, kappa	Invitrogen
anti-human CD271 (NGFR) APC	ME20.4	Mouse IgG1 kappa	BioLegend
anti-mouse CD8a PE-Cy7	53-6.7	Rat IgG2a kappa	BD Biosciences
anti-mouse CD4 FITC	GK1.5	Rat IgG2b, κ	BioLegend
anti-human CD3 FITC	UCHT1	Mouse IgG1, κ	BioLegend

Antibodies used for stimulation – unless otherwise indicated– were used at a concentration of 20 µg/ml.

Table 9: Monoclonal antibody used for stimulation.

Name	Clone	Isotype	Source
AffinityPure anti-human IgG F(ab)$_2$´, unconjugated	polyclonal	Goat IgG	Jackson Immuno Research

3.1.9 Primers

All oligonucleotide primers were synthesized by Eurofins Genomics.

Table 10: Primers used in this study.

Primer name	Sequence 5'→3'	Application
PGK-ENB-fwd	AAC GAA TTC TAG CGG CCG CGA TGG ATC CTC TAC CGG GTA GGG AGG CGC	Generation of pMSCVpuro II vector
PGK-HIND-rev	GGT AAG CTT GGG CTG CAG GTC G	Generation of pMSCVpuro II vector
CD8a-UTR-XEN-fwd	AAG TCT AGA GAT GAA TTC AGC GGC CGC GCT TCT ACT GAT	Addition of unique restriction sites – XbaI, EcoRI and NotI
MEM262_VL-XbaI rev	AAG CTC TAG ACG CGT ACG TCT GAT TTC CAG	Addition of a unique restriction site -XbaI
Hu-kappaV1L-VJMEM fwd	GAT CTC GAG AGA TCT ACC ACC ATG GAC ATG AGG GTC CCC GCT CAG CTC CTG GGG CTC CTG CTA CTC TGC CTG CAG GGT GCC AGA TGT GAT ATC CAG ATG ACA CAG ACT	Generation of light chain constructs of anti-Vβ 5.3 dcCAR construct
Hu-kappaV1L-VJMEM rev	GAC AGA TGG CGC CGC CAC AGT TCT GAT TTC CAG TTT GGT GCC	Generation of light chain construct of anti-Vβ 5.3 dcCAR construct
Hu-kappaC fwd	GGC ACC AAA CTG GAA ATC AGA ACT GTG GCG GCG CCA TCT GTC	Generation of kappa light chain construct of anti-Vβ 5.3 dcCAR construct
Hu-kappaC rev	CTA ACA CTC TCC CCT GTT GAA	Generation of kappa light chain construct of anti-Vβ 5.3 dcCAR construct
Hu-lambda-VJMEM rev	GGG CGC GCC CTT TGG CTG CCC TCT GAT TTC CAG TTT GGT GCC	Generation of lambda light chain construct of anti-Vβ 5.3 dcCAR construct
Hu-lambdaC fwd	GGC ACC AAA CTG GAA ATC AGA GGG CAG CCA AAG GGC GCG	Generation of lambda light chain construct of anti-Vβ 5.3 dcCAR construct
Hu-lambdaC rev	CTA TGA ACA TTC TGT AGG GGC	Generation of lambda light chain construct of anti-Vβ 5.3 dcCAR

		construct
EcoRI-MMVH fwd	GAT GAA TTC ACC ACC ATG GCT CTG CCT GTC ACC	Generation of heavy chain-CAR construct of anti-Vβ 5.3 dcCAR construct
MMVH rev	CGA TGG GCC CTT GGT GGA GGC TGA GGA GAC GGT GAC TGA GGT	Generation of heavy chain-CAR construct of anti-Vβ 5.3 dcCAR construct
Hu IgG1-HC fwd	ACC TCA GTC ACC GTC TCC TCA GCC TCC ACC AAG GGC CCA TCG	Generation of heavy chain-CAR construct of anti-Vβ 5.3 dcCAR construct
Hu IG1-HC rev	AAA TTT GGG ATC CAA TTG TTT TTT ACC CGG AGA CAG GGA GAG	Generation of heavy chain-CAR construct of anti-Vβ 5.3 dcCAR construct
Hu CD28TM fwd	CTC TCC CTG TCT CCG GGT AAA AAA CAA TTG GAT CCC AAA TTT	Generation of heavy chain-CAR construct of anti-Vβ 5.3 dcCAR construct
Hu CD3zIC-NotI rev	ATC GCG GCC GCA TCA GGG GCC AGG TGT AGG GTT	Generation of heavy chain-CAR construct of anti-Vβ 5.3 dcCAR construct
Hu CD28TM modif fwd	CTC TCC CTG TCT CCG GGT AAA AAA CAA TTG GAT CCC AAA TTT TGG	Generation of heavy chain-CAR construct of anti-Vβ 5.3 dcCAR construct
Hu CD3zIC-NotI modif rev	ATC GCG GCC GCA TCA GGG GCC AGG TGT AGG	Generation of heavy chain-CAR construct of anti-Vβ 5.3 dcCAR construct
Nv (hPO) hu CD3z int NotI rev	ATC GCG GCC GCC TAG CGA GGG GGC AGG GCC TG	Generation of heavy chain-CAR construct of anti-Vβ 5.3 dcCAR construct
NV(hPB) hu CD3z intr NotI rev	ATC GCG GCC GCC TAT CGT GGA GGC AGA GCC TG	Generation of heavy chain-CAR construct of anti-Vβ 5.3 dcCAR construct

huDAP10-ITT- fwd_1	GAG TAA GAG GAG CAG GGA AGA TGG CAA AGt CTA CAT GAA CAT GAC TC	Exchange of CD28 ITT sequence with DAP10ITT (D-V amino acid substitution) in anti-Vβ 5.3 dcCAR construct
huDAP10-ITT- rev_1	GAG TCA TGT TCA TGT AGa CTT TGC CAT CTT CCC TGC TCC TCT TAC TC	Exchange of CD28 ITT sequence with DAP10ITT (D-V amino acid substitution) in anti-Vβ 5.3 dcCAR construct
huDAP10-ITT- fwd_3	AGC AAG CGG AGC AGA gaa gat CAC AGC GAC TAC ATG	Exchange of CD28 ITT sequence with DAP10ITT (LL-ED amino acid substitution) in anti-Vβ 5.3 dcCAR construct
huDAP10-ITT- rev_3	CAT GTA GTC GCT GTG atc ttc TCT GCT CCG CTT GCT	Exchange of CD28 ITT sequence with DAP10ITT (LL-ED amino acid substitution) in anti-Vβ 5.3 dcCAR construct
huDAP10-ITT-(G-K) fwd_4	GCG GAG CAG AGA AGA Tgg caa aGA CTA CAT GAA CAT G	Exchange of CD28 ITT sequence with DAP10ITT (HS-GK amino acid substitution) in anti-Vβ 5.3 dcCAR construct
huDAP10-ITT- (G-K) rev_4	CAT GTT CAT GTA GTC ttt gcc ATC TTC TCT GCT CCG C	Exchange of CD28 ITT sequence with DAP10ITT (HS-GK amino acid substitution) in anti-Vβ 5.3 dcCAR construct
huDAP10-ITT- (I-P) fwd_5	GAT GGC AAA GTC TAC ATc AAC ATG cCA CCT AGA CGG CCC GGA	Exchange of CD28 ITT sequence with DAP10ITT (MT-IP amino acid substitution) in anti-Vβ 5.3 dcCAR construct
huDAP10-ITT- (I-P) rev_5	TCC GGG CCG TCT AGG TGg CAT GTT gAT GTA GAC TTT GCC ATC	Exchange of CD28 ITT sequence with DAP10ITT (MT-IP amino acid substitution) in anti-Vβ 5.3 dcCAR construct

3.1.10 Reaction Systems and Kits

Ready-to-use kits were used according to the manufacturer's recommendations.

Table 11: Reaction systems and kits used in this study.

Name	Manufacturer	Application
Human Pan T cell Isolation Kit™	Miltenyi Biotec	Isolation of primary human T cells from peripheral blood
QIAprep® Spin Miniprep Kit	Qiagen	Plasmid DNA isolation
TA cloning Kit™	Invitrogen	Molecular Cloning
Wizard® SV Gel and PCR Clean-Up System	Promega	DNA purification

3.1.11 Synthetic DNA Constructs

Table 12: Synthetic DNA constructs and manufacturers.

Name	Manufacturer	Application
pEX-A128-MEM262VH+VL	Eurofins Genomics	Sequence of V (D) J regions encoding anti-human TCR Vβ 5.3 variable heavy and light chain regions (MEM 262 antibody)
pEX-A128-HPB-ALL TCRB chain	Eurofins Genomics	Sequence of VDJ regions encoding human TCR Vβ 5.3 receptor

3.1.12 Software

Table 13: Softwares used in this study.

Application	Name	Source
Flow cytometer data acquisition software	BD FACS Diva 8	BD Biosciences
Flow cytometer data analysis	FlowJo 7.5	Treestar
Sequence data analysis	Clone Manager	Sci-ed Central
Sequence raw data visualization	Finch TV	Geospiza
Text processing	Microsoft Word	Microsoft
Citation management software	Mendeley	Elsevier
Graphing and statistical analysis	Prism 7	GraphPad
Graphical tool	Biorender	Biorender.com

3.1.13 Universal Primer List

Primers for Sanger DNA sequencing were used according to the recommendations given by the sequencing company – Microsynth Seqlab GmbH.

Table 14: Universal primer list used for sequencing.

Name	Sequence 5' ->3'
M13 fwd	TGT AAA ACG ACG GCC AGT
M13 rev	CAG GAA ACA GCT ATG ACC
MSCV fwd	CCC TTG AAC CTC CTC GTT CGA CC
MSCV rev	CAG ACG TGC TAC TTC CAT TTG TC
pEX fwd	GGA GCA GAC AAG CCC GTC AGG
pEx rev	CAG GCT TTA CAC TTT ATG CTT CCG GC

3.1.14 Vector backbones

Table 15: Vector backbones used in this study.

Name	Source
pCR2.1	Invitrogen
pMSCV puro	Clontech
pMSCV puro II	this study
pEX-A128	Eurofins Genomics
pMIRFP	Lars König
pMIGRII	E. Vigorito

3.2 Methods

3.2.1 Molecular Biology

3.2.1.1 Bacteria

Chemically competent E. coli TOP10 F′ (Invitrogen, F'[lacI^{q} Tn10 (tet^{R})] mcrA Δ(mrr-hsdRMS-mcrBC) φ80lacZΔM15 ΔlacX74 deoR nupG recA1 araD139 Δ(ara-leu)7697 galU galK rpsL(Str^{R}) endA1 λ^{-}) were used for all transformations with plasmids.

3.2.1.2 Medium for bacterial cultivation

Bacterial growth medium used in all experiments was Lysogeny Broth (LB), containing 10 g/L Trypton, 5 g/L Yeast extract and 5 g/L NaCl at pH 7. The bacterial medium was autoclaved before use and supplemented with the respective antibiotics when required, either - 100 µg/ml Ampicillin or 50 µg/ml Kanamycin.

Solid bacterial growth medium was prepared by dissolving 2% agarose in LB medium, autoclaved, supplemented with the respective antibiotic after cooling down and casted on Petri dishes. Before use, the Petri dishes were stored at 4°C.

When required for blue-white colony screening in Lac operon inducible plasmids, agar plates were supplemented with 50 µl 0.1 M Isopropyl-β-D-thiogalactopyranosid (IPTG) and 50 µl of 5-bromo-4-chloro-3-indolyl-beta-D-galacto-pyranoside solution (XGal, 50 mg/ml in DMF).

3.2.1.3 Transformation of bacteria with plasmid DNA

50 µl aliquots of chemically competent *E.coli* TOP10F´ bacteria were incubated after thawing on ice for approximately 5 min. For transformation after DNA ligation 1-3 µl from the ligation mixture were pipetted to the bacterial suspension, gently vortexed and put back on ice for 5 min. Subsequently, a heat-shock was performed by incubating the *E.coli* TOP10`F cells for 1 min. at 42°C. After the incubation, the cells were put back on ice for 5 min. For regeneration of bacteria after the heat-shock, 100 µl of pre-warmed LB medium without antibiotic was added and the bacterial suspensions were kept on 37°C, 300 rpm for at least 15 min. before plating out on agar plates.

For inoculating bacterial suspensions, a single colony from the agar plate was picked and cultivated in 5 ml LB medium containing the respective antibiotic. Incubation of all bacterial cultures was performed overnight at 37°C, on a shaker with constant agitation at 220 rpm for a maximum of 16 h.

3.2.1.4 Isolation of plasmid DNA (Mini-Preparation)

Isolation of plasmid DNA was performed by harvesting the bacterial pellet from inoculated liquid cultures by centrifugation at 7,500x g at room temperature for 3 min. Plasmid isolation was performed with Qiaprep Spin Miniprep kit (Qiagen) according to the manufacturer's instructions.

3.2.1.5 DNA concentration measurement

DNA concentration was measured by NanoDrop 2000 instrument according to the manufacturer's instructions. The optical density at 260 nm wavelength was measured in 1 µl volume of the DNA samples.

3.2.1.6 Molecular cloning techniques

3.2.1.6.1 Restriction digestion of DNA samples

DNA samples of plasmids and PCR products were subjected to restriction digestion with endonuclease enzymes from New England Biolabs (NEB). The enzyme concentration was adjusted according to manufacturer's instructions (approximately 10 units per 1 µg DNA), reconstituted in the appropriate buffer providing 100% endonuclease activity. Incubations were performed at 37°C for 1 h or overnight when required. Digested DNA samples were assessed on agarose gel electrophoresis.

When a linearization of vector backbones with only one restriction enzyme was required, the linearized vector was additionally treated with 1 µl (5 units) of Calf Intestinal Alkaline

Phosphatase (CIP) for 30 min. This procedure is required in order to cleave 5' phosphate groups in the digested vector and to prevent backbone self-ligation during ligation reactions.

3.2.1.6.2 Agarose gel electrophoresis

Quality of isolated plasmids, PCR products, digested plasmids, as well as products of molecular cloning were assessed by using agarose gel electrophoresis. The products were mixed with 1x loading dye (Fermentas), separated on 1% or 1.5% agarose gels containing 0.1 µl/ml ethidium bromide, and run in a horizontal chamber containing 1x TAE running buffer. For DNA size estimation, 1 kb DNA Ladder (Fermentas) was run alongside at 120 V for 30 - 45 min.

3.2.1.6.3 DNA gel extraction

DNA fragments obtained by PCR amplification or restriction digestion were excised from agarose gels and purified using Wizard SV Gel and PCR Clean-up kit (Promega) according to the manufacturer's instructions. The final DNA elution step was performed in 35 µl nuclease-free water.

3.2.1.6.4 Ligation of DNA fragments

Ligation of DNA fragments was performed by preparing a reaction mixture, containing 1 µl linearized vector backbone 3 µl DNA insert, 1 µl T4 DNA ligase enzyme, 1x T4 DNA ligase buffer and brought to 10 µl total reaction volume with ddH_20. Incubation was performed at 22°C for 1 h followed by transformation into chemically competent *E.coli* TOP10F` cells.

3.2.1.6.5 Sub-cloning of blunt end PCR-amplified DNA

For cloning of PCR-amplified blunt-end DNA fragments into linearized pCR2.1 backbone was performed an additional reaction to add 3` adenine overhangs ('A-tailing'). 15.5 µl from gel-purified DNA fragments were incubated with 0.5 µl Taq Polymerase enzyme in a reaction containing 1x Taq Polymerase Buffer, and 1 µM dATPs. Incubation was performed at 72°C for 30 min. Subsequently, the DNA was purified with the Wizard SV Gel and PCR Clean-up kit (Promega) followed by elution with 35 µl nuclease-free water.

3.2.1.7 Polymerase Chain Reaction (PCR)

The Polymerase Chain Reaction is a technique used to generate multiple copies of nucleic acids by utilizing the process of DNA replication *in vitro*[128]. A PCR is divided into three essential steps: First, a double-stranded DNA template is subjected to denaturation allowing the formation of single-stranded DNA templates. Second, specific DNA fragments (Primers) which are complementary to the region of interest, specifically bind and hybridize to those regions, the so-called Annealing Step. Third, there is an elongation process, where the polymerase enzymatic machinery is assembled to the regions of interest, flanked by the primers, to generate a copy DNA (cDNA) of the desired region. Multiple repetition cycles of the described above essential steps leads to exponential amplification of double-stranded cDNA.

3.2.1.7.1 Standard PCR

In this study, all PCR reactions were performed by using Pfu DNA Polymerase (Promega), as it provides high fidelity of replication. A control sample containing all components of the Master Mix except Pfu DNA Polymerase was used in all PCR reactions.

For all reactions at least 400 ng DNA template was used in a Master Mix containing:

Table 16: Master Mix composition for standard PCR

	Components	**Volume**
1.	10x Pfu buffer	5 µl
2.	dNTPs mix (10 mM each)	1 µl
3.	10 µM Forward Primer	1 µl
4	10 µM Reverse Primer	1 µl
5.	Pfu Polymerase	0.6 µl
6	Template DNA (at least 400 ng)	Required volume based on the template DNA concentration
7.	ddH_20	Adjusted to 50 µl total reaction volume

PCR program:

1. Initial Denaturation: 95°C – 2 min.
2. Denaturation: 95°C – 30 sec.
3. Annealing – 55 - 66°C based on the calculated Tm of the primers – 30 sec } 32 cycles
4. Elongation: 72°C – 2 min. per kb
5. Final Elongation: 72°C –2 min.
6. Cool down: 4°C - ∞

The PCR-amplified products were then analyzed by agarose gel electrophoresis (see section **3.2.1.6.2 Agarose gel electrophoresis**)

3.2.1.7.2 Overlap extension PCR

Overlap extension PCR technique can be used to incorporate genetic constructs into plasmids without the need for endonuclease restriction digestion and subsequent ligation reaction[129]. The principle behind the technique lies in the design of primers that carry 5' overhangs, complementary to the desired joining sites of each plasmid molecule. When subjected to a PCR reaction, the primers extend the template DNA molecules with complementary regions from the other genetic constructs at the desired junction sites. The two amplified genetic constructs are subjected to a third PCR reaction where the extended complementary regions in each genetic construct hybridize together and the hybrid molecule is amplified by the forward and reverse primer complementary to the first and the second genetic construct, respectively (figure 3.1). The procedure can be repeated as many times as required based on the number of genetic elements that need to be incorporated in one plasmid molecule. At the end of the reaction, the samples are being subjected to DpnI enzymatic digestion. DpnI digests methylated DNA, produced as a result of post-transcriptional modifications in bacterial strains. Thus, the methylated template DNA molecules are being degraded and only the non-methylated fused plasmids will remain in the reaction mixture. The latter can be then subjected to bacterial transformation (See **3.2.1.3 Transformation of bacteria**).

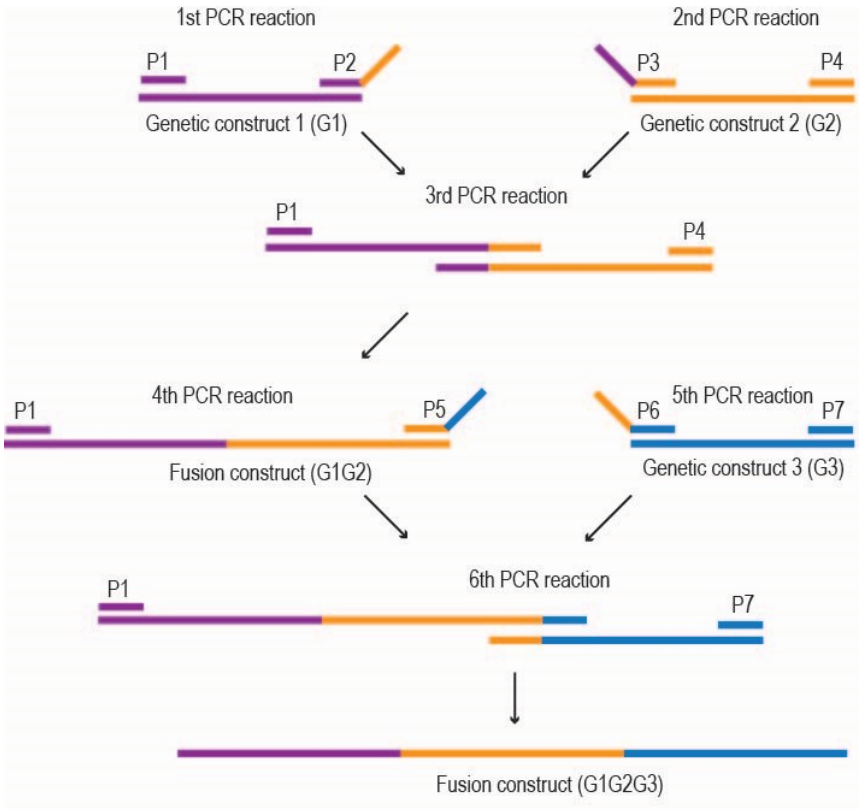

Figure 3.1: Schematic representation of the principle of overlap extension PCR assay. Primer sets are designed with 5' overhangs complementary to the ends of the desired joining sites of the genetic constructs to be fused (Primers P2, P3, P5 and P6). Two PCR reactions are performed to extend each DNA molecule with the respective complementary region from the other. Then the extended DNA molecules are being mixed and subjected to a third PCR reaction with primer set P1 and P4 to amplify the fused genetic construct (G1G2). If more genetic constructs need to be fused together, the reaction is repeated following the same principle to combine as many genetic constructs as required (i.e fusion construct containing 3 genetic constructs G1G2G3).

Overlap extension PCR technique was used to generate the genetic constructs encoding the anti-Vβ 5.3 kappa/lambda light chains and the anti-Vβ 5.3 heavy chain ectodomain of the 2nd generation dc CAR. In order to generate the anti-Vβ 5.3 kappa/lambda light chain constructs, several consecutive PCR reactions were performed. The reactions were performed to fuse kappa V1L leader peptide sequence to the genetic construct encoding anti-Vβ 5.3 variable light chain domain and a second round for the addition of the respective immunoglobulin constant domain (kappa or lambda).

The anti-Vβ 5.3 heavy chain ectodomain of the second generation dcCAR was generated by overlap extension PCR also in several consecutive rounds. The reactions were performed to fuse together human IgG1 spacer region (CH1-CH2-CH3) to the genetic construct encoding the anti-Vβ 5.3 variable heavy chain domain and the sequences encoding the intracellular CD3ζ and CD28 domains.

All overlap extension PCR reactions in this study were performed with Pfu DNA polymerase and according to the reaction conditions described below.

Table 17: Master Mix composition for overlap extension PCR

		1st PCR reaction	**2nd PCR reaction**	**3rd PCR reaction**
	Components	Volume	Volume	Volume
1.	10xPfu buffer	5 µl	5 µl	5 µl
2.	dNTPs mix	1 µl	1 µl	1 µl
3.	10 µM Forward Primer – Genetic construct 1	1 µl	-	1 µl
4	10 µM Reverse Primer - Genetic construct 1	1 µl	-	-
	10 µM Forward Primer- Genetic construct 2	-	1 µl	-
	10 µM Reverse Primer Genetic construct 2	-	1 µl	1 µl
5.	Pfu Polymerase	0.2 units	0.2 units	0.2 units
6	Template DNA (at least 400 ng)	Required volume based on the template DNA concentration	Required volume based on the template DNA concentration	Products from 1st and 2nd PCR reactions - Required volume based on the template DNA concentration
7.	ddH_20	Adjusted to 50 µl total reaction volume	Adjusted to 50 µl total reaction volume	Adjusted to 50 µl total reaction

PCR program

1. Initial Denaturation: 95°C – 2 min.
2. Denaturation: 95°C – 30 sec.
3. Annealing: 55 - 66°C based on the calculated Tm of the primers – 30 sec } 30 cycles
4. Elongation: 72°C – 2 min. per kb
5. Final Elongation: 72°C – 2 min.
6. Cool down: 4°C - ∞

The PCR amplified final products were then split into two samples: 15 µl were analyzed by Agarose Gel Electrophoresis (see section **3.2.1.6.2 Agarose gel electrophoresis**) and 25 µl were subjected to restriction digestion with 1 µl (20 units) Dpn1 in Cutsmart buffer (37°C for 1 h) for degradation of the methylated template DNA. Subsequently, they were transformed into *E.coli* TOP10F` cells (see section **3.2.1.3 Transformation of bacteria**).

3.2.1.7.3 Site-directed mutagenesis

Specific mutations within a plasmid were introduced by site-directed mutagenesis. The principle of this technique lies in the generation of primers that are complementary to the region of interest but also carry the desired nucleotide mismatch sequence. The PCR reaction mixture is then subjected to Dpn I digestion for degradation of the methylated template plasmid.

For site-directed mutagenesis, the following reaction was prepared:

Table 18: Master Mix composition for site-directed mutagenesis

	Components	**Volume**
1.	10xPfu buffer	5 µl
2.	dNTPs mix (10 mM each)	1 µl
3.	10 µM Forward Primer	1 µl
4	10 µM Reverse Primer	1 µl
5.	Pfu Polymerase	0.6 µl (0.2 units)
6	Template DNA (at least 400 ng)	Required volume based on the template DNA concentration
7.	ddH_20	Adjusted to 50 µl total reaction volume

PCR program:

1. Initial Denaturation: 95°C – 2 min.
2. Denaturation: 95°C – 30 sec.
3. Annealing: 55 - 60 °C – 60 sec.
4. Elongation: 72°C – 2 min. per kb
5. Final Elongation: 72°C –10 min.
6. Cool down: 4°C - ∞

} 30 cycles

The PCR-amplified final products were split into two samples: 15 µl were analyzed by agarose gel electrophoresis (see section **3.2.1.6.2 Agarose gel electrophoresis**) and 25 µl were subjected to restriction digestion with 1 µl (20 units) Dpn1 in Cutsmart buffer (37°C for 1 h) for degradation of the methylated template DNA. Subsequently, they were transformed into *E.coli* TOP10F` cells (see section **3.2.1.3 Transformation of bacteria**).

3.2.1.8 Sanger sequencing

All DNA sequencing reactions were performed by the company Microsynth Seqlab GmbH (Göttingen).

Sample reactions were prepared as follows:

1.2 µg DNA was filled up to 12 µl with ddH_20. Subsequently, 3 µl of the respective sequencing primers (10 µM stock) were added. Post-sequencing data analysis was performed by using Finch TV raw data analysis and Clone manager software for further analysis and annotations.

3.2.2 Cell biology

3.2.2.1 Cell culture medium

The medium used for cell culture of all eukaryotic cells was RPMI 1640 + GlutaMAX with addition of the following additives:

10% heat-inactivated FCS

1 mM sodium pyruvate

1% Penicillin/Streptomycin

1 mM L-glutamine

50 µM β-mercaptoethanol

3.2.2.2 Cell lines

Bw58-NF-AT

The murine thymoma cell line Bw58-NF-AT was used for expression of the CAR constructs. The cell line was kindly provided by Prof. Dr. Ludger Klein (Munich). Bw58-NF-AT cells are described to lack endogenous expression of functional TCR α/β[130]. Additionally, the cell line contains a cassette of enhanced green fluorescent protein (eGFP) that is under the control of NF-AT. Upon activation of the cell line, downstream signaling events lead to GFP expression in the cells.

Jurkat

The cell line Jurkat was kindly provided by Prof. Dr. Holger Reichard. It is a human T cell leukemic cell line derived from peripheral blood of a 14-year old boy with Acute T cell Leukemia[131].

PLAT-E

The cell line PLAT-E was derived from an adhesive 293T cell line. It contains genes from Moloney Murine Leukemia Virus (MMLV) and is equipped with an enhanced EF1a promoter for an efficient and high-yield retroviral protein expression of gag, pol and env genes, that are required for virus particle packaging[132]. To produce virus particles that are able to infect human T cell lines, PLAT-E cells were also transfected with Vesicular stomatitis virus glycoprotein (VSV-G) plasmid that encode surface glycoprotein structures required for retroviral particle tropism and highly efficient retroviral infection of human T cell lines[133].

Ramos
Ramos cells are a human Burkitt lymphoma-derived cell line. They express an mIgM-containing BCR and were used in this study as a positive control for cell surface expression of an immunoglobulin lambda light chain[134].

DG75
DG75 is a human mIgM-expressing B cell line that was used in this study as a positive control for surface expression of immunoglobulin kappa light chain. The cell line was established in 1975 from a 10-years old patient with a primary abdominal lymphoma[135].

MEM 262 hybridoma cell line
The MEM262 hybridoma cell line was kindly provided by Prof. Dr. Horejsi (Prague). The cell line secretes an anti-human TCR Vβ 5.3 monoclonal antibody, which specifically recognizes the Vβ 5.3 TCR chain of a HPB-TALL cell line [136].

3.2.2.3 Cell counting
10 µl cell suspension was mixed with 10 µl 0.4% Trypan Blue in PBS for exclusion of dead cells and subjected to counting in a Neubauer chamber.

3.2.2.4 Cell culture
All cell lines were cultured in R10 medium under optimal growth conditions – humidified atmosphere, 37°C and a constant supply of 5% CO_2. All cell lines were maintained in culture for no longer than 2 months after thawing.

The cell lines Bw58–NF-AT were passaged in a ratio of 1:5 every second day. For functional assays they were split in a ratio of 1:1 the day prior to the experiment (unless otherwise indicated for specific assays) (see **3.2.4.1 Ca^{2+} mobilization assay**).

The cell lines Jurkat were passaged in a ratio of 1:4 every second day of culture.

Primary human T cells isolated from PBMCs were cultured in R10 medium for no more than 1 day prior to use in functional assays.

The adherent PLAT-E cells used for retroviral transfection were passaged by removing the supernatant, washing once with 5 ml PBS (sterile) and incubation with 0.8 µl Trypsin-EDTA at 37°C for 4 min. Then 6 ml fresh R10 medium was added to block the effect of Trypsin-EDTA and cells were split in a ratio of 1:6 to reach confluence of 60-70% at the day of transfection. For long-term cell culture, cells were treated as indicated above and split in a ratio of 1:10 every third day to maintain an exponential phase of growth.

3.2.2.5 Freezing of mammalian cell cultures
Approximately $2x10^6$ cells were harvested for each cryo-vial. Cells were centrifuged at 300x g for 5 min. at room temperature. Supernatants were discarded and the cell pellets were resuspended in sterile heat-inactivated Fetal Calf Serum (FCS) containing 10% DMSO. Then 1 ml cell suspension was aliquoted into cryo-vials and kept on ice before transfer to -80°C freezer for short-term storage. For long-term storage cells were transferred and kept in a -150°C freezer.

3.2.2.6 Thawing of mammalian cell cultures

Cryo-vials were kept on ice before thawing in a water bath at 37°C. The cell suspension was rapidly transferred to 9 ml R10 medium and spun down at 300x g for 5 min at RT. The supernatant was discarded, cells were reconstituted in 10 ml fresh R10 medium and seeded onto a 10 cm dish. All cell lines were cultured under optimal conditions at least 3-5 days post-thawing before they were used in experiments.

3.2.2.7 Isolation of human PBMCs from peripheral blood

Peripheral blood from healthy donors was obtained from the Department of Transfusion Medicine of the UMG. Blood samples were diluted in sterile ice-cold PBS supplemented with 2 mM EDTA (PBS/EDTA).

BD Leukocept 50 ml Falcon tubes with 15ml sterile Ficoll were spun down at 300x g for 5 min at room temperature. Approximately 50 ml diluted peripheral blood was added and centrifuged at 800x g (with slow acceleration and without rotor brake) at 20°C for 20 min. The PBMC layer was collected, diluted with 50 ml sterile ice-cold PBS/EDTA and washed 4-5 times (400x g for 10 min at room temperature) to obtain a thrombocyte-free fraction of PBMCs. After the last washing step the PBMC suspension was reconstituted in approximately 10 ml sterile ice-cold PBS/EDTA and the total cell number was determined by counting.

3.2.2.8 Magnetic isolation of human primary T cells from PBMCs

Isolation was performed with the human Pan T cell Isolation Kit from Miltenyi Biotec. Separation was performed manually. Approximately 4 x 10^7 PBMCs were spun down (300x g, 5 min, RT) and reconstituted with 40 µl per 10^7 cells sterile ice-cold PBS/EDTA. Subsequently, the cell suspension was incubated for 5 min at 4°C with 10 µl per 1 x 10^7 cell Pan T cell cocktail. After incubation, 30 µl sterile ice-cold PBS/EDTA per 10^7 cells was added to the cell suspension and the sample was then incubated with 20 µl of Pan T cell Microbead Coctail per 10^7 cells for 5 min at 4°C. Total volume was brought to 500 µl with sterile ice-cold PBS/EDTA if necessary. The cell suspension was ran through a wetted LS-column, installed on a magnet stand. The fraction of human primary pan T cells was collected and the total cell count was determined. The purity of the separation was evaluated by surface staining with a FITC-conjugated anti-human CD3 monoclonal antibody (see section **3.2.3.1 Analysis of cell surface molecules**) and subsequent FACS analysis. The percentage of TCR Vβ 5.3-positive cells was assessed by surface staining with anti-human TCR Vβ 5 (MEM262) FITC-conjugated monoclonal antibody and FACS analysis.

3.2.2.9 Retroviral transduction of mammalian cell lines

Retroviral transfection was performed by using ecotropic PLAT-E packaging cell line, cultured in 60-70% confluence before transfection with the respective genetic constructs. On the day of transfection, the following reaction mixture was prepared and incubated for 15 min. at RT:

16 µl TransIT (Mirus)

500 µl R0 medium

1 µg of VSV-G plasmid

After incubation, approximately 6 µg DNA of the respective genetic construct was added to the reaction mixture, followed by vigorous resuspension and incubation for 25 min at RT. In the meanwhile, R10 from cultured PLAT-E cells was carefully removed without detaching the cells from the bottom of the dish and it was added 5 ml fresh pre-warmed R10. At the end of the incubation time, the transfection mixture was applied drop wise onto the PLAT-E cells, followed by gentle mixing to allow even distribution. Transfected PLAT-E cells were cultured and handled under biosafety level 2 (BSL-2) conditions at humidified atmosphere, 37°C and constant flow of 5% CO_2. At the day after transfection, 3 ml pre-warmed R10 medium was added to the cells.

Retroviral Transduction of the target mammalian cell lines was performed on day 3 after transfection of the PLAT-E cells with the respective genetic construct. Approximately 3 x 10^6 cells from the target cell lines were harvested and reconstituted in 2.5 ml pre-warmed R10, containing 3 mg/ml Polybrene. 8 ml of the PLAT-E medium containing virus particles was collected and centrifuged at 300x g, 5 min at RT. 7.5 ml of the latter was then collected and applied to the target cell suspension. Subsequently, the cells were transferred to a 10 cm culture dish and incubated under optimal growth conditions. One day after the transduction, the cells were washed once with 10 ml R10. Subsequently, the cells were cultured for about 1-2 days before estimation of the transduction efficiency by FACS analysis. After transfection, in some cases the eGFP reporter function upon activation of Bw58 cell line was impaired. To overcome this limitation, cells were stimulated with suboptimal concentration of PMA/Ionomycin cocktail (5 ng/ml PMA and 1 µM Ionomycin) for 24 h. Subsequently, cells expressing the highest amount of GFP (~10% of the cells) were subjected to FACS sorting and were used in further experiments.

3.2.3 Flow cytometry

3.2.3.1 Analysis of cell surface molecules

All surface stainings with monoclonal antibodies, unless specifically indicated elsewhere, were performed on ice with 15-20 min incubation time, followed by washing with 2 ml ice-cold PBS and reconstitution in 300 µl ice-cold PBS prior to the FACS measurement.

The analysis of CD4 and CD8 expression in Bw58-NF-AT cells was performed by staining with PE-Cy7-conjugated anti-mouse CD8 (BD Biosciences, 53-6, dilution 1:200) or FITC-conjugated anti-mouse CD4 (BioLegend, GK1.5, dilution 1:100) monoclonal antibodies.

To evaluate the surface expression of dcCAR molecules on the plasma membrane of Bw58-NF-AT cells, approximately 1 x 10^6 cells were harvested and washed once with ice-cold PBS. Subsequently, the cells were stained with a polyclonal AF647-conjugated anti-human IgG antibody (Southern Biotech, polyclonal, dilution 1:5.000) in 100 µl PBS.

Surface expression analysis of kappa or lambda light chains from dcCARs in Bw58-NF-AT cells was performed by addition of FITC-conjugated anti-human kappa light chain or FITC-conjugated anti-human lambda light chain monoclonal antibodies (ImmunoTools, A8B5 and 4C2, dilution 1:40), respectively.

Evaluation of TCR Vβ 5.3 surface expression on transfected Jurkat T cell line was performed by staining with a FITC-conjugated anti-human TCR Vβ 5 monoclonal antibody (Biolegend, MEM-262, dilution 1:40).

Assessment of the purity of the isolated human primary T cells was performed by staining 1 x 10^6 cells with a FITC-conjugated anti-human CD3 monoclonal antibody (BioLegend, UCHT1, dilution 1:80) in 100 µl ice-cold PBS for 15 minutes on ice. Evaluation of the percentage of TCR Vβ 5.3^+ T cells was performed by staining with FITC-conjugated TCR Vβ 5 monoclonal antibody (Biolegend, MEM-262, dilution 1:40). The percentage of TCR Vβ 8^+ T cells was performed by staining with eFluor 450-conjugated TCR Vβ 8 monoclonal antibody (Invitrogen, JR-2, dilution 1:100)

3.2.3.2 Cell sorting

Cell sorting was performed in cooperation with the FACS sorting facility of the University Medical Center Göttingen. Approximately 5-10 x 10^6 cells were harvested and washed once with 5 ml ice-cold PBS (300x g, 5 min, RT). In case surface staining with monoclonal antibodies was required, the procedure was kept as described above. After the final washing step, the cell pellet was reconstituted in 1 ml PBS and sorted into tubes pre-filled with 5 ml R10 medium.

3.2.4 Functional assays

3.2.4.1 Ca^{2+} mobilization assay

Changes in intracellular Ca^{2+} levels can be detected via flow cytometry by using the Ca^{2+} sensitive ratiometric dye Indo-1[137]. The ester form of Indo-1, Indo-1 AM, can diffuse passively through the cell membrane of the treated cells. When the ester enters cells, it is cleaved by esterases and serves as a fluorescent indicator that binds to Ca^{2+} present within the cell. When excited by a UV (355nm) laser, the cells in resting state emit fluorescence at about ~475 nm. Stimulation of the cells with antibodies that cross-link surface receptors leads to triggering of intracellular signaling events, Ca^{2+} influx and shift of the Indo-1 excitation maximum to ~400 nm. In this work, the assay was utilized to measure the signaling potential of different CARs. To this end, anti-human IgG $(Fab')_2$ was used to cross-link the dcCARs on the membrane of Bw58-NF-AT cells. The concentrations used for stimulation was 20 µg/ml, unless otherwise specified.

The day before the experiment, the respective Bw58-NF-AT cells were seeded at a density of 1.5 x 10^6 cells per sample to avoid overstimulation. On the next day, approximately 2-3 x 10^6 cells were harvested and reconstituted in 500 µl of R10 medium. A master mix containing 200 µl R10, 2 µl 5% Pluronic F127 acid and 0.7 µl Indo1-AM per sample (1 µM Indo1-AM and 0.015% Pluronic Acid per reaction) was added. Subsequently, incubation of the cell samples was performed at 30°C under mild agitation (600 rpm) for 40 min. After incubation, the cells were washed twice with 1 ml Krebs-Ringer buffer (K-R buffer) solution containing 1 mM $CaCl_2$ and reconstituted in 1 ml K-R buffer. Prior to the FACS measurement, cells were rested at 30°C, 300 rpm for 15 min. A 24 sec baseline level was recorded prior to stimulation with the antibody and the measurement was terminated after 5 min.

3.2.4.2 Cytotoxic cellular assays with Bw58 cells

Co-culture experiments were performed in various ratios of effector (Bw58 anti-Vβ 5.3 lambda/kappa dc CAR T cells) and target cells (TCR Vβ 5.3^+ Jurkat cells). – 1:1, 1:2, 1:3, 2:1, 2:3 (E:T). Cells were incubated in 24-well plates with 2.5 ml R10 medium. A minimum of 0.5 x 10^6 cell density (which corresponds to ratio factor 1) was used for both effector and target cells. Samples were collected at time points 0, 24, 48 h, washed once with ice-cold PBS and stained with monoclonal antibodies prior to FACS analysis. To determine the percentage of Jurkat target cells, the collected samples were stained with a BV421-conjugated anti-human CD38 monoclonal antibody (BioLegend, HB-7, dilution 1:200) in 100 µl PBS for 15 min on ice. Bw58 CAR T cells were identified by RFP fluorescence.

CAR-expressing Bw58 cells were stimulated with a cocktail of PMA (20 ng/ml) and Ionomycin (1µM) as a positive control for maximum GFP expression. To determine the antigen-specific interaction between Bw58 dcCAR T cells and TCR Vβ 5.3^+ Jurkat cells, the CAR-expressing T cells were cultured with Jurkat cells as a specificity control. Additionally, TCR Vβ 5.3^+ Jurkat cells were cultured with Bw58 cells, which do not express the CAR as additional specificity control.

Co-culture experiments in the presence of GolgiStop reagent (Monensin) were performed under the same conditions. The optimal concentration of the reagent was calculated based on the manufacturer's recommendations. Shortly, 1.7 µl of inhibitor was added per 2.5 ml R10 (~1 x 10^6 cells) in co-culture. Time points of collecting samples were in this case 0, 6, 12, and 24 h, followed by FACS measurement to determine the percentage of live cells within each population.

3.2.4.3 Apoptosis Assay

Apoptosis assays were performed to assess the cytotoxic activity of CAR-expressing Bw58 cells in co-cultures with Jurkat cells. Apoptosis was assessed by staining with APC-conjugated Annexin V, which binds to phosphatidylserine (PS) during the early and late stages of apoptosis. 7-AAD dye was used as a marker for late stage apoptosis, which diffuses through the cell membrane and intercalates with DNA.

The cytotoxicity assay was set up as described above (see **3.2.4.2 Cytotoxic cellular assays**). Samples were collected at 0, 24, and 48 h time points. Subsequently, the cell samples were washed once with ice-cold PBS and reconstituted in 100 µl Annexin V binding buffer. The following reagents were added:

anti-human CD38-BV421 (BioLegend, HB-7, dilution 1:200)

Annexin V APC (BioLegend, dilution 1:200)

7-AAD (BD Biosciences, dilution 1:30)

Incubation was performed at RT for 15 min, followed by washing once with 500 µl Annexin V binding buffer. After washing, cells were reconstituted in 300 µl Annexin V binding buffer and subjected to FACS measurement.

3.2.4.4 Blocking of Fas-Ligand

To evaluate whether the killing mechanism of the effector anti-Vβ 5.3 lambda dcCAR Bw58 cells is mediated by Fas/FasL interaction, I used a purified anti-mouse FasL monoclonal antibody (BioLegend, clone MFL3) for blocking. 5 x 10^5 anti-Vβ 5.3 lambda dcCAR Bw58 cells were pre-incubated with 20 µg/ml MFL3 antibody in 100 µl PBS for 15 min at 37°C. Subsequently, the cell samples were mixed with TCR Vβ 5.3^+ Jurkat cells (1:1 ratio) in 2.5 ml R10 medium. The cells were incubated for 24 h and 48 h at 37°C, 5% CO_2. Samples were collected at time points 0 h, 24 h and 48 h, followed by staining with a master mix with the following composition and subjected to FACS analysis:

anti-human CD38-BV421 (BioLegend, HB-7, dilution 1:200)

Annexin V-APC (BioLegend, dilution 1:200)

7-AAD (BD Biosciences, dilution 1:30)

3.2.4.5 Co-culture experiments with primary human T cells

After isolation of pure fraction of primary human pan T cells, they were counted and subjected to FACS measurement for evaluation of the percentage of TCR Vβ 5.3^+ T cells. The co-culture ratio between Bw58 anti-Vβ 5.3 lambda dcCAR T cells (Effector cells) and primary human TCR Vβ 5.3^+ T cells (Target cells) in total human pan T cells population was approximately 7:1 (E:T). It was calculated as per approximately 3% (around $4.5x10^4$ TCR Vβ 5.3^+ T cells) of primary human TCR Vβ 5.3^+ T cells in a pool of 1.5 x 10^6 pan T cells per sample, co-cultured with 3 x 10^5 effector cells. As a positive control was used 3% TCR Vβ 5.3^+ Jurkat cells in a pool of 1.5 x 10^6 Jurkat cells co-cultured with the same cell density of effector Bw58 dc CAR T cells. As a specificity control in the co-culture experiment were used Bw58 lambda LC cells co-cultured with primary human pan T cells. The co-cultured cells were incubated in 2.5 ml R10 medium for 24 h and 48 h (37°C, 5% CO2). Samples for FACS analysis were taken at 0h (prior to addition of effector cells and after the addition of effector cells), 24 h and 48 h. Samples were washed once with ice-cold PBS, stained in 100 µl total PBS and incubated on ice for 15 min with the following antibodies:

anti-human TCR Vβ 5 FITC (BioLegend, MEM-262, dilution1:40)

anti-human CD2 APC (BioLegend, RPA-2.10, dilution 1:200)

anti-human TCR Vβ 8 eFluor 450 (Invitrogen, JR-2, dilution 1:200)

Then cell samples were washed once with 2 ml PBS, the cell pellets were dissolved in 300 µl PBS and subjected to flow cytometry.

4. Results

4.1 Generation of a conventional anti-Vβ 5.3 CAR

To adapt the CAR T platform for selective elimination of individual T cell subpopulations, I explored the possibility to redirect CAR T cells against the TCR Vβ chain. There are several monoclonal antibodies reported to specifically recognize TCR Vβ families[36]. One of those, the murine monoclonal antibody MEM262, recognizes the human TCR Vβ 5.3 domain[136]. The variable regions of the IgH and IgL chains of MEM262 were used to engineer a second generation scCAR to specifically target TCR Vβ 5.3^{+} T cells. The DNA sequences encoding the variable domains of MEM262 were previously PCR-amplified in our group from genomic DNA of the MEM262 hybridoma. They were additionally verified by mRNA sequencing by the company Absolute Antibody, which furthermore confirmed that the hybridoma cells are monospecific (i.e. they produce only one set of IgH and IgL chains).

Subsequently, a chemically synthesized scFv sequence was ligated in-frame into a cloning vector encoding a second generation scCAR backbone. This backbone consists of a CD8-derived spacer region, the transmembrane region of CD8a, and the intracellular domains of CD28 and CD3ζ. The scCAR open reading frame is followed by an internal ribosomal entry site (IRES) for bi-cistronic expression of a truncated variant of the human nerve growth factor receptor (tNGFR). Thus, the expression of tNGFR can serve as a surrogate marker for successful transfection. The entire construct was ligated into the retroviral expression vector pMSCVpuro II, followed by transduction of Bw58-NF-AT-eGFP cells (hereafter referred to as Bw58 cells). Bw58 is a murine thymoma cell line that lacks the expression of a functional TCR[130]. The cell line is further modified by stable integration of an eGFP cDNA that is under the control of a nuclear factor of activated T cells (NF-AT)-responsive promotor. Thus, activation of NF-AT in these cells results in the expression of eGFP, which can be monitored by e.g. flow cytometry. Figure 4.1 shows the principle of action of Bw58 cells expressing the scCAR upon the cognate antigen encounter.

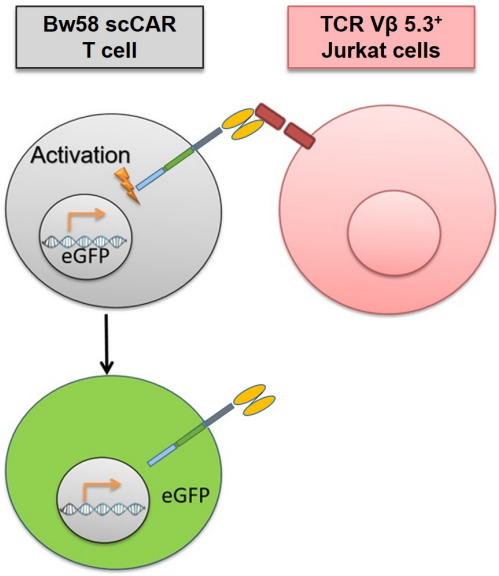

Figure 4.1 Principle of action of Bw58 anti-Vβ 5.3 scCAR T cells. Schematic representation of the principle of action of Bw58 cells transfected with genetic constructs encoding the anti-Vβ 5.3 scCAR (shown in grey). The Bw58 cells used here contain eGFP cassette that is under the control of a nuclear factor of activated T cells (NF-AT)-responsive promotor. When the CAR-expressing Bw58 cells recognize their cognate antigen-expressing cells (shown in red), they activate NF-AT, which leads to the expression of eGFP (shown in green) and can be monitored by FACS analysis.

To assess the transfection efficiency of Bw58 cells with the scCAR vector, the expression of tNGFR was analyzed by flow cytometry using an anti-NGFR antibody. Next, tNGFR-positive cells were sorted, expanded, and re-analyzed (Figure 4.2 A), showing that this strategy principally resulted in successful transfection and stable transgene expression. Unfortunately, the scCAR could not be stained directly on the surface of Bw58 cells, since there was no suitable epitope present in the extracellular domain. Thus, I had to use an indirect assay to test for the presence and functionality of the anti-Vβ 5.3 scCAR in Bw58 cells. Since the cells contain an NF-AT-eGFP reporter cassette, I analyzed the inducible expression of GFP in the scCAR-transfected cells. To this end, I first established a cellular ‘antigen’ for the scCAR-expressing Bw58 cells by expressing a Vβ 5.3-containing TCR β chain in the human T cell line Jurkat (Figure 4.2 B).

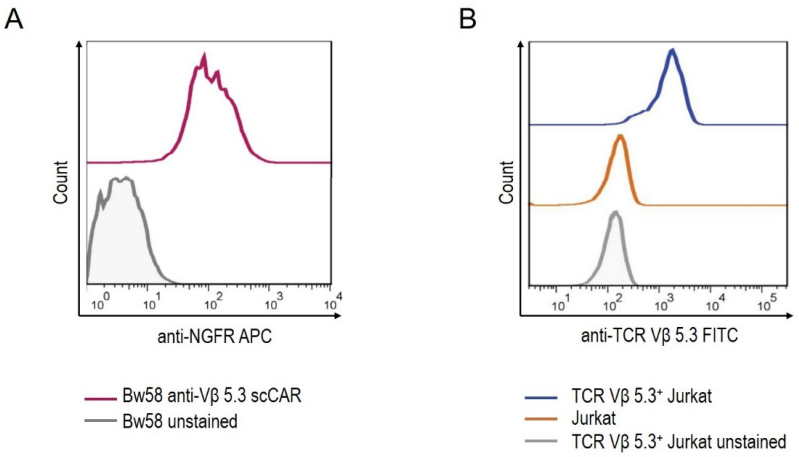

Figure 4.2 Cell surface expression of the anti-Vβ 5.3-specific scCAR in Bw58 cells and the Vβ 5.3-containing TCR in Jurkat cells. (A) Bw58 cells were transfected with the anti-Vβ 5.3 scCAR-encoding vector and sorted based on surface expression of tNGFR. Unstained Bw58 cells served as a negative control. **(B)** FACS analysis of TCR Vβ 5.3 expression by Jurkat cells. Cells were stained with a FITC-conjugated anti-human TCR Vβ 5 antibody (MEM262). The unstained TCR Vβ 5.3$^+$ Jurkat cells and Jurkat cells served as controls.

Next, to assess the functionality of the anti-Vβ 5.3-reactive scCAR, I tested for the induction of GFP in the Bw58 scCAR T cells. In this assay, I co-cultured the TCR Vβ 5.3$^+$ Jurkat cells (the 'antigen') with the Bw58 scCAR T cells and analyzed the induction of GFP expression after 8 and 48 h (Figure 4.3). Unfortunately, there was hardly any GFP signal detectable in the Bw58 scCAR T cells neither after 8 nor after 48 h (Figure 4.3 A and B), whereas stimulation of the Bw58 scCAR T cells with PMA/ionomycin gave rise to strong expression of GFP in roughly one-third of the cells (Figure 4.3 C). Moreover, the percentage of viable TCR Vβ 5.3$^+$ Jurkat cells (anti-NGFR$^-$) remained in a similar range in co-culture with Bw58 scCAR T cells (Figure 4.3 A and B).

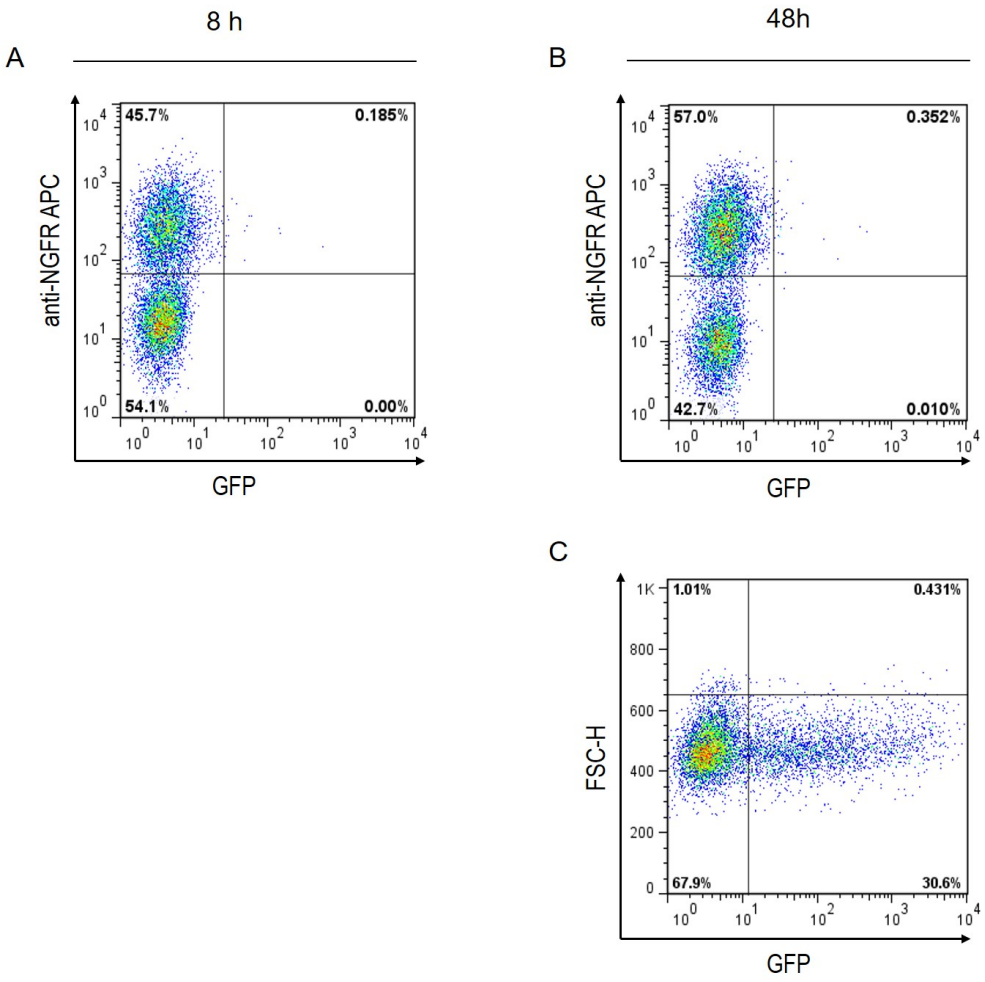

Figure 4.3 The anti-Vβ 5.3 scCAR does not induce GFP expression in Bw58 cells. (A, B) FACS analysis of a co-culture between Vβ 5.3-specific Bw58 scCAR T cells and TCR Vβ 5.3$^+$ Jurkat cells. Cells were co-cultured in a 1:1 ratio for 8 **(A)** and 48 **(B)** hours. Subsequently, the cells were stained with an APC-conjugated anti-NGFR antibody (Y-axes) to distinguish the Bw58 scCAR T cells (NGFR$^+$) from the Jurkat target cells (NGFR$^-$). GFP-expressing cells are shown on the X-axes. **(C)** Unstained anti-Vβ 5.3 scCAR Bw58 cells were stimulated with PMA/ionomycin and the activated, GFP-expressing cells were measured after 48h.

In conclusion, neither could the expression of the scFv-based scCAR in Bw58 cells be satisfactorily tested, nor could its functionality be shown in a cellular assay. Thus, to circumvent these problems, I decided to pursue an alternative strategy. Instead of using a scCAR, I generated a dcCAR with the same specificity as outlined below.

4.2 Generation of an anti-Vβ 5.3 CAR in an alternative dual chain format

The lack of antigen-specific activation and cytotoxicity against TCR Vβ 5.3^{+} Jurkat cells, when co-cultured with Bw58 scCAR cells raised the question of whether the conventional scFV design is the only possible approach to be applied in the generation of the CAR. Moreover, the lack of a suitable extracellular epitope for direct detection of the scCAR expression, respectively to monitor the CAR-mediated signaling potential, were limiting factors in the assessment of the anti-Vβ 5.3 scCAR functionality. To circumvent these limitations, I generated an anti-Vβ 5.3 CAR in an alternative dual chain format. In the dcCAR design, the anti-Vβ 5.3 – specific VH and VL were expressed as a complete IgG antibody, anchored by the transmembrane domain and coupled to the T cell intracellular signaling domains of CD3ζ and CD28.

To express the anti-Vβ 5.3 dcCAR, I generated genetic constructs, encoding the anti-Vβ 5.3 IgG heavy and light chain, respectively. To this end, the sequences encoding the anti-Vβ 5.3 kappa or lambda light chain were generated by overlap extension PCR. Next, they were ligated into retroviral expression vector MIRFP, followed by retroviral transduction of Bw58 cells. In the MIRFP backbone, the open reading frame of anti-Vβ 5.3 kappa/lambda LC-encoding sequence is followed by the IRES site for bi-cistronic expression of red fluorescent protein (RFP) (Figure 4.4 A). Hence, the transfection efficiency of Bw58 cells with the anti-Vβ 5.3 light chain genetic constructs could be assessed by FACS analysis of the RFP fluorescent emission. Next, the transduced Bw58 anti-Vβ 5.3 kappa/lambda LC cells were sorted, expanded, and re-analyzed (Figure 4.4 B).

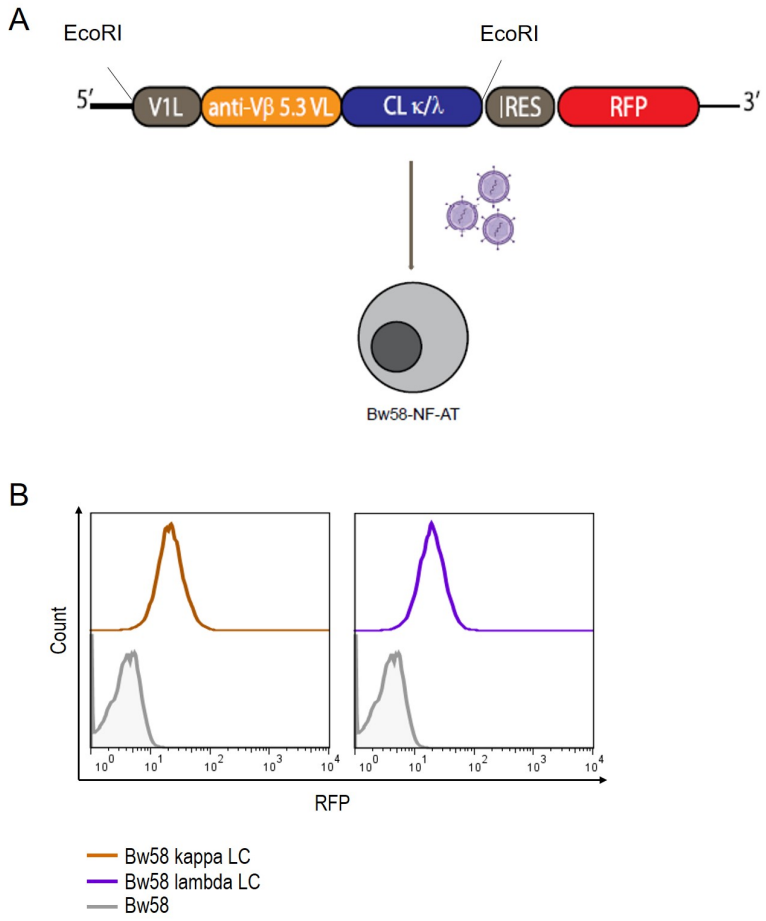

Figure 4.4 Transfection of Bw58 cells with anti-Vβ 5.3 light chain-encoding vectors. (A) Schematic representation of the sequence encoding the anti-Vβ 5.3 kappa/lambda light chain. The VL sequence from MEM262, preceded by a VL1 leader sequence, was fused to the constant domains of either human kappa or lambda light chain and subsequently cloned into the expression vector MIRFP via EcoRI restriction sites. The vector backbone contains an IRES that allows co-expression of a red fluorescent protein (RFP). The respective plasmids were then delivered into the Bw58 cell line via retroviral transfection. **(B)** FACS analysis of Bw58 cells expressing either anti-Vβ 5.3 kappa (orange) or anti-Vβ 5.3 lambda light chains (violet). The parental Bw58 cell line is represented as a negative control.

The genetic construct encoding the MEM262-derived anti-Vβ 5.3 heavy chain was generated in a similar way by fusing individual sequences to create a second generation CAR construct. First, the VH sequence was fused to sequences encoding three human γ1 heavy chain constant domains (CH1-CH2-CH3). These domains represent the spacer region of the dcCAR and at the same time serve as an epitope for its detection. Next, the complete fragment was fused to sequences encoding the CD28 TM domain and the cytoplasmic domains of CD28 and CD3ζ (Figure 4.5 A).

The respective anti-Vβ 5.3 heavy chain sequence was cloned into the expression vector pMSCVpuro II, which I generated from pMSCVpuro by introducing an additional NotI cloning site. Next, the plasmid was delivered to Bw58 cells, transfected with either kappa or lambda light chain constructs, by a second round of retroviral transfection. This strategy allows for the pairing of the heavy and light chain and subsequent surface expression of the assembled anti-Vβ 5.3 dcCAR.

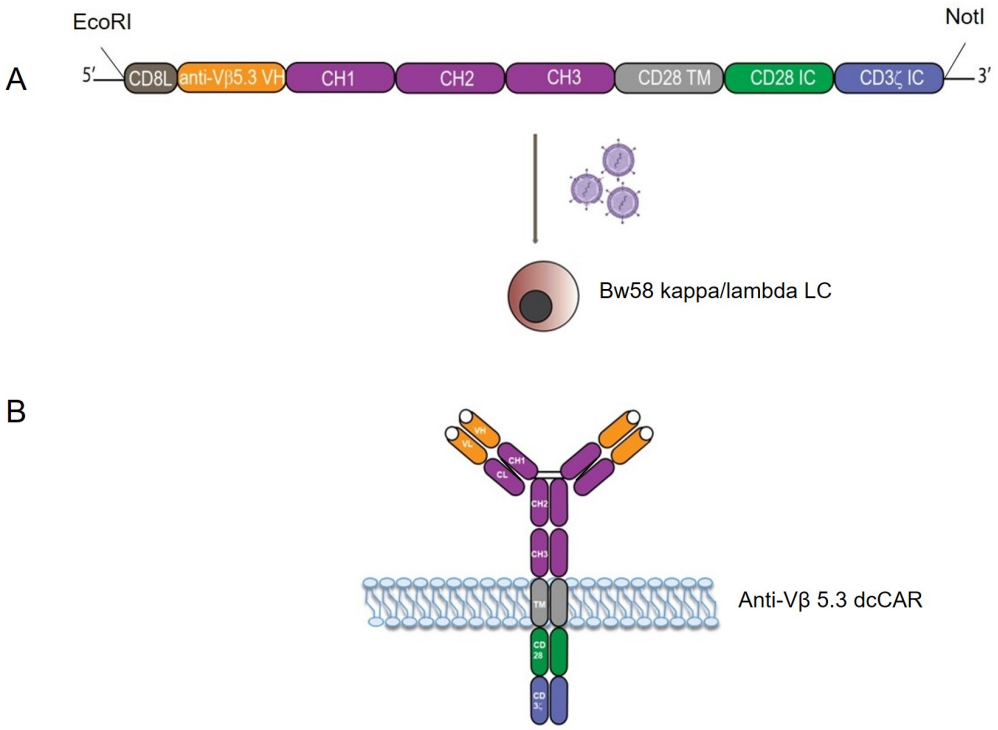

Figure 4.5 Generation of Bw58 cells expressing an anti-Vβ 5.3 dcCAR. **(A)** Schematic representation of the gene sequence encoding the anti-Vβ 5.3 heavy chain construct in the dual chain format. The VH sequence from MEM262, preceded by a CD8 leader sequence, was fused via overlap extension PCR to human IgG1 heavy chain constant domains (CH1-CH2-CH3) and human CD28 transmembrane domain. In additional PCR reaction, the construct was fused to human CD3ζ and CD28-encoding genetic sequences. The amplified genetic construct was cloned into pMSCV puro II expression vector via EcoRI and NotI restriction sites. The respective plasmid was then delivered into previously sorted Bw58 kappa or lambda LC transfected cells. **(B)** The delivery of the heavy chain-CAR construct allows paring of the heavy and light chain and surface expression of the anti-Vβ 5.3 kappa or lambda dcCAR, respectively.

To assess the transfection efficiency of the anti-Vβ 5.3 dcCAR 'heavy chain', the Bw58 cells were analyzed by staining with polyclonal IgG antibody and FACS (Figure 4.6 A and B). To evaluate the light chain surface expression, I stained the Bw58 cells with FITC-conjugated antibodies recognizing either the kappa or the lambda light chain (Figure 4.6 C and D). As positive controls, I used human cell lines expressing IgM with either kappa (DG75) or lambda (Ramos) light chains, respectively.

The analysis of the surface expression of both kappa and lambda light chains in Bw58 cells showed that they were expressed on the cell surface, most likely as a part of the anti-Vβ 5.3 dcCAR. I observed a slightly higher expression level of the lambda chain-containing dcCAR in comparison to the kappa dcCAR. However, both dcCARs were expressed on the surface of the Bw58 cells, which showed that this strategy resulted in a stable transgene expression.

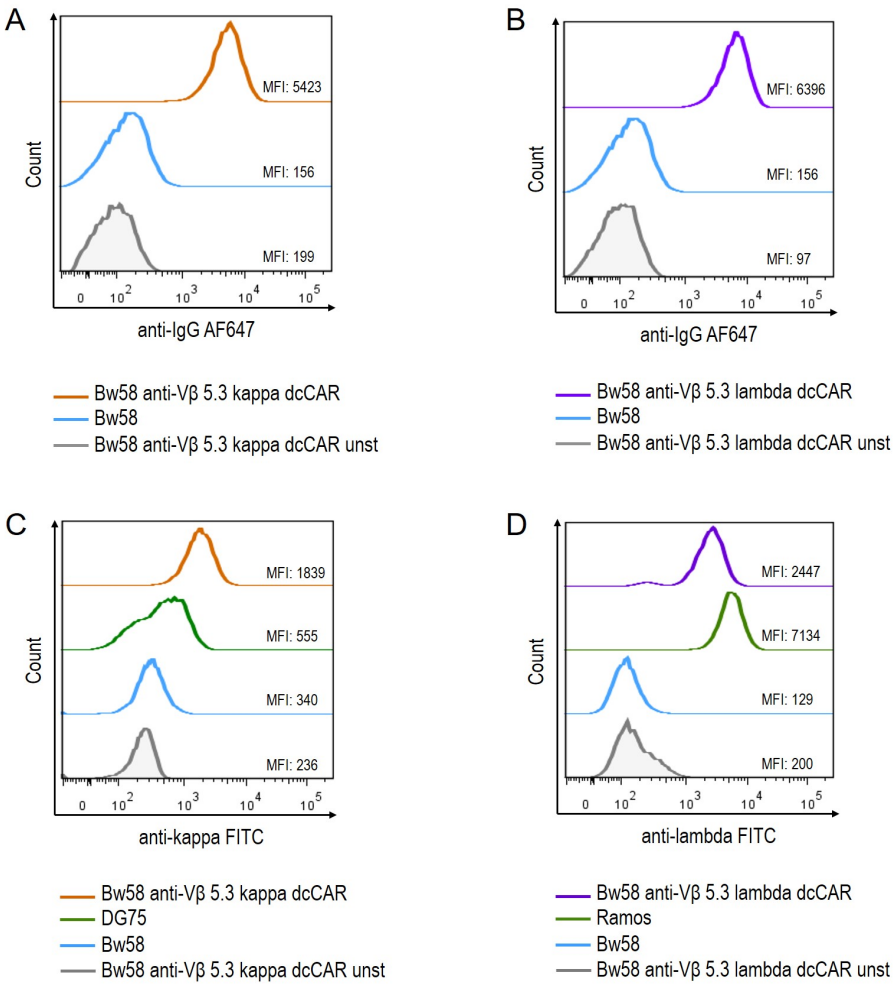

Figure 4.6 Anti-Vβ 5.3 kappa/lambda dcCAR expression on the surface of Bw58 cells. To detect the heavy chain of the anti-Vβ 5.3 kappa/lambda dcCAR, cells were stained with AF647-conjugated anti-human IgG polyclonal antibody and analyzed by flow cytometry (**A** and **B**). Surface staining of the light chain was performed with FITC-conjugated anti-human kappa or lambda monoclonal antibodies, respectively (**C** and **D**). The human B cell lines DG75 and Ramos served as positive controls for the respective light chain expression. DG75 cell line – expressing kappa light chain (**C**, in dark green) and Ramos cells – expressing lambda light chain (**D**, in light green). The graphs are representative of three independent experiments.

In conclusion, the anti-Vβ 5.3 dcCARs were successfully expressed on the surface of Bw58 cells, showing that this alternative CAR design resulted in a stable expression. Moreover, the incorporation of an IgG1 spacer allows for further assessment of the signaling properties of the anti-Vβ 5.3 dcCAR, upon stimulation with anti-IgG F(ab´)$_2$ fragments and the resulting intracellular Ca^{2+} mobilization as discussed below.

4.3 Stimulation of the anti-Vβ 5.3 dcCAR induces Ca^{2+} mobilization in Bw58 cells

To evaluate the functionality and the signaling capacity of the anti-Vβ 5.3 dcCAR, the Bw58 cells were subjected to Ca^{2+}mobilization assay. For stimulation I used polyclonal anti-human IgG F(ab)$_2$' fragment, which cross-links the dcCARs and leads to a change in the Ca^{2+} level in the cells. Both dcCARs (containing either kappa or lambda light chains) were capable to transmit intracellular signaling to a comparable extent as shown by the Ca^{2+} mobilization upon stimulation (Figure 4.7). The kappa dcCAR (Figure 4.7 A) showed slightly reduced signaling capacity in comparison to the lambda dcCAR (Figure 4.7 B). As a control in this experiment were used stimulated Bw58 cells, transfected with the light chains only (Bw58 kappa and lambda LC).

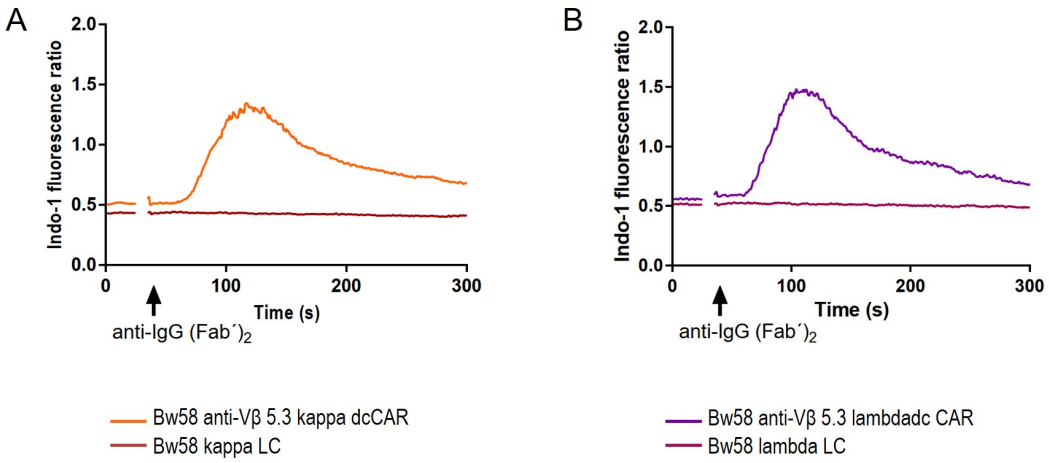

Figure 4.7 Stimulation of dcCARs induces Ca^{2+} signaling in Bw58 cells. Analysis of Ca^{2+} mobilization to assess the signaling capacity of kappa **(A)** or lambda light chain-containing dcCARs in Bw58 cells **(B).** Either kappa or lambda light chain transfected Bw58 cells – Bw58 kappa/lambda LC cells served as controls. All cells were loaded with the Ca^{2+} sensitive dye Indo-I AM. After recording a 25-second baseline, the cells were stimulated with 20 µg/ml goat anti-human IgG (Fab´)$_2$ fragment. The fluorescence was recorded for 300 seconds. The graphs are representative of three independent experiments.

Taken together, these results demonstrate that the Bw58 cells express the respective dcCARs which are capable of initiating intracellular Ca^{2+}-mobilization upon stimulation. Therefore, the alternative design of the anti-Vβ 5.3 CAR has proven to be beneficial for the direct evaluation of the surface expression and the functionality of the respective CAR molecules.

To my knowledge, it has not been reported in the literature whether the Bw58 cell line has cytotoxic potential. To shed some light on the phenotype of this cell line, I performed FACS analysis after staining with monoclonal antibodies against either CD8 or CD4 (Figure 4.8). The results demonstrated that the Bw58 is a $CD8^+$ cell line (Figure 4.8 A) and $CD4^-$ (Figure 4.8 B).

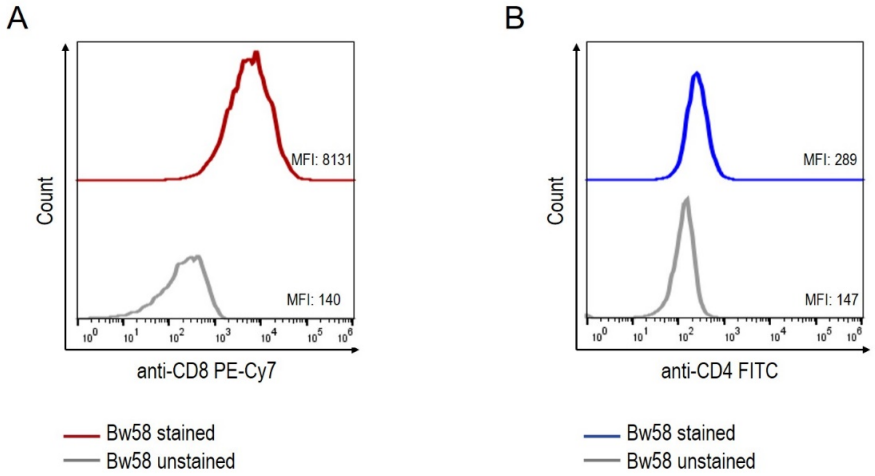

Figure 4.8 Bw58 cells have the phenotype of a cytotoxic T cell line. Bw58 parental cells were stained with anti-mouse PE-Cy7-conjugated CD8 **(A)** or anti-mouse FITC-conjugated CD4 **(B)** and analyzed via FACS. The graphs are representative of two independent experiments.

Having shown that the Bw58 cells have a phenotype of a cytotoxic cell line and are equipped with a functional anti-Vβ 5.3 dcCAR receptor, I evaluated their cytotoxic response against target cells in cellular assays. To this end, the Bw58 anti-Vβ 5.3 dcCAR T cells were co-cultured with TCR Vβ 5.3^+ Jurkat and Jurkat non-target cells to evaluate their antigen-specific cytotoxic response.

4.4 Bw58 dcCAR T cells exert cytotoxicity towards target T cells

The dcCAR has proven to be beneficial in terms of the possibility to directly detect its surface expression on Bw58 and also to assess the signaling capacity of the receptor via stimulation and monitoring of CAR-induced Ca^{2+} mobilization. Furthermore, to evaluate the selective targeting of the dcCAR-expressing cells and their potential to exert a cytotoxic response, I performed a similar *in vitro* cytotoxicity assay as shown before for the anti-Vβ 5.3 scCAR. To this end, I co-cultured either Bw58 anti-Vβ 5.3 kappa or lambda dcCAR T cells (effector cells) with the TCR Vβ 5.3^+ Jurkat cells (target cells). The effector and target cells were co-cultured in varying ratios and incubated for 24 and 48 h before FACS analysis. Jurkat cells were identified by expression of CD38, whereas Bw58 effector cells by the expression of RFP (as illustrated in

Figure 4.4). As a specificity control, I co-cultured them also with Jurkat cells, which do not express the cognate TCR Vβ 5.3 antigen.

The analysis of live cells in co-culture of Bw58 anti-Vβ 5.3 lambda dcCAR T cells (referred hereafter to simply as Bw58 lambda dcCAR T cells) with target cells at an equal ratio showed already at the beginning of the incubation a formation of a high percentage of doublets (Figure 4.9 B, right panel). Interestingly, the majority of these doublets appeared to be double-positive cells (RFP^+CD38^+), which suggests that those were already interacting cells (Figure 4.9 C, right panel and E). Although there was a doublet formation (Figure 4.9 B, left panel) and some double-positive cells in co-culture with non-target Jurkat cells (Figure 4.9 C, left panel and D), the percentage of this population was lower and remained in a similar range both after 24 and 48 h (Figure 4.9 C, middle and left panel). Furthermore, the percentage of viable non-target Jurkat cells remained high at each time point (Figure 4.9 C, left panel).

Strikingly, after 24 h in co-culture of Bw58 lambda dcCAR T cells with target cells, I observed a drastic decrease in the percentage of live TCR Vβ 5.3^+ Jurkat cells (Figure 4.9 C, right panel). Moreover, after 48 h, there were almost no viable target Jurkat cells (Figure 4.9 C, bottom panel). In addition, after 24 h and 48 h when almost all target cells were eliminated, the respective double-positive population was not present. This suggests further that its formation was due to interaction between effector and target cells (Figure 4.9 C, middle and bottom right panels).

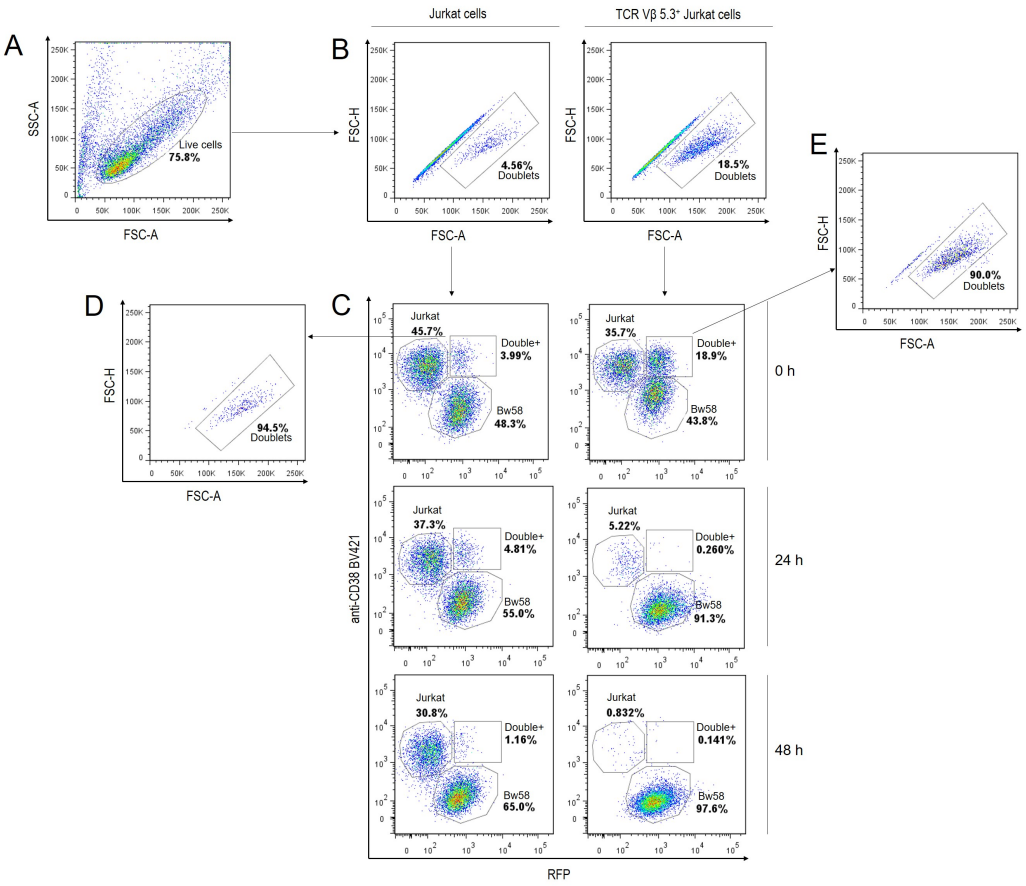

Figure 4.9 Bw58 dcCAR T cells form a distinct population of interacting cells at 0 h and eliminate the target cells after 24 h. FACS analysis of cytotoxicity assay between Bw58 dcCAR T cells and TCR Vβ 5.3⁺ Jurkat cells or non-target Jurkat cells (specificity control) at 1:1 ratio**. (A)** Gating of live cells. **(B)** The doublet formation between Bw58 dcCAR T cells in co-culture of Jurkat (left) or target cells (right) are shown on FSC-A (X-axis) and FSC-H (Y-axis). **(C)** The percentage of live cells within each population was assessed by the RFP fluorescence from Bw58 dcCAR T cells and additional staining with BV421-conjugated anti-human CD38 monoclonal antibody to monitor the percentage of Jurkat cells. Samples were taken at 0, 24, and 48 h. **(D)** The percentage of doublets shown on FSC-A (X-axis) and FSC-H (Y-axis) within the gate of double-positive cells in co-culture of Bw58 dcCAR T cells and Jurkat cells and **(E)** with TCR Vβ 5.3⁺ Jurkat cells. The data is representative of three independent experiments.

To address the question of whether the cytotoxic response of Bw58 cells is mediated by the dcCAR expression, in a separate specificity control, I co-cultured Bw58 lambda LC (RFP⁺) transfected cells with the TCR Vβ 5.3⁺ Jurkat cells. Similar to the specificity control with non-target Jurkat cells, there was no drastic decrease in the percentage of viable target cells (Figure 4.10 C, red line).

The analysis of inducible GFP expression of Bw58 lambda dcCAR T cells showed that they become activated only in co-culture with the respective antigen-expressing Jurkat cells (Figure 4.10 A, green line). Within the first 24 h, the percentage of activated GFP-expressing Bw58

lambda dcCAR T cells was increased which correlated with the complete elimination of target cells (Figure 4.10 A, red line). Furthermore, there were no GFP-expressing Bw58 cells in both specificity controls (Figure 4.10 B and C, green line), where the viability of Jurkat cells did not decrease drastically (Figure 4.10 B and C, blue and red line).

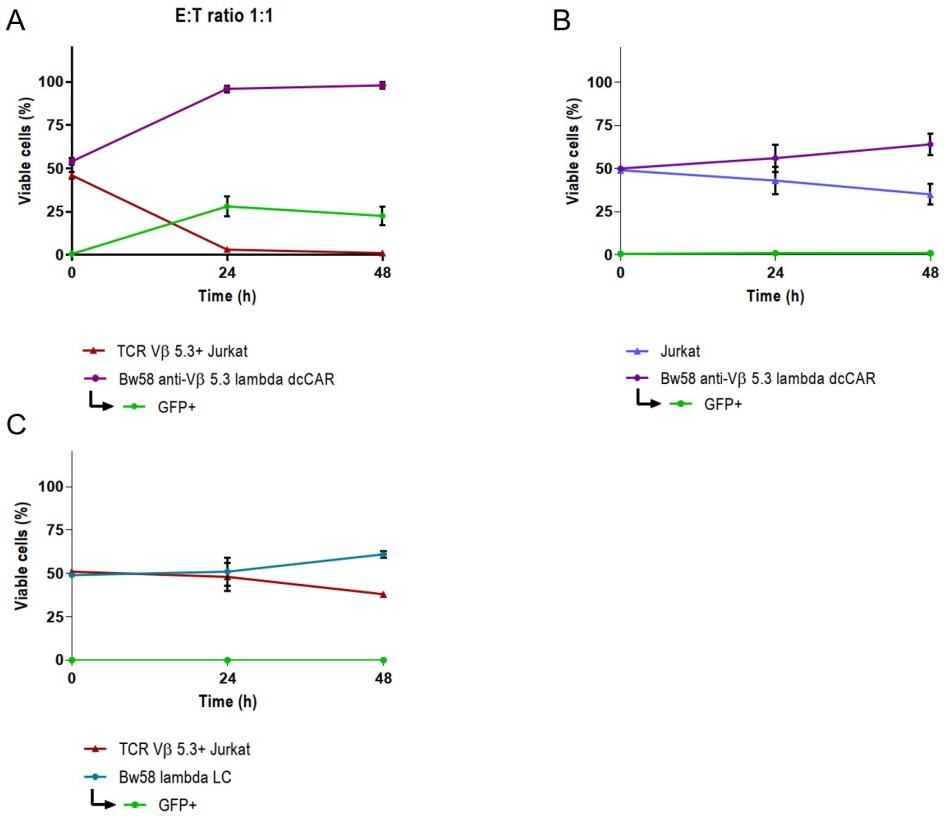

Figure 4.10 Bw58 lambda dcCAR T cells became activated only in co-culture with target cells. Analysis of the percentage of viable cells in co-culture at effector to target (E:T) ratio 1:1 during 0, 24, and 48 h of **(A)** Bw58 cells lambda dcCAR T cells (violet line) and TCR Vβ 5.3$^+$ Jurkat T cells (red line) **(B)** Bw58 lambda dcCAR T cells (violet line) and Jurkat cells (blue line). **(C)** Bw58 lambda LC (light blue) and TCR Vβ 5.3$^+$ Jurkat cells (red line). The green line in all plots shows the percentage of activated, GFP-expressing Bw58 cells. The graphs represent the mean percentage ±SD of three independent experiments.

In conclusion, these results show that the Bw58 lambda dcCAR T cells become specifically activated by target cells, which is demonstrated by the increased percentage of activated GFP-expressing cells after 24 h. Furthermore, after this time point, there were no viable TCR Vβ 5.3$^+$ Jurkat cells. To address the question of whether the cell density of target cells would have an impact on the percentage of GFP-expressing effector cells and their cytotoxic efficiency, I assessed additional E:T ratios of co-culture.

4.4.1 Bw58 dcCAR T cells demonstrate similar cytotoxic efficiency in varying E:T ratios

The Bw58 dcCAR T cells demonstrated high cytotoxic efficiency in co-culture with TCR Vβ 5.3⁺ Jurkat cells in equal effector to target ratio. Next, to evaluate the impact of varying cell ratios on the cytotoxic response of the Bw58 lambda dcCAR T cells, I co-cultured them either with a lower or higher cell density of target cells. I observed that irrespective of the co-culture ratio between effector and target cells, the majority of TCR Vβ 5.3⁺ Jurkat cells were efficiently eliminated already within 24 h (Figure 4.11 A and B, red bars). In excess of effector cells (E:T 2:1), TCR Vβ 5.3⁺ Jurkat cells were almost completely eliminated after 24 h (Figure 4.11 A, red bars). Furthermore, in co-culture with a higher cell density of target cells, I also observed a drastic decrease in the percentage of viable TCR Vβ 5.3⁺ Jurkat cells after 24 h and a complete elimination after 48 h (Figure 4.11 B, red bars). Consistent with the previous findings, the viability of Jurkat cells in both specificity controls did not decrease significantly irrespective of the co-culture ratio (Figure 4.11 A and B, blue and orange bars).

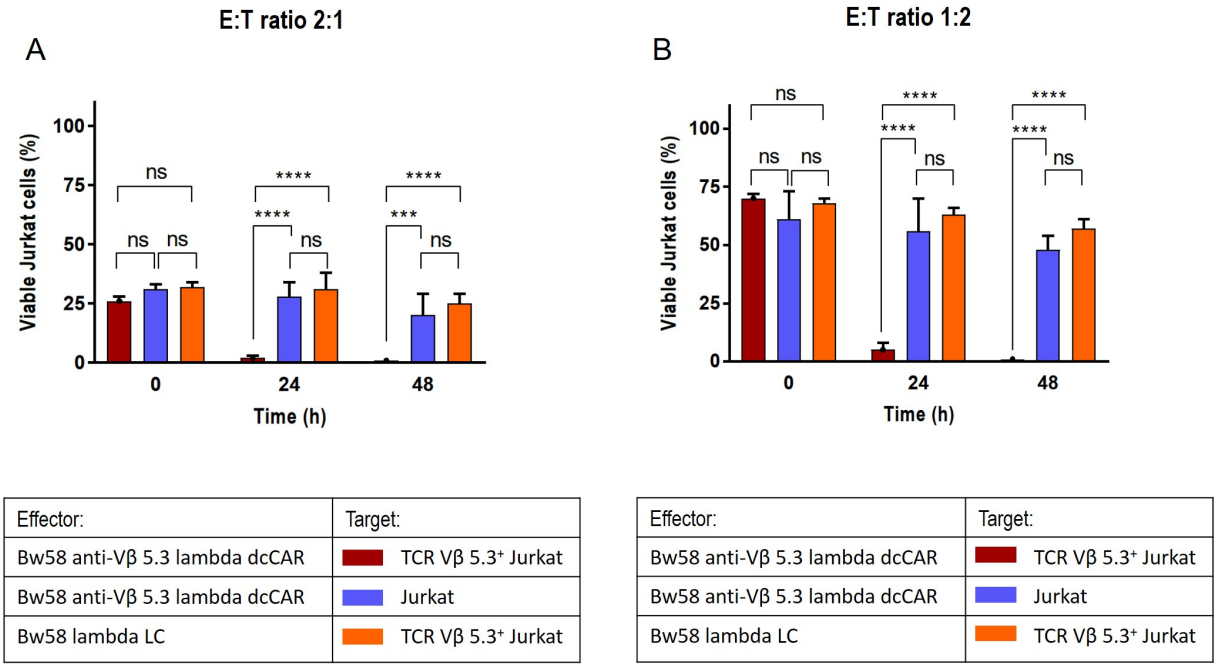

Figure 4.11 Bw58 lambda dcCAR T cells eliminate target cells within 24 h irrespective of the E:T ratio. (A) Percentage of viable TCR Vβ⁺ 5.3 Jurkat (red bars) in co-culture with an excess of Bw58 lambda dcCAR T cells (E:T 2:1) during 0, 24 and 48 h and comparison to the Jurkat cell viability in specificity controls (Bw58 lambda dcCAR T with Jurkat cells – blue bars; Bw58 lambda LC with TCR Vβ 5.3⁺ Jurkat cells – orange bars). **(B)** Percentage of viable TCR Vβ⁺ 5.3 Jurkat co-cultured in high cell density (E:T 1:2) with Bw58 lambda dcCAR T cells and comparison to the specificity controls. The graphs represent the mean percentage ± SD of three independent experiments. Statistical analysis was performed using the two-way ANOVA test with Tukey's multiple comparison test. **** <0.0001, *** 0.0040.

To investigate whether the Bw58 kappa dcCAR T cells would demonstrate similar cytotoxic efficiency, I used the same experimental setup as for the lambda dcCAR T cells. The majority of TCR Vβ 5.3⁺ Jurkat cells in co-culture with Bw58 kappa dcCAR T cells were also eliminated within the first 24 h of co-culture in E:T ratio 1:1 and 2:1 (Figure 4.12 A and B, red bars). After 48 h, there was a complete elimination of the target cells. Additionally, no antigen-independent cytotoxicity was observed in the respective specificity controls (Figure 4.12 A, and B, blue and orange bars).

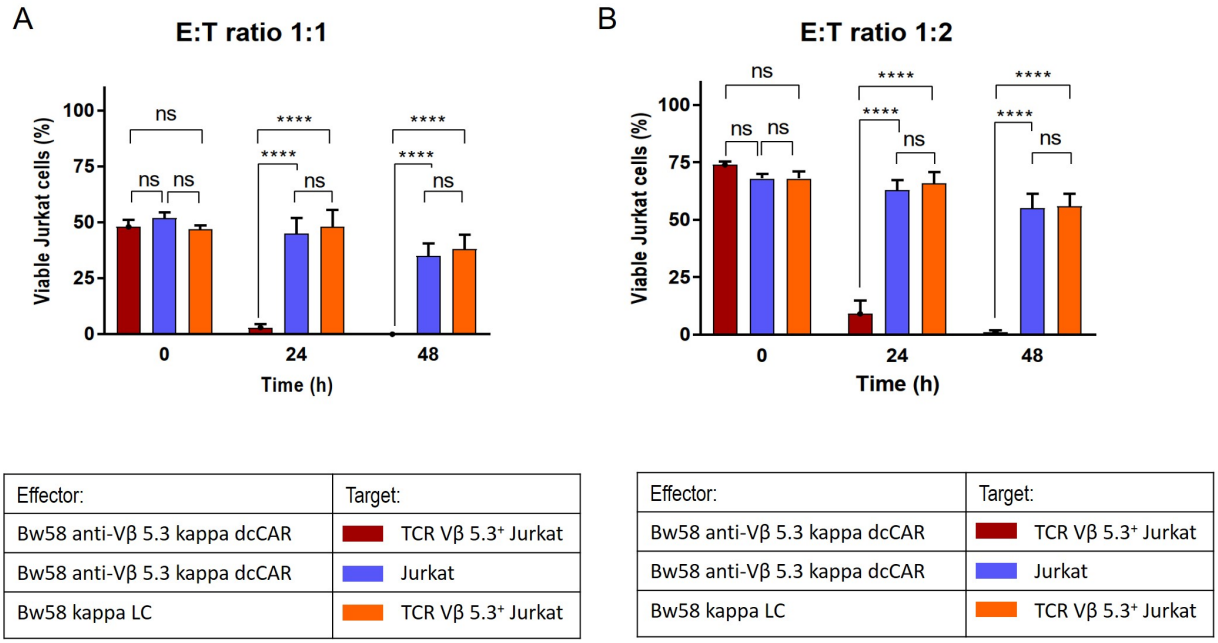

Figure 4.12 Bw58 kappa dcCAR cells demonstrated a comparable cytotoxic efficiency to Bw58 lambda dcCAR T cells. (A) Percentage of viable TCR Vβ 5.3⁺ Jurkat (red bars) in co-culture with Bw58 kappa dcCAR T cells at equal ratio during 0, 24 and 48 h and comparison to the viability of Jurkat cells in the specificity controls (Bw58 kappa dcCAR T with Jurkat cells – blue bars; Bw58 kappa LC with TCR Vβ 5.3⁺ Jurkat cells – orange bars). **(B)** Percentage of viable TCR Vβ 5.3⁺ Jurkat co-cultured in high cell density with Bw58 kappa dcCAR T cells and comparison to the specificity controls. The graphs represent the mean percentage ± SD of three independent experiments. Statistical analysis was performed using the two-way ANOVA test with Tukey's multiple comparison test. **** <0.0001.

Taken together, these findings indicated that Bw58 lambda dcCAR T cells demonstrated comparable cytotoxic efficiency against TCR Vβ 5.3⁺ Jurkat cells within the assessed E:T ratios. Thus, even in a high density of target cells, the majority of the target cells were already eliminated after 24 h. Furthermore, these findings demonstrate that both Bw58 lambda or kappa dcCAR-expressing T cells elicit comparable cytotoxic response against target cells.

4.4.2 The percentage of GFP-expressing Bw58 dcCAR T cells correlates with the target cell density

The analysis of the percentage of activated, GFP-expressing Bw58 lambda dcCAR T cells in co-culture with TCR Vβ 5.3⁺ Jurkat cells at the different ratios are summarized in Figure 4.13. In co-culture of a higher cell density of effector cells (Figure 4.13 A), at 24 h the percentage of activated GFP-expressing Bw58 cells is significantly lower (E:T 2:1 and 3:1, orange and blue bars) in comparison to co-culture at equal cell densities with target cells (E:T 1:1, violet bars). At the same time point, the high cell density of TCR Vβ 5.3⁺ target cells (Figure 4.13 B) correlates with a high percentage of activated GFP-expressing Bw58 lambda dcCAR cells (Figure 4.13 B, E:T 1:2 and 1:3, pink and light-blue bars). Moreover, after the complete elimination of the target cells at 48 h, the percentage of GFP-expressing Bw58 lambda dcCAR T cells decreases in comparison to the 24 h time point, which indicates that the Bw58 dcCAR T cell activation is dependent on the target cell density (Figure 4.13 A and B). As a control to assess the maximum GFP expression upon activation, are shown Bw58 lambda dcCAR cells treated with a cocktail of PMA/ionomycin (Figure 4.13 A and B, green bars).

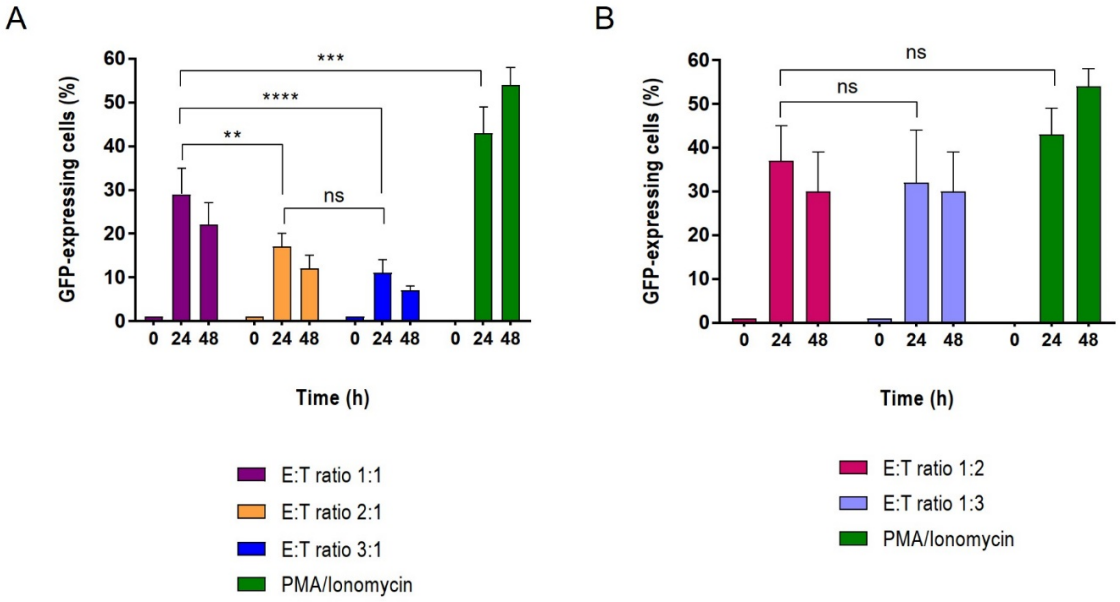

Figure 4.13 The percentage of the activated GFP-expressing Bw58 lambda dcCAR T cells correlates with the cell density of target cells. (A) Percentage of GFP-expressing Bw58 lambda dcCAR T cells in co-culture with increasing effector cell densities in 1:1, 2:1, 3:1 (E:T) during 0, 24, and 48 h. **(B)** Percentage of GFP-expressing Bw58 lambda dcCAR T cells in co-culture with increased target cells densities in ratio 1:2, 1:3 (E:T) during 0, 24, and 48 h. As a control for maximum GFP expression served PMA (20 ng/ml) /ionomycin (1μM) treated Bw58 lambda dcCAR T cells. The graphs represent the mean percentage ± SD of three independent experiments. Statistical analysis was performed using the two-way ANOVA test with Tukey's multiple comparison test. **** <0.0001, *** 0.0002, ** 0.0014.

In conclusion, both Bw58 lambda and kappa dcCAR T cells demonstrated high cytotoxic efficiency in the elimination of target cells. Moreover, the cytotoxic response by Bw58 lambda dcCAR T cells was comparable irrespective of the assessed effector to target ratios, evidence for which was the elimination of the majority of TCR Vβ 5.3$^+$ Jurkat cells within 24 h. Furthermore, the percentage of the activated GFP-expressing Bw58 lambda dcCAR T cells correlated with the cell density of the Jurkat target cells. Since the Bw58 lambda dcCAR T cells demonstrated slightly higher dcCAR expression and signaling capacity, all further experiments were performed with this effector cell line (referred hereafter to simply as Bw58 dcCAR T cells).

4.5 Cytotoxic mechanisms involved in the elimination of Jurkat target cells

4.5.1 Jurkat target cells underwent apoptosis in co-culture with Bw58 dcCAR T cells

The *in vitro* cytotoxicity assay showed that there is rapid antigen-specific elimination of target cells by the Bw58 dcCAR T cells. To investigate the mechanism by which the target cells were eliminated, I performed an Annexin V apoptosis assay. The analysis of Annexin V revealed that the TCR Vβ 5.3$^+$ Jurkat cells in co-culture with an equal percentage of effector cells underwent programmed cell death (Figure 4.14). After 24 h, the majority of the target cells had undergone late apoptosis and there was also an increased percentage of early apoptotic cells (Figure 4.14 D, left panel 24 h). This tendency was preserved after 48 h (Figure 4.14 D, left panel 48 h). The percentage of apoptotic cells in the population of Bw58 dcCAR T cells is shown as a comparison (Figure 4.14 D, right panel).

The vast majority of Jurkat target cells underwent apoptosis irrespective of the tested E:T ratios (Figure 4.14 E and F) as shown in the statistical analysis. As a comparison to the target cell apoptosis, the early and late apoptosis observed in the specificity control with Jurkat non-target cells are shown as well. I observed a low percentage of early and late apoptotic Jurkat cells, which was consistent within the two-time points. In conclusion, these results showed that the elimination of the TCR Vβ 5.3$^+$ Jurkat cells was due to apoptosis, triggered by the cytotoxic response of the Bw58 dcCAR T cells.

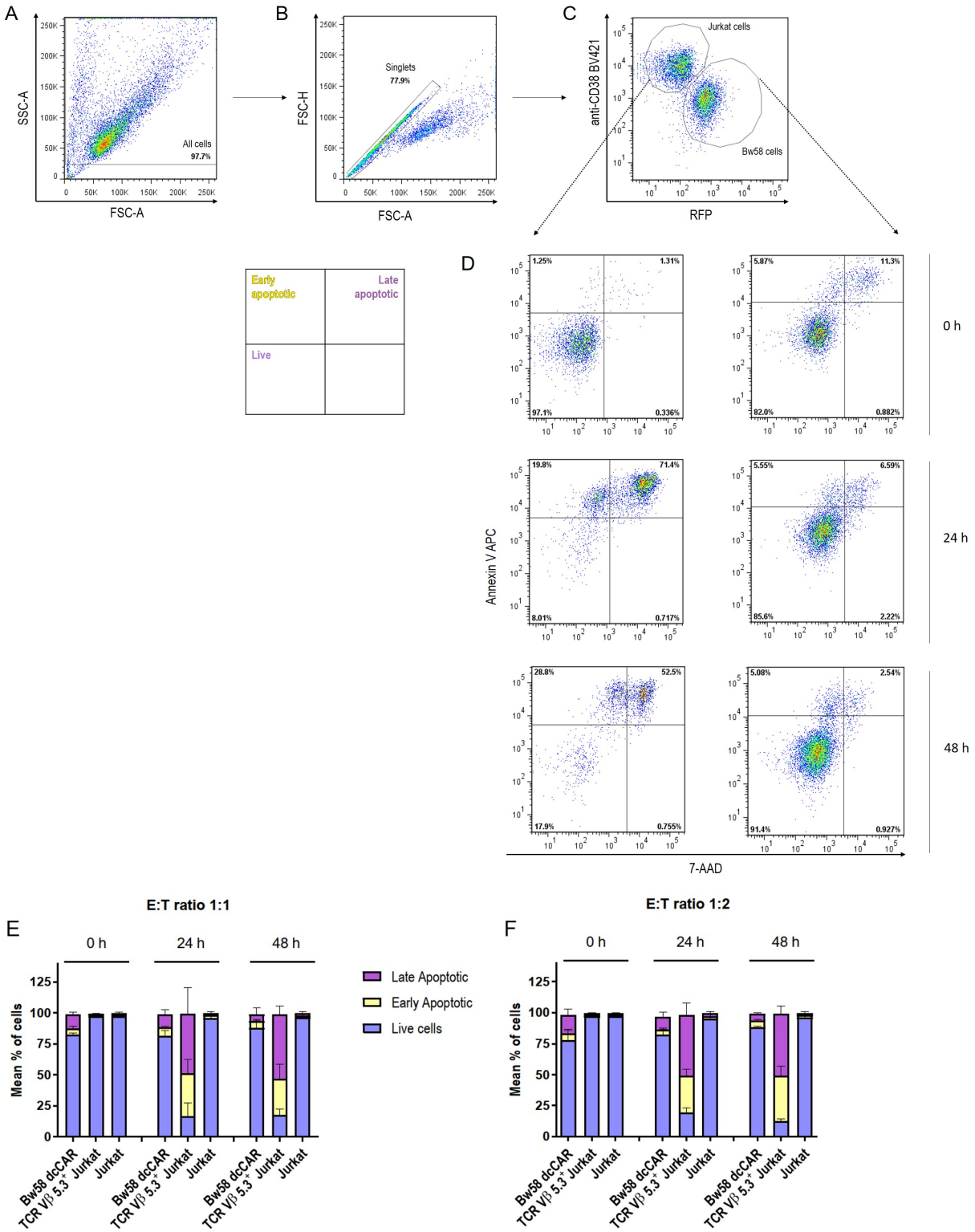

Figure 4.14 TCR Vβ 5.3⁺ Jurkat cells underwent apoptosis in co-culture with Bw58 dcCAR T cells.
(for legend see next page)

(A) Gating strategy of co-culture assay in ratio 1:1 (E:T). All cells except the debris were gated, followed by exclusion of doublets **(B)**. The percentage of the individual populations was assessed by staining with BV421-conjugated CD38 (Jurkat cells) and RFP fluorescence from Bw58 dcCAR T cells **(C)**. On **(D)** is shown the apoptosis rate within the respective populations of effector or target cells assessed at 0, 24, and 48 h of co-culture by staining with Annexin V APC and 7-AAD dye**.** The left panels show the percentage of viable, early, and late apoptotic cells within the population of TCR Vβ 5.3^{+} Jurkat T cells. The right panels show the percentage of viable, early, and late apoptotic cells within the population of Bw58 dcCAR T cells. The analysis of live, early and late apoptotic cells, co-cultured with Bw58 dcCAR T cells in ratio 1:1 (E:T) with TCR Vβ 5.3+ Jurkat cells and Jurkat cells, is shown on **(E)**. **(F)** shows the analysis of the apoptotic cells in ratio 1:2 (E:T). The graphs represent the mean percentage ± SD of three independent experiments.

There are two major cytotoxic mechanisms utilized by CTLs to eliminate target cells: the release of lytic granules, with granzyme and perforin, and triggering of programmed cell death via interaction with death domain-containing receptors (i.e. FasL-Fas interaction). Hence, the involvement of these mechanisms was further investigated as outlined below.

4.5.2 Monensin treatment abrogates the elimination of Jurkat target cells by Bw58 dcCAR T cells.

One of the cytotoxic mechanisms utilized by CTLs to eliminate target cells is the exocytosis of lytic granules containing granzyme and perforin, which disrupt the membrane of the target cells and trigger cell death[138]. To evaluate whether treatment with protein transport inhibitor would impair the elimination of Jurkat target cells, I performed the same *in vitro* cytotoxic assay in E:T ratio of 1:2 as shown before with or without the addition of monensin. Monensin is known to prevent acidification of lytic vesicles and interferes with vesicle transport from the Golgi apparathus[139,140]. Since the main mechanism of delivery of granzyme and perforin to the membrane of target cells is mediated by the transport of lytic granules in the proximity of target cells, I evaluated whether blocking of the intracellular protein transport would have an impact on the efficiency of TCR Vβ 5.3^{+} Jurkat cell elimination.

According to my results, the cytotoxicity against Jurkat target cells was impaired when co-cultured with effector cells in the presence of monensin (Figure 4.15 A, red line), whereas without the inhibitor, the majority of target cells were eliminated after 24 hours as shown before (Figure 4.15 B, red line). Furthermore, the percentage of GFP-expressing Bw58 dcCAR T cells in co-culture with target cells was preserved irrespective of the addition of monensin (Figure 4.15 A and B, green line). This observation suggests that the inducible GFP-expression upon antigen-specific recognition of target cells by the Bw58 dcCAR T cells was preserved. The addition of protein transport inhibitor did not affect the overall viability of Jurkat cells in the specificity control (Figure 4.15 B, blue line). In both monensin-treated co-culture samples (Figure 4.15 A and C), I observed a decreasing percentage of live effector cells at 24 h (Figure 4.14 A and C, violet line), which might be caused by the accumulation of proteins within the cells and the cytotoxic effect of the reagent after the long exposure[141].

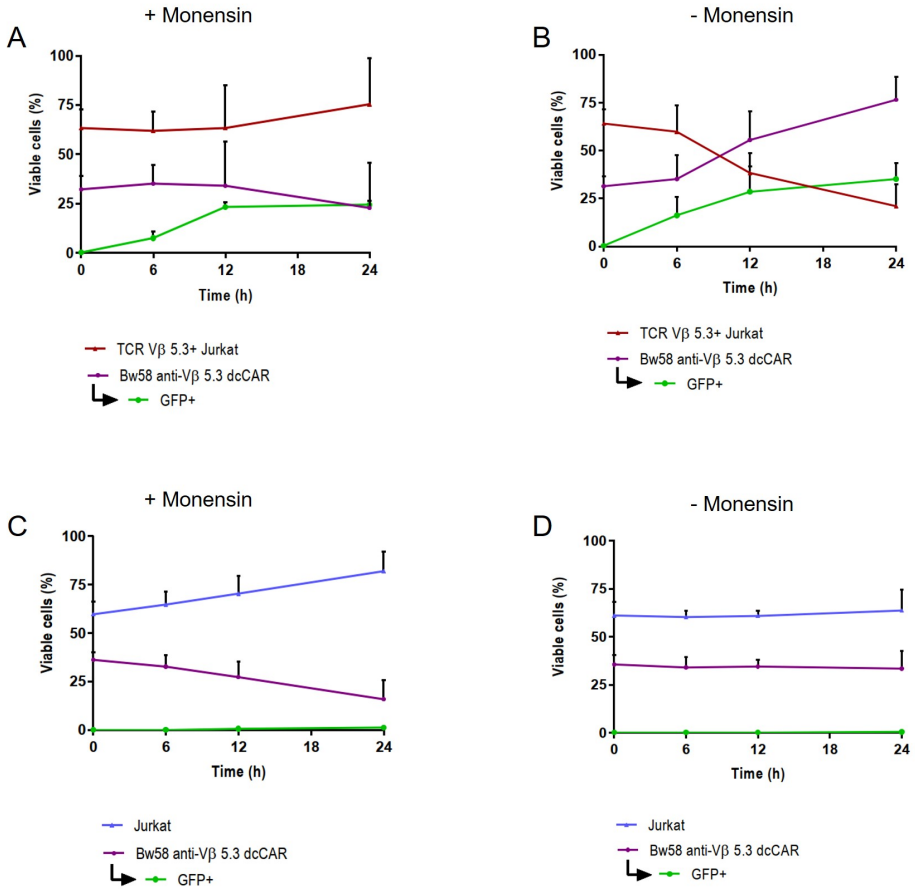

Figure 4.15 Monensin impairs the cytotoxic response of Bw58 dcCAR T cells against target cells. Bw58 dcCAR T cells (violet line) were incubated in ratio 1:2 (E:T) with TCR Vβ 5.3$^+$ Jurkat cells (red line) **(A, B)** or Jurkat parental cells (blue line) **(C, D)** in the presence **(A, C)** or absence **(B, D)** of monensin in the culture medium. The green line represents the percentage of activated GFP-expressing Bw58 dcCAR T cells. Samples were taken at 0, 6, 12, and 24 h of co-culture and stained with BV421-conjugated CD38 to assess the percentage of viable cells within the Jurkat population. The graphs represent the mean percentage ± SD of two independent experiments.

In conclusion, these findings suggest that blocking of the protein transport with monensin affects the efficiency of cytotoxic elimination of TCR Vβ 5.3$^+$ Jurkat cells, which might suggest that there was an impaired granzyme and perforin delivery. To address the question of whether death-receptor mediated apoptosis has a role in the elimination of target cells, the involvement of death-domain receptor interactions, in particular FasL-Fas, was tested as well.

4.5.3 Fas-FasL interaction contributes as a mechanism of the elimination of Jurkat target cells

Another mechanism of target cell elimination by CTLs is the interaction between FasL-Fas[110]. To investigate whether death-receptor mediated apoptosis also has an impact on the observed apoptosis of TCR Vβ 5.3$^+$ Jurkat cells, I blocked FasL on Bw58 CAR T cells with monoclonal

antibody to prevent its interaction with FAS on Jurkat target cells and analyzed cytotoxicity as before.

After blocking of FasL on Bw58 dcCAR T cells, I observed significantly impaired cytotoxic response against Jurkat target cells both after 24 h and 48 h in comparison to untreated effector cells (Figure 4.16 A, purple and orange bars). Furthermore, after 24 h of co-culture, the percentage of apoptotic TCR Vβ 5.3⁺ Jurkat cells was decreased in comparison to co-culture conditions without the anti-FasL antibody (Figure 4.16 B, light blue and dark blue bars). Treatment of the Bw58 dcCAR T cells with anti-FasL antibody prior to co-culture with Jurkat non-target cells had no significant effect neither on the percentage of viable cells, nor on the observed apoptosis rate.

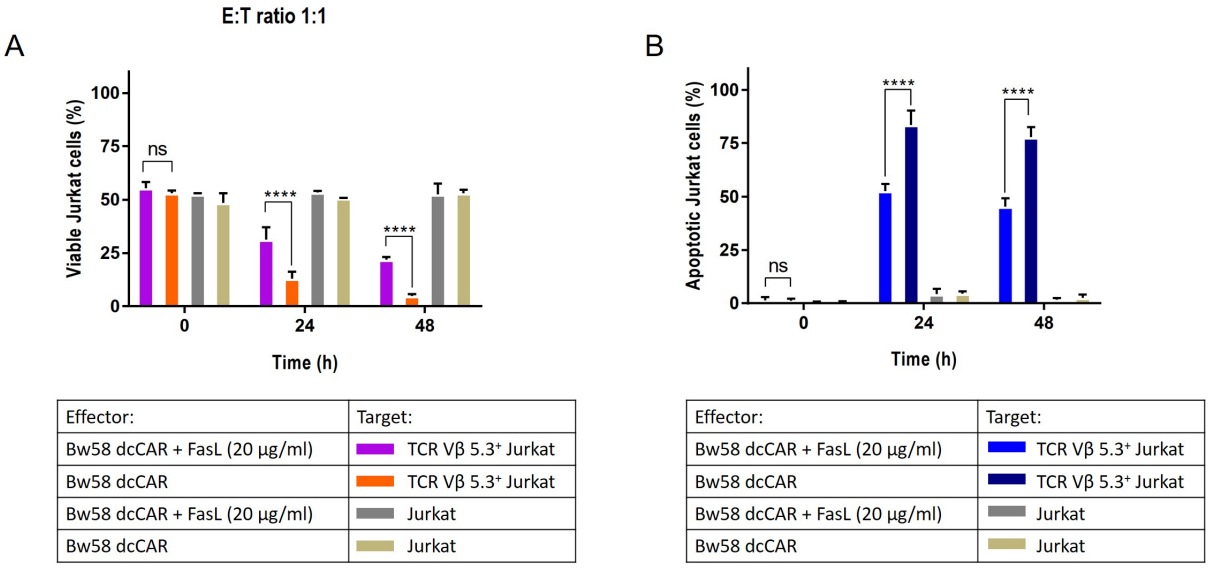

Effector:	Target:
Bw58 dcCAR + FasL (20 µg/ml)	TCR Vβ 5.3⁺ Jurkat
Bw58 dcCAR	TCR Vβ 5.3⁺ Jurkat
Bw58 dcCAR + FasL (20 µg/ml)	Jurkat
Bw58 dcCAR	Jurkat

Effector:	Target:
Bw58 dcCAR + FasL (20 µg/ml)	TCR Vβ 5.3⁺ Jurkat
Bw58 dcCAR	TCR Vβ 5.3⁺ Jurkat
Bw58 dcCAR + FasL (20 µg/ml)	Jurkat
Bw58 dcCAR	Jurkat

Figure 4.16 FasL block on Bw58 dcCAR T cells impairs their cytotoxic response. (A).Bw58 dcCAR T cells were pre-incubated with 20 µg/ml purified anti-mouse FasL monoclonal antibody and co-cultured with TCR Vβ 5.3⁺ Jurkat cells in a ratio of 1:1 (E:T). Samples were taken at 0, 24, and 48 h and stained with BV421-conjugated CD38 monoclonal antibody to distinguish the population of Jurkat cells, and additionally with APC-conjugated Annexin V and 7-AAD to evaluate the percentage of apoptotic cells. The graphs represent the percentage of viable TCR Vβ 5.3⁺ Jurkat cells, co-cultured with FasL-blocked Bw58 dcCAR cells (purple) and untreated cells (orange). The same conditions were applied to the specificity control with non-target Jurkat cells**,** where FasL-blocked Bw58 dcCAR cells (grey) or untreated cells (yellow) were added, respectively. **(B)** The total percentage of apoptotic cells, in co-culture with FasL-blocked Bw58 dcCAR cells (light blue) or with untreated effector cells (dark blue). The apoptosis rate was assessed also in the specificity control with Jurkat cells, co-cultured with FasL-blocked Bw58 dcCAR cells (grey) or with untreated cells (yellow). The graphs represent the mean percentage ± SD of three independent experiments, whereas the specificity control with Jurkat cells of two independent experiments. Statistical analysis was performed using the two-way ANOVA test with Sidak's multiple comparison test. **** <0.0001

Taken together, these findings demonstrate that treatment of Bw58 dcCAR cells with purified-FasL antibody impaired the cytotoxic response against Jurkat target cells. Therefore, the FasL-Fas interaction has a contribution as a cytotoxic mechanism in the elimination of target cells.

The results of the *in vitro* cytotoxicity assay with TCR Vβ 5.3$^+$ Jurkat cells demonstrated that there is an antigen-specific activation of Bw58 dcCAR T cells and selective elimination of the majority of target cells within the first 24 h of co-culture, irrespective of the assessed E:T ratio. Next, it was of interest to investigate the potential of the Bw58 dcCAR T cells to target selectively human TCR Vβ 5.3$^+$ primary T cells. Thus, I performed a similar *in vitro* cytotoxicity assay with isolated human peripheral blood T cells as discussed below.

4.6 Bw58 dcCAR T cells target human primary TCR Vβ 5.3$^+$ T cells *ex vivo*

The percentage of TCR Vβ 5.3$^+$ T cells is in the range between 1-3 % of all T cells in peripheral blood of healthy individuals[36]. Therefore, to achieve optimal distribution between effector and target cells, the Bw58 dcCAR T cells were co-cultured with primary T cells in an increased E:T ratio of 7:1. Although the primary T cells differ significantly in scatter morphology from the Bw58 dcCAR T cells, to distinguish between the two populations, I performed additional staining with anti-CD2 to identify the primary T cells (Figure 4.17). Next, to assess the targeting of TCR Vβ 5.3$^+$ primary T cells, I additionally stained them with FITC-conjugated anti-TCR Vβ 5 and eFluor450-conjugated anti-TCR Vβ 8 monoclonal antibodies. The latter was used as a control to exclude unspecific targeting effects of the Bw58 dcCAR T cells. To evaluate the percentage of TCR Vβ 5.3$^+$ and Vβ 8$^+$ T cell subpopulations, I performed FACS analysis before (Figure 4.17 and 4.18, A) and after the addition of the respective Bw58 cells (Figure 4.17 and 4.18, D) and after 24 h of co-culture (Figure 4.17 and 4.18, I).

Immediately after the addition of Bw58 dcCAR T cells to the primary T cells, I observed doublets formation (Figure 4.17, G). Moreover, this doublet population was composed of double-positive cells comprising of effector cells and primary T cells, which implies that most probably these were already interacting cells (Figure 4.17, E) as shown earlier in the *in vitro* cytotoxicity assay with Jurkat target cells (Figure 4.9).

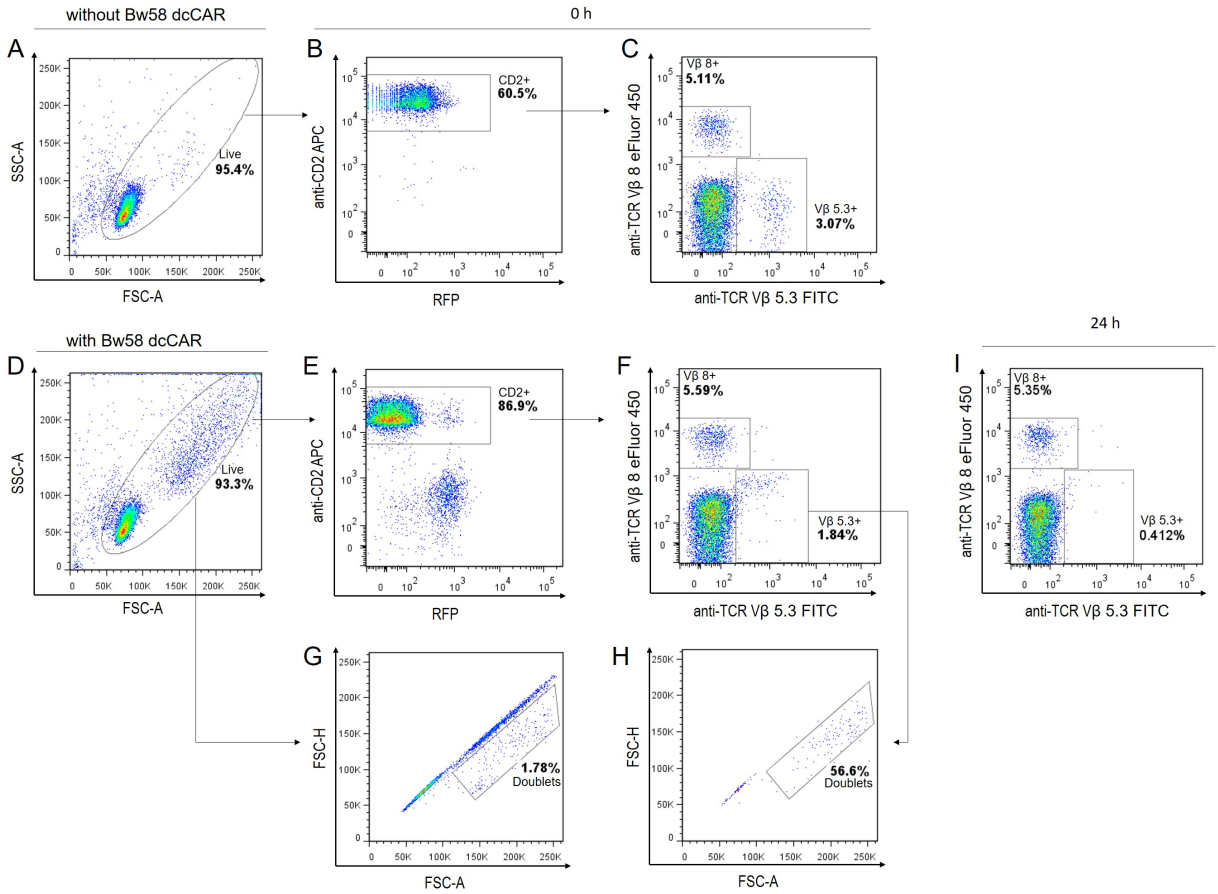

Figure 4.17 Bw58 dcCAR T cells interact with TCR Vβ 5.3⁺ primary T cells at 0 h. Isolated primary pan T cells were co-cultured with Bw58 dcCAR Tcells in ratio 7:1 (E:T) for 24 h. Two samples were taken at 0 h – before and after the addition of the Bw58 cells to monitor the percentage of TCR Vβ 5.3⁺ and TCR Vβ 8⁺ T cell subpopulations. The samples were stained with APC-conjugated CD2 monoclonal antibody to distinguish the subpopulation of primary T cells. The percentage of effector Bw58 cells was assessed by the RFP fluorescence. **(A, D)** Live cells were gated before and after the addition of Bw58 cells. **(G)** shows the doublet formation after the addition of Bw58 dcCAR T cells. **(B, E)** CD2⁺ cells before and after the addition of Bw58 dcCAR T cells and the formation of a distinct double-positive (CD2⁺RFP⁺) population. **(C)** shows the percentage of the individual TCR Vβ 5.3⁺ or TCR Vβ 8⁺ primary T cells before addition of Bw58 dcCAR T cells and **(F)** after addition of Bw58 dcCAR T cells. **(H)** shows the percentage of doublets within the gate of TCR Vβ 5.3⁺ cells. **(I)** shows the percentage of the individual TCR Vβ 5.3⁺ or TCR Vβ 8⁺ primary T cells after 24 h of co-culture with Bw58 dcCAR T cells. The results are representative of two independent experiments.

The analysis of TCR Vβ 5.3⁺ and TCR Vβ 8⁺ subpopulations showed that before the addition of Bw58 cells both subpopulations are present (Figure 4.17, C). Notably, after the addition of Bw58 dcCAR T cells, the majority of target primary T cells were no longer detected, while the subpopulation of TCR Vβ 8⁺ T cells remained unaltered (Figure 4.17, F). This phenomenon was observed immediately after mixing primary T cells and Bw58 dcCAR T cells, but also after 24 h (Figure 4.17, I). The analysis of the remaining cells within the gate of TCR Vβ 5.3⁺ cells

immediately after the addition of Bw58 dcCAR T cells showed that these cells were doublets (Figure 4.17, H), which further suggests that they were likely already interacting cells.

The inability to stain TCR Vβ 5.3⁺ primary T cells at the beginning of co-culture might have been caused by epitope masking by the dcCAR since it recognizes the same epitope as the anti-Vβ 5.3 antibody (MEM262) that was used to generate the dcCAR. These observations were further strengthened by the results of co-culture in the specificity control with Bw58 Lambda LC cells (Figure 4.18).

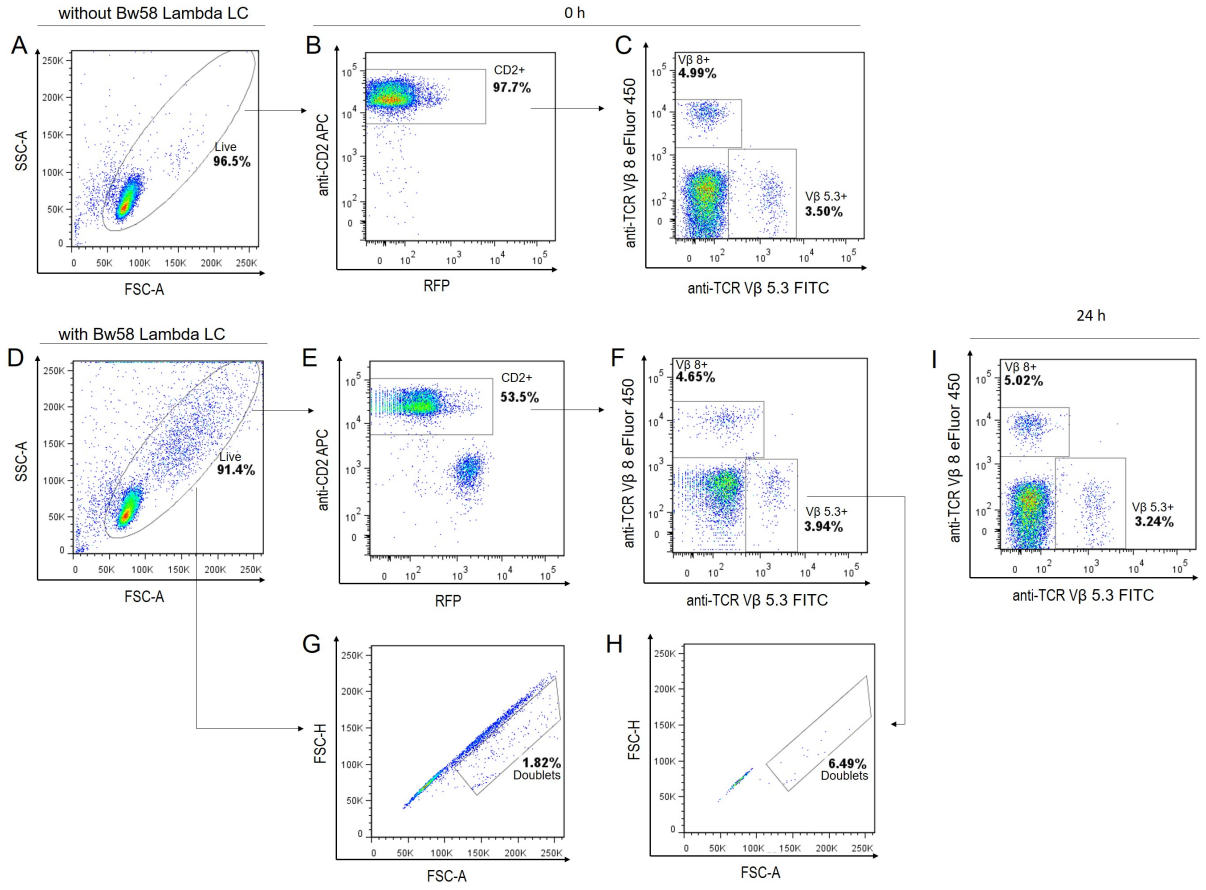

Figure 4.18 TCR Vβ 5.3⁺ primary T cells remain unaffected in co-culture with Bw58 lambda LC T cells. Isolated primary pan T cells were co-cultured with Bw58 lambda LC T cells in ratio 7:1 (E:T) for 24h. Two samples were taken at 0 h – before and after the addition of the Bw58 cells to monitor the percentage of TCR Vβ 5.3⁺ and TCR Vβ 8⁺ T cell subpopulations. The samples were stained with APC-conjugated CD2 monoclonal antibody to distinguish the subpopulation of primary T cells. The percentage of effector Bw58 cells was assessed by the RFP fluorescence. **(A, D)** Live cells were gated before and after addition of Bw58 Lambda LC cells. **(G)** shows the doublet formation after addition of Bw58 lambda LC T cells. **(B, E)** CD2⁺ cells before and after the addition of Bw58 lambda T cells. **(C)** shows the percentage of the individual TCR Vβ 5.3⁺ or TCR Vβ 8⁺ primary T cells before addition of Bw58 lambda LC T cells and **(F)** after addition of Bw58 lambda LC T cells. **(H)** shows the percentage of doublets within the gate of TCR Vβ 5.3⁺ T cells. On **(I)** is shown the percentage of the individual TCR Vβ 5.3⁺ or TCR Vβ 8⁺ primary T cells after 24 h of co-culture with Bw58 dcCAR T cells.

Analysis of the live cells after the addition of Bw58 Lambda LC cells showed also a doublet cell formation (Figure 4.18, G), which appeared to be composed of some double-positive $CD2^+RFP^+$ cells (Figure 4.18, E). However, this population was not so prominent as compared to the one formed by Bw58 dcCAR T cells (Figure 4.17 E). Moreover, the percentage of both TCR Vβ 5.3^+ and TCR Vβ 8^+ primary T cells remained similar irrespective of the addition of Bw58 cells both at 0 h (Figure 4.18, C and F) and after 24 h (Figure 4.18, I). Furthermore, the gating on the TCR Vβ 5.3^+ cells showed the presence of a very low percentage of doublets (Figure 4.18, H).

The co-culture conditions with primary T cells differ from those with Jurkat cells as there are only a small percentage of target cells in a much bigger population of non-target cells. To recapitulate these conditions in the Jurkat system, I mixed TCR Vβ 5.3^+ Jurkat cells with non-target Jurkat cells to obtain approximately 2% of the target cell population. Subsequently, I performed the cytotoxicity assay with Bw58 dcCAR T cells in the same 7:1 E:T ratio. Similar to the cytotoxicity assay with human primary T cells, the population of the target Jurkat cells was present at the 0 h before co-culture with Bw58 dcCAR T cells (Figure 4.19 C) and it was undetectable after the addition of the effector cells (Figure 4.19 F).

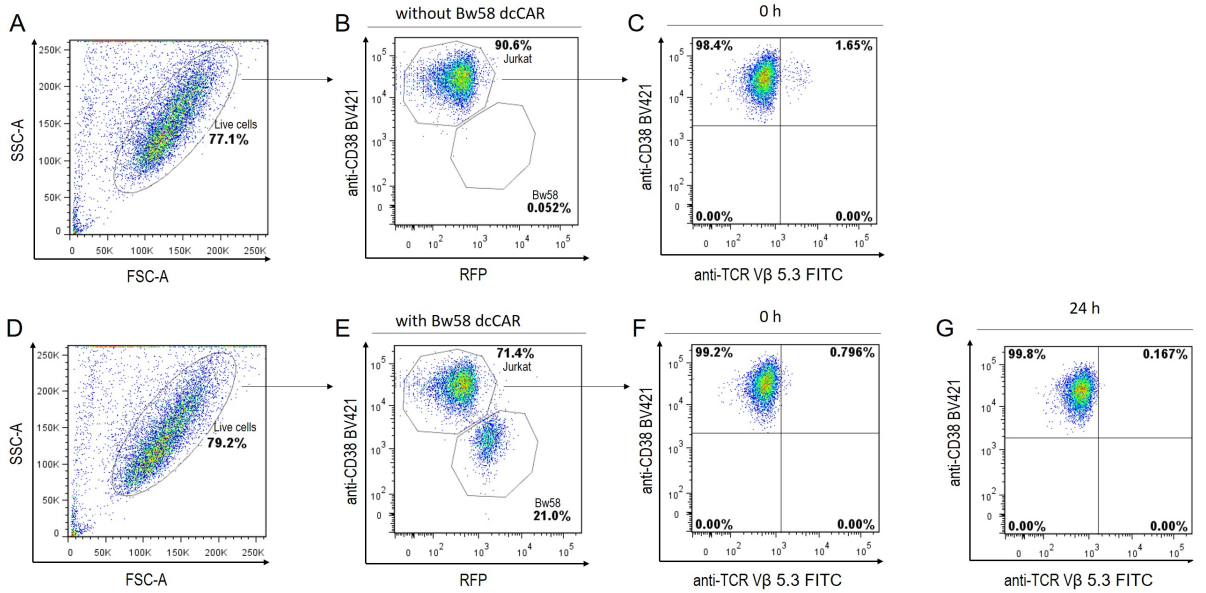

Figure 4.19 2% Jurkat target cells in a pool of non-target cells were undetectable after the addition of Bw58 dcCAR cells. Target cells were mixed with Jurkat cells in a similar distribution ratio of the target TCR Vβ 5.3^+ primary T cell subpopulation. To distinguish the population of Jurkat cells, it was performed staining with BV421-conjugated anti-CD38 and additional staining with FITC-conjugated TCR Vβ 5 monoclonal antibody. **(A, D)** Gating strategy for the analysis of the percentage TCR Vβ 5.3^+ Jurkat cells**.** First live cells were gated and then the percentage of Jurkat cells was assessed at 0 h before **(B)** and after the addition of Bw58 dcCAR T cells **(E)**. On **(C)** is shown the percentage of TCR Vβ 5.3^+ Jurkat cells before and after the addition of Bw58 dcCAR T cells **(F)**. **(G)** Percentage of live TCR Vβ 5.3^+ Jurkat cells after 24 h of co-culture with the effector cells.

This observation implies further that most probably the TCR Vβ 5.3 epitope might have been masked by the binding of the Bw58 dcCAR T cells. Consistent with the observation with primary T cells, after 24 h of co-culture, the 2% TCR Vβ 5.3$^+$ target cells were not present (Figure 4.19 G), while the majority of Jurkat parental cells remained viable. However, in concordance with the previous results, where I could show that Jurkat target cells were eliminated after 24 h by the Bw58 dcCAR T cells, this experiment imply that the Jurkat target cells were depleted.

In conclusion, these findings show that there was a selective targeting of TCR Vβ 5.3$^+$ primary T cells by the Bw58 dcCAR T cells, evidence for which might be the presence of a double-positive RFP$^+$CD2$^+$ population of interacting cells at the beginning of co-culture. Moreover, this double-positive population was not present after 24 h of co-culture. Furthermore, the subpopulation of TCR Vβ 5.3$^+$ primary T cells is undetectable after the addition of the Bw58 dcCAR T cells and after 24 h, in comparison to co-culture with Bw58 lambda LC cells. The monitoring of the TCR Vβ 8$^+$ primary T cell subpopulation, which remains unaffected at each time point, further showed the specificity of interaction. Altogether, these results indicate that there was a selective recognition of TCR Vβ 5.3$^+$ primary T cells, although whether they have been eliminated by the Bw58 dcCAR T cells would require further investigation.

4.7 DAP10ITT motif improves the signaling capacity of the dcCAR

Having shown that the dcCAR, expressed by Bw58 cells is functional and induces an effective cytotoxic response, it was of interest to explore whether modification of the ITT motif in the CAR construct would affect the signaling capacity of the receptor. Previous work by our group has demonstrated that the exchange of the mIgG2a ITT-motif with that of DAP10 in B cells leads to increased Ca^{2+} mobilization and enhanced signaling, whereas the CD28 was ineffective[142]. Therefore, the hypothesis was that the exchange of CD28 ITT-motif with DAP10ITT in the dcCAR would also potentiate the signaling and the effector response, demonstrated by the Bw58 cells. To test this, the dcCAR (referred to hereafter as a conventional dcCAR) heavy chain-encoding genetic construct was modified by site-directed mutagenesis to substitute six amino acids (Figure 4.20 A, in black letters) within the CD28ITT motif in the cytoplasmic tail of the dcCAR and to express the DAP10ITT-motif instead (Figure 4.20 B).

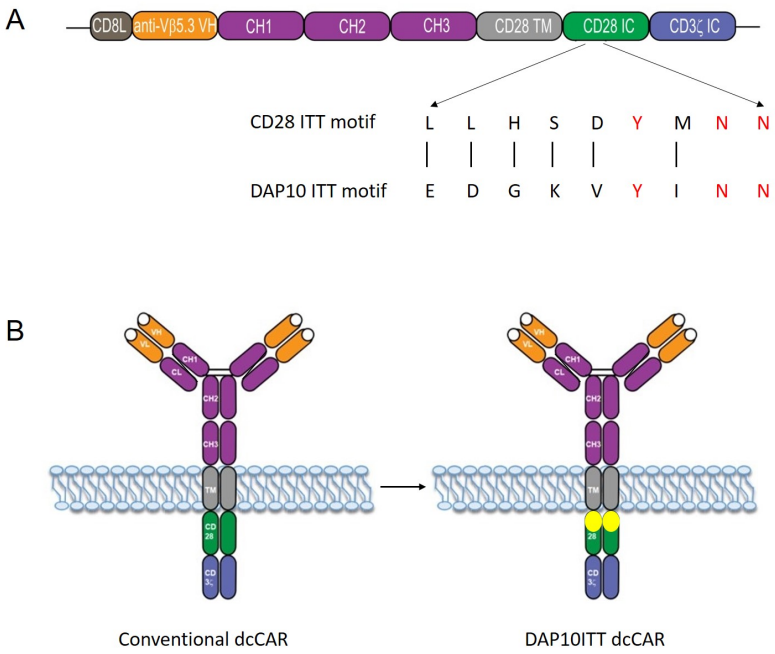

Figure 4.20 Generation of DAP10ITT-modified dcCAR. (A) To exchange the CD28 ITT motif in the cytoplasmic tail of the CAR backbone, I performed site-directed mutagenesis to generate the DAP10ITT-encoding genetic sequence. The substituted amino acids (in a single-letter code) are shown in black, and the conserved amino acids are marked in red. The modified genetic construct was then delivered to Bw58 lambda LC cells via retroviral transfection. **(B)** Schematic representation of the DAP10ITT dcCAR.

Next, a retroviral transfection of the respective Bw58 lambda LC cells was performed. To assess the surface expression of the DAP10ITT dcCAR, I performed FACS analysis with the anti-human AF647-conjugated IgG polyclonal antibody. The surface expression of the DAP10ITT dcCAR on Bw58 cells was compared to the conventional dcCAR. Notably, the expression level of the latter was higher in comparison to the DAP10ITT dcCAR (Figure 4.21 A).

To address the question of whether the DAP10ITT-motif would improve the signaling capacity of the receptor, I compared the dcCAR-mediated Ca^{2+} mobilization upon stimulation of DAP10ITT and conventional dcCAR-expressing Bw58 cells with anti-human IgG $(Fab´)_2$ fragment. The results revealed a stronger Ca^{2+} flux by the Bw58 cells, expressing the DAP10ITT dcCAR, despite the lower expression level of the receptor in comparison to the conventional dcCAR (Figure 4.21 B). These findings suggest that the DAP10ITT motif itself served as a signal amplifier. To test if this effect would be preserved upon stimulation with different concentrations, I also evaluated lower concentrations of the IgG $(Fab´)_2$ fragment (Figure 4.21 C and D). In all stimulations, the DAP10ITT dcCAR demonstrated a stronger Ca^{2+} influx as compared to the conventional dcCAR. These observations indicate that the DAP10ITT exchange in the dcCAR improved the signaling capacity of the receptor.

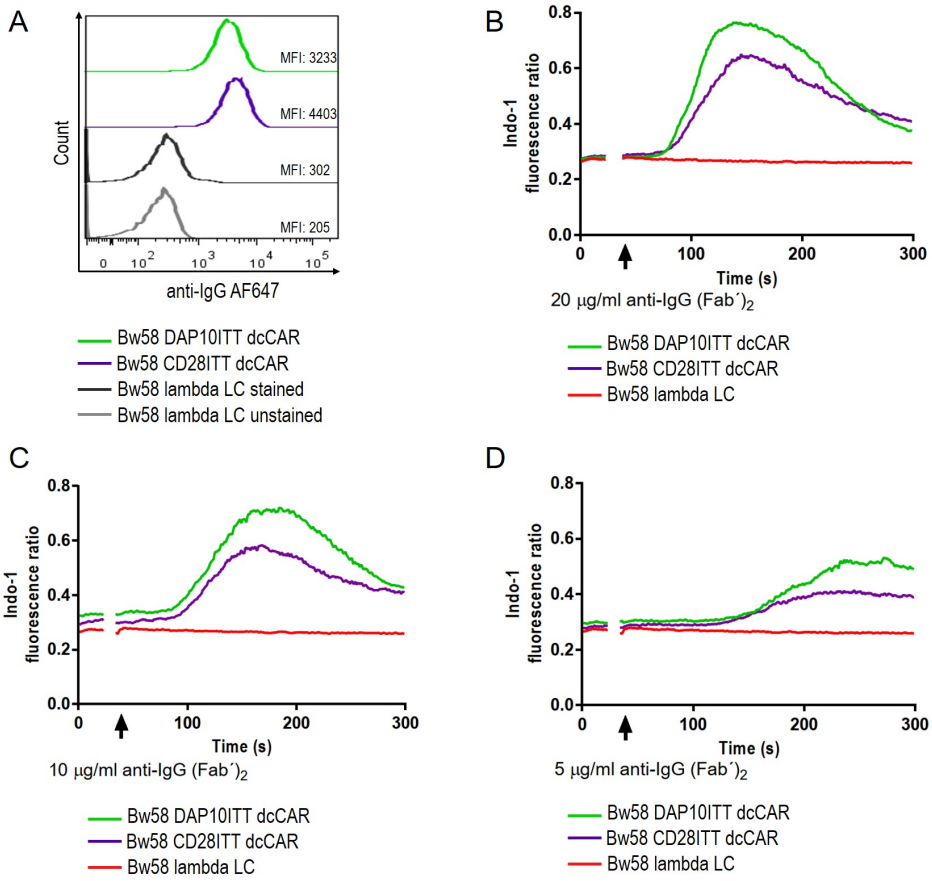

Figure 4.21 DAP10ITT-motif improves the signaling capacity of the dcCAR. (A) Surface expression of DAP10ITT dcCAR and comparison to the conventional dcCAR. Staining was performed with AF647-conjugated anti-human IgG. Bw58 lambda LC transfected cells served as a negative (grey) and background control (black). **(B, C, D)** Ca^{2+} mobilization upon stimulation of DAP10ITT and conventional dcCAR-expressing Bw58 cells. All cells were loaded with the Ca^{2+} sensitive dye Indo-I AM. 25 seconds baseline was recorded and cells were stimulated with anti-human IgG $(Fab')_2$ in concentrations of 20 µg/ml **(B)**, 10 µg/ml **(C)**, 5 µg/ml **(D)**. The signal was recorded for 300 seconds. The results are representative from one of three independent experiments.

To address the question of whether the increased signaling capacity of the DAP10ITT dcCAR would potentiate the cytotoxic efficiency of Bw58 cells against Jurkat target cells, I performed a similar *in vitro* cytotoxicity assay in equal effector to target cell ratio. Having shown that the Bw58 dcCAR T cells eliminate the majority of target cells rapidly and taking into account the increased signaling potential of the DAP10ITT-modified receptor, in addition to the 24 and 48 h time points, I evaluated the percentage of viable Jurkat target cells after 6 and 12 h after co-culture.

According to my findings, the Bw58 DAP10ITT dcCAR T cells demonstrated similar cytotoxic efficiency against target cells at each time point (Figure 4.22 A). Unfortunately, the inducible GFP expression of the Bw58 DAP10ITT dcCAR T cells was impaired. Hence, it was not

possible to compare directly the percentage of activated GFP-expressing cells between the two types of dcCAR-expressing Bw58 cells. In concordance with the previous findings, the percentage of viable Jurkat non-target cells remained high irrespective of the time points in co-culture with effector cells (Figure 4.22, B).

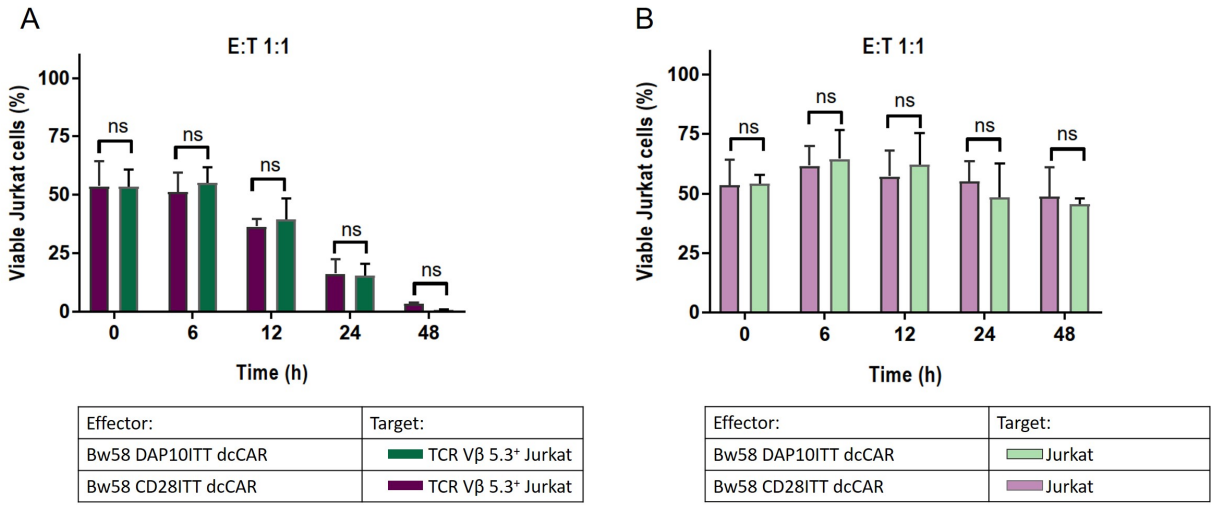

Figure 4.22 Bw58 DAP10ITT dcCAR T cells demonstrate similar cytotoxic efficiency against target cells. Analysis of co-culture between Bw58 DAP10ITT and conventional dcCAR-expressing Bw58 cells with Jurkat target cells **(A)** or with non-target Jurkat cells (specificity control) **(B)** at 1:1 E:T ratio. Samples were taken at 0, 6, 12, 24, and 48 h. The percentage of viable cells within each population was assessed by the RFP fluorescence from Bw58 cells and additional staining with anti-human BV421-conjugated CD38 monoclonal antibody to distinguish the Jurkat cell population. The graphs represent the mean percentage ± SD of three independent experiments. Statistical analysis was performed using the two-way ANOVA test with Sidak's multiple comparison test.

In conclusion, the DAP10ITT dcCAR showed improved signaling capacity in comparison to the conventional dcCAR as indicated by the increased Ca^{2+} mobilization level upon stimulation. Furthermore, the substitution of the ITT motif alone in the dcCAR served as a signal amplifier, which was indicated by the higher surface expression of the conventional dcCAR in comparison to DAP10ITT dcCAR. Thus, these findings demonstrate that the ITT-motif exchange in co-stimulatory domains might be considered as a possible signal amplifier in the context of CARs. However, the improved signaling capacity did not have a significant effect on the cytotoxic efficiency of the Bw58 DAP10ITT dcCAR T cells in co-culture with Jurkat target cells as compared to the conventional dcCAR-expressing cells. Whether the ITT exchange would affect distinct signaling pathways upon CAR stimulation, thereby leading to a shift of the cytokine profile or enhancing the response by the CAR-expressing T cells upon re-encounter with target cells would need further investigation. The demonstrated here findings serve as a basis for expanding the current knowledge about the potential role of additional signaling elements such as the ITT-motif in CAR activity-modulating co-receptors.

5. Discussion

The application of the CAR T cell platform for treatment of T cell malignancies is rather limited to date. The main reason is the choice of suitable target antigens expressed on malignant but also on healthy T cells. The careful selection of T cell markers to redirect CARs is of great importance since an elimination of the entire T cell population would lead to severe immunodeficiency and thus is not a feasible strategy[126].Therefore, there is an urgent need for investigation of novel targeting approaches that would be effective in the elimination of only defined T cell subpopulations and would allow preservation of the majority of the T cell compartment. Thus, during my PhD, I evaluated the potential of redirecting CAR T cells against the TCR Vβ unit in order to achieve selective targeting of individual T cell subpopulations. Here, as a proof-of-principle I developed and functionally characterized an anti-Vβ 5.3 CAR, which when expressed in T cells enables them to specifically eliminate TCR Vβ 5.3^+ T cells. Hence, my findings provide a basis for the improvement of the selectivity of CAR T cell platform as immunotherapy for treatment of T cell disorders in the future.

The main objectives achieved during the course of my PhD project are as follows:

1. Generation of a prototypic anti-Vβ 5.3 dcCAR, which enables selective targeting of the cognate TCR Vβ-expressing subpopulation. Upon transfection of a mouse T cell line, the dcCAR sensitize the cells to recognize the cognate antigen-expressing T cells.

2. Demonstration that the Bw58 dcCAR-expressing T cells become activated in an antigen-specific manner and exert efficient cytotoxic response against T cell line *in vitro.* Moreover, the Bw58 dcCAR T cells specifically recognize the target human primary TCR Vβ 5.3^+ T cells *ex vivo,* which shows the potential of this targeting approach as a basis for future development of immunotherapies to treat T cell malignancies or autoimmune diseases.

3. Improvement of the signaling capacity of the dcCAR. The replacement of the CD28ITT-motif with DAP10ITT improves the signaling potential of the dcCAR. Thus, the exchange of the ITT motif in the cytoplasmic part of co-receptors might be used to modulate the signaling capacity of CARs.

5.1 TCR Vβ unit as a potential target for selective elimination of T cells by CAR-T cells

So far, several possible T cell surface markers have been evaluated to adapt the CAR T cell platform for the treatment of T cell malignancies[123,143]. Among these are pan-T cell surface markers (i.e. CD3, CD5, CD7) that have been identified to have a high frequency of expression in T cell acute lymphoblastic and chronic lymphocytic leukemia[126,143,144,121]. Despite the successful design of CAR-expressing T cells, which further demonstrated cytotoxic responses against tumor cells *in vitro*, the persistency of these CAR T cells during *ex vivo* expansion in pre-clinical conditions was reported to be low due to fratricide occurring caused by shared marker expression between the CAR-modified T cells. Although this limitation could be overcome by using gene-editing tools to disrupt the expression of the respective surface markers on the CAR T cells, targeting pan-T cell markers and elimination of the majority of T cells would compromise the immune response by eliminating polyclonal T cell subsets.

Pule and colleagues showed that targeting the TCR with CAR T cells is also a feasible approach. They have taken advantage of the knowledge about the recombination events involved in the generation of the TCR during T cell development and in particular the re-arrangement of one of the two mutually exclusive gene segments encoding the constant domain of the TCR β chain[127]. By utilizing the variable domains of a monoclonal antibody, which specifically recognizes the TCR VβC1 domain, they have generated CAR T cells that possess the specificity to target only the respective TCR VβC1-expressing T cell subpopulations[127]. This targeting approach would spare the remaining TCR α/β T cells, which express the TCR VβC2. However, a clinical limitation for the application of such CAR T cells might be the safety concerns with regards to the risk of development of severe cytokine-release syndrome associated with the high percentage of target T cells. Thus, identifying new suitable target antigens on T cells, which would allow selective targeting, which might minimize the risk for the aforementioned effect, would benefit the improvement of the CAR T cell platform to treat T cell malignancies or autoimmune diseases.

During my Ph.D., I have explored the potential of targeting the TCR Vβ unit as a suitable marker for redirecting CAR T cells. There are available monoclonal antibodies recognizing the majority of TCR Vβ families, which makes it a feasible approach to be applied for adapting the CAR T cell platform for selective targeting. Recently, many efforts are directed toward the sequencing of the TCR Vβ repertoire both in healthy individuals and in patients with cancer or autoimmune diseases[36,43,145]. Some studies report a clonotypic expansion of defined TCR Vβ subpopulations in T cell malignancies and autoimmune diseases in comparison to their distribution in healthy individuals[45,146,147,148]. Therefore, targeting individual TCR Vβ families might benefit the immunotherapy of T cell-mediated disorders, where expanded TCR Vβ subpopulations are reported as main drivers of the pathogenesis. Moreover, targeting the Vβ region may limit the possibility of fratricide between CAR T cells only to those belonging to the same subpopulation.

So far, there are a few studies reporting that targeting of the TCR Vβ unit is a feasible approach for application in immunotherapies. Jie Wang et al. have demonstrated that targeting individual TCR Vβ families could be achieved by modification of T cells to express high-affinity receptor CD64 in combination with application of Vβ-directed monoclonal antibodies that leads to selective T cell cytolysis *in vitro* and *in vivo* in mice[149]. However, the authors themselves acknowledge that the clinical application of such approach would not be feasible due to the possibility for unspecific binding of patient's immunoglobulins to the modified CD64-expressing T cells, thus reducing the efficacy of the treatment[149].

The findings demonstrated in this study could contribute to expanding of the T cell targeting approaches by providing a basis for the generation and functional characterization of an anti-Vβ-directed CAR T cells. As a proof of principle for the applicability of this approach, I generated anti-Vβ 5.3-directed CAR T cells and could show that adaptation of the CAR platform to target individual T cells subpopulations is a feasible strategy for improvement of the selectivity in treatment of T cell malignancies or autoimmune diseases.

5.2 Considerations about the CAR design - the anti-Vβ 5.3 CAR in a dual chain format showed improved properties

The majority of CAR designs are based on the scFv format as an extracellular antigen-binding domain[150]. The conventional scCARs have proven to be a "golden standard" for targeting and elimination of tumor cells in hematological malignancies and some solid tumors[52,151–154]. Therefore, I first generated the anti-Vβ 5.3 CAR in an scFv format. However, the transfection of Bw58 cells with the scCAR-encoding genetic construct did not result in antigen-specific activation of the transfected cells upon co-culture with the TCR Vβ 5.3$^+$ Jurkat cell line *in vitro*. Moreover, I did not observe a cytotoxic response against the target cells (Figure 4.3). The reason could be the lack of surface expression of the anti-Vβ 5.3 scCAR in Bw58 T cells, despite the expression of the surrogate marker tNGFR from the bi-cistronic scCAR-encoding vector. The attempts to directly detect the expression of the scCAR by staining with polyclonal IgG antibodies were not successful, most probably due to the lack of suitable extracellular epitopes.

In some cases, the conventional design of CARs containing scFvs as antigen-binding moiety requires further "fine-tuning" to be effective in binding the selected target antigen[155]. In some cases, the spacer length of the CAR molecule might need to be optimized depending on the particular target antigen. It has been demonstrated by several groups that the spacer length could be an important parameter in order to enhance the anti-tumor reactivity of the CARs. Moritz et al. reported a correlation between the spacer length and the antigen-binding of HER2-directed scCAR[156]. In contrast, Hombach et al. did not observe the same effect with an anti-CD30 scCAR[157]. Furthermore, Watanabe and colleagues demonstrated that the inclusion of a longer spacer region in a prostate stem cell antigen-directed CAR resulted in a more potent anti-tumor effect[155]. Considering these observations, it is tempting to speculate that the CD8 spacer length of the anti-Vβ 5.3 scCAR might not have been optimal to provide the necessary distance to the TCR Vβ 5.3 epitope. Therefore, suboptimal spacer length could also be a reason for the lack of antigen-specific activation and cytotoxic response by the Bw58 scCAR T cells.

Another possible explanation for the lack of scCAR-mediated cytotoxic response might be a reduced antigen-binding affinity upon conversion into an scFV format. Some groups studying the biophysical properties of scFVs have reported lower affinities of such fusion proteins in comparison to the native antibody structures[158]. Therefore, the conversion of the MEM262 monoclonal antibody into an scFV might have led to loss of binding of the extracellular domain of the CAR. Furthermore, several studies report that the artificial linker included in the scFV format may lead to aggregation of scCARs, which could impair the binding to the target antigen[159,160]. Taken together, all the aforementioned limitations in the scCAR design could impede the successful generation of functional CARs.

Faitschuk et al. have proposed an alternative CAR design, which is based on a dual chain (dc) format thus preserving the native structure of an immunoglobulin[64]. Moreover, they have reported that the dcCAR-expressing T cells demonstrated efficient target cell elimination comparable to the scCAR-expressing T cells with the same specificity. Thus, I pursued a similar strategy and generated an anti-Vβ 5.3 CAR in a native Ig-like dual chain format. The alternative design of the anti-Vβ 5.3 dcCAR allowed me to directly assess the surface expression of the receptor in the Bw58 T cell line. Moreover, the heavy and light chain domains were both detected on the cell surface, which suggested that they most probably pair to form the dcCAR. Although, the lambda light chain-containing dcCAR had a slightly higher surface expression as compared to the kappa dcCAR in Bw58 cells, the type of the light chain included in the dcCARs did not have a major impact on the overall dcCAR expression. Furthermore, I could show that the dcCAR is functional and successfully induced intracellular Ca^{2+} mobilization upon stimulation. The observed slightly higher signaling capacity of the lambda dcCAR in comparison to the kappa dcCAR-expressing T cells could be explained by the higher surface expression level, which would allow cross-linking of more receptors.

In accordance with the report from Faitschuk and colleagues, the dcCAR format appeared to be a more robust approach to generate the anti-Vβ 5.3 CAR. However, for a direct comparison between the surface expression and functionality of the two types of CARs, it would be necessary to generate identical constructs that differ only in the format of the antigen-binding ectodomains. That way, it would be possible to compare the target recognition and the cytotoxic response exerted by the CAR-expressing Bw58 cells against target T cells. In the study of Faitschuk and colleagues, the dcCAR format induces lower cytokine secretion by the modified T cells, which could also be beneficial for the clinical application of the CAR-expressing T cells, by reducing the cytokine-release syndrome as a life-threatening side effect of the application of the CAR platform[64]. Thus, the anti-Vβ 5.3 dcCAR might exhibit better properties in terms of future evaluation in *in vivo* experiments.

5.3 Bw58 dcCAR-expressing T cells demonstrate selective cytotoxicity against Jurkat target cells *in vitro*

The mouse T cell line Bw58 serves as a good model system for the evaluation of the CAR-mediated antigen-specific cytotoxic response. The cell line lacks expression of an endogenous TCR and it is widely used for transfection with various antigen-specific TCR-encoding constructs to investigate cellular activation and IL-2 secretion[161,162,163]. Moreover, its modification with an

NF-AT-responsive eGFP cassette provides an additional read-out system to monitor the activation of the cells upon stimulation. To my knowledge, there are no reports showing that Bw58 cells have been used in cytotoxic cellular assays. According to my findings, the cell line expresses CD8 similar to conventional CTLs. In addition, my results demonstrate that Bw58 can exert a cytotoxic response against target cells.

The Bw58 dcCAR T cells in co-culture with TCR Vβ 5.3$^+$ Jurkat cells revealed the formation of a distinct double-positive population already at the beginning of the incubation, which was less prominent in co-culture with non-target cells. These observations imply that effector and target cells interacted already at early time points of their co-culture. Furthermore, the Bw58 dcCAR T cells eliminated the majority of target cells after 24 h of co-culture, which indicates the high cytotoxic efficiency of the Bw58 cells (Figure 4.9). I also showed that the elimination of Jurkat target cells *in vitro* is selective, evident from the preserved viability of Jurkat cells in both specificity controls (Figure 4.10). Moreover, the Bw58 dcCAR T cells in co-culture with target cells demonstrated antigen-specific activation, indicated by the expression of GFP. In addition, I could show that the percentage of the GFP-expressing Bw58 effector cells correlated with the cell density of the target cells, but the cytotoxic response was comparable within the assessed E:T ratios and similar among the kappa and lambda dcCAR-expressing Bw58 cells. Investigation of the mechanism involved in the elimination of the target TCR Vβ 5.3$^+$ Jurkat cells, showed that Bw58 dcCAR T cells are triggering programmed cell death in target cells. The majority of them were late apoptotic cells after 24 h, which highlighted the efficient cytotoxic response occurring early after the exposure of Bw58 dcCAR T cells to the target cells.

To date, it is considered that CAR T cells are acquiring the respective effector properties of the transfected T cells[164,165]. The Bw58 cells demonstrated a cytotoxic response, hence it was of interest to shed a light on the underlying cytotoxic mechanism involved in the elimination of the Jurkat target cells. The cytolytic activity of CAR-expressing T cells is thought to be achieved mainly via the faster granzyme and perforin secretory pathway[166,167,168]. For example, CD5 CAR-expressing primary T cells, whose perforin secretion was blocked by an inhibitor (i.e egtazic acid), were shown to have impaired killing efficiency against Jurkat cells[144] . In my experiments, monensin treatment impaired the cytotoxic response of the Bw58 dcCAR T cells (Figure 4.14), while the percentage of GFP-expressing Bw58 dcCAR T cells was preserved. These observations suggest that there was an antigen-specific activation of the effector cells, but the cytotoxic response had been diminished by the treatment with monensin. A possible reason for that could be an inhibition of the exocytosis of lytic granules. However, since monensin might also have an effect on the surface expression of receptors, it cannot be excluded that it might be affecting other pathways to abrogate the cytotoxic response (i.e blocking of the expression of FasL or the secretion of soluble FasL).

The second pathway utilized by CTLs to trigger programmed cell death upon target antigen recognition involves the engagement of TNF family receptors (i.e. Fas, TNFR1, TNF-related apoptosis-inducing ligand receptors). Blocking of FasL on the surface of activated T cells would lead to their inability to interact with Fas on the target cells and abrogation of programmed cell death[169]. According to my findings, the FasL-Fas interaction contributes to the elimination of the Jurkat target cells. However, whether FasL-Fas is the main mechanism or it is having rather a

complementary role, would need further investigation. Mamonkin and colleagues have also reported that CD5 CAR-expressing autologous primary T cells eliminated Jurkat cells by using the Fas-mediated cytotoxic mechanism in addition to the perforin secretory pathway[144]. These results among others, suggest that the two cytotoxic mechanisms could have complementary roles in the cytotoxicity of Bw58 against target cells [7, 109, 106].

5.4 Human primary TCR Vβ 5.3$^+$ T cells are selectively recognized by the Bw58 dcCAR T cells

The results from the *in vitro* cellular assays with Jurkat cells showed efficient elimination of the target cells by Bw58 dcCAR T cells. Therefore, it was of great interest to transfer these finding and to evaluate whether Bw58 dcCAR T cells would selectively target human primary TCR Vβ 5.3$^+$ T cells. Although TCR Vβ 5.3$^+$ cells constitute only a small subpopulation of all T cells, co-culture with Bw58 dcCAR demonstrated selective recognition of the target cells. Similar to the cytotoxicity assay with Jurkat target cells, I observed a doublet formation of Bw58 dcCAR T cells in co-culture with primary T cells immediately after mixing the cells. Moreover, this doublet population was composed of double-positive cells comprising of the effector cells and primary T cells, which implies that most probably these were already interacting cells (Figure 4.17 E and H). Furthermore, I could show that the human primary TCR Vβ 5.3$^+$ T cells are undetectable after the addition of Bw58 dcCAR T cells, but also after 24 h (Figure 4.17, F and I). Thus, these findings suggest that there is an antigen-dependent interaction already at the beginning of the co-culture. The less prominent double-positive population and the similar percentage of TCR Vβ 5.3$^+$ primary T cells during all time points in co-culture with CAR-less Bw58 cells is also supporting this hypothesis (Figure 4.18). Furthermore, I could show that the recognition of the target primary T cells is selective, since the TCR Vβ 8$^+$ subpopulation remained unaffected by the Bw58 dcCAR T cells.

The inability to detect the TCR Vβ 5.3$^+$ primary T cells immediately after mixing with the Bw58 dcCAR T cells could also be due to epitope masking by the dcCAR, which has the same target specificity as the monoclonal antibody (MEM262) used for detection. Similar observations were made when mimicking the physiological distribution of target primary T cells in peripheral blood within the Jurkat T cell system. Importantly, in both systems I could show that there are almost no target cells left after 24 h of co-culture with Bw58 dcCAR T cells (Figure 4.17 and 4.19). These observations corroborate my previous findings and suggest that the low target cell density might have led to the fast and efficient elimination of TCR Vβ 5.3$^+$ T cells by the CAR-expressing T cells. Although, the exact fate of the target primary T cells remains elusive, to investigate further whether the target primary T cells were eliminated by Bw58 dcCAR T cells similar to Jurkat cells would be beneficial to apply this approach with donor samples, which have overrepresented TCR Vβ 5.3 primary T cells. There are T cell malignancies such as cutaneous T cell lymphoma, in which the T cell repertoire in donor samples is skewed toward the preferential expression of TCR Vβ 5$^+$ malignant T cells (approx. 26%) in comparison to healthy individuals[170]. Thus, it would be possible to assess the Bw58 dcCAR cytotoxic response against malignant T cells *in vitro*.

In conclusion, my results demonstrate that the Bw58 dcCAR T cells selectively bind human target primary cells *in vitro*. Therefore, the findings of this work indicate the promising potential of this approach for application of the CAR T cell platform in targeting individual T cell subpopulations. Moreover, adapting this system with ectodomains derived from monoclonal antibodies specific for other TCR Vβ families, possess a potential for the generation of a CAR library to target additional T cell subpopulations.

5.5 The modification of the ITT-motif could serve as a signal amplifier in CARs

The properties of the ITT motif on B cell signaling have been extensively studied by our group [21,23,91,92,142,171], more specifically with regards to the investigation of the role of the ITT motif for the enhanced signaling response in mIgG-expressing or mIgE-expressing B cells. Previous reports from our group have demonstrated the importance of the tyrosine-containing evolutionarily conserved ITT-motif, located in the cytoplasmic tail of mIgG molecules, as a signal amplifier in mIgG-expressing memory B cells[21]. Apart from its role in B cells, ITT-like motifs are present also in the cytoplasmic tails of co-receptors such as CD28 and DAP10 in cytotoxic T cells [91]. Therefore, I explored the effect of the modification of the ITT motif and its role on the signaling capacity of the dcCAR. I hypothesized that the DAP10ITT motif might enhance the signaling capacity of the dcCAR and thus influence the cytotoxic response toward target cells by the Bw58 DAP10ITT dcCAR T cells.

In line with the hypothesis, the exchange of the ITT motif in the dcCAR backbone with a DAP10 ITT demonstrated higher signaling potential followed by an increased Ca^{2+} mobilization in the Bw58 dcCAR T cells (Figure 4.21). The surface expression level of the conventional dcCAR was higher in comparison to the expression level of DAP10ITT dcCAR in Bw58 cells. This observation indicated that the surface expression level is not directly contributing to the increased signaling capacity upon stimulation. Hence, these findings demonstrate that the improved signaling potential of the DAP10ITT dcCAR is due to the incorporation of the ITT motif itself. The exact signaling pathways underlining the signal amplification by the DAP10ITT dcCAR were not investigated in detail in this work. However, it would be beneficial to further characterize and compare the intracellular levels of signaling molecules, involved in potentiating the signal transduction in order to identify differences, which might contribute to expanding the current knowledge about the CAR-mediated signaling.

According to my findings, the DAP10ITT exchange in the dcCAR did not affect significantly the cytotoxic response exerted by the Bw58 dcCAR T cells. A possible explanation might be the already high efficiency of cytotoxic response toward target cells by Bw58 dcCAR T cells, containing the CD28ITT motif. Similar to these findings, Peng Li and colleagues have investigated the impact of the DAP10 included as a costimulatory domain into a second generation CAR targeting mesothelin. They have compared the cytotoxic response of human T cells, expressing a conventional CD28-containing second generation CAR with DAP10-containing CAR and have demonstrated comparable cytotoxic efficiency exhibited by both CAR-expressing T cell[172]. Therefore, the two co-stimulatory modules might contribute similarly to the cytotoxicity of the CAR-expressing T cells. However, I could demonstrate that the DAP10ITT

dcCAR has an improved signaling capacity over CD28ITT dcCAR. Depending on the signaling pathways involved in potentiating the signaling, the exchange of the ITT might contribute to a shift of the cytokine secretion profile or enhanced cytotoxic response by the CAR-expressing cells after re-exposure to target cells. Moreover, exchanging solely the ITT-motif in the dcCAR preserved the proline-rich motifs of CD28 co-receptor, which are known to be binding sites for Itk that triggers signaling pathways responsible for IL-2 production of the activated cells [179,180]. Thus, it might be beneficial to further investigate the properties of the hybrid DAP10ITT dcCAR in primary T cells or *in vivo*.

In conclusion, my results demonstrate that the modification of the ITT-motif in co-stimulatory domains included in the CAR backbones could serve as a potential tool to ´fine-tune´ the signaling capacity of the receptor. Thus, it can be used as a signal amplifier where modulation of the signal strength is required for more efficient CAR-mediated response.

6. Conclusion and Outlook

The results of this study reveal the potential of TCR Vβ-directed dcCAR T cells as a novel tool for selective and efficient elimination of individual T subpopulations *in vitro*. Characterization of the type of TCR Vβ-expressing T cell subpopulations that are predominantly over-represented in hematological or autoimmune diseases is currently an expanding research field. The generated prototypic anti-Vβ 5.3 dcCAR serves as a proof-of-principle that Vβ-redirected CARs may be utilized for the specific elimination of clonotypically distinct T cells. Since monoclonal antibodies are available against the majority of TCR Vβ subpopulations, this approach could be applied for the specific elimination of other subsets by exchanging the respective CAR ectodomains. Moreover, the results demonstrated here, show that the design of CARs in a dual chain format is a robust approach to generate functional CARs, at least in terms of circumventing the major limitations of the conventional scCAR platform.

Besides the antigen-binding format, the acquired effector functions of CAR-transfected T cells depend on the included signaling elements. The impact of the ITT motif in the cytoplasmic part of co-stimulatory domains included in CARs has not been investigated so far. Therefore, the results of this work demonstrate that modification of the signaling capacity via ITT substitution from various co-receptors might be an attractive strategy in the optimization of the signaling potential of CARs. Taken together, the described findings lay a foundation for the improvement of the CAR T cell platform in targeting T cell subpopulations in the future and provides a basis for futher investigation of additional signaling components for ´fine-tuning´ of the CAR-mediated signaling.

7. Bibliography

1. Chaplin, D. D. Overview of the immune response. *J. Allergy Clin. Immunol.* 125, S3 (2010).

2. Storey, M. & Jordan, S. An overview of the immune system. *Nurs. Stand.* 23, 1777–1789 (2008).

3. Gonzalez, H., Hagerling, C. & Werb, Z. Roles of the immune system in cancer: From tumor initiation to metastatic progression. *Genes and Development* vol. 32 1267–1284 (2018).

4. Biron, C. A. Innate Immunity: Recognizing and Responding to Foreign Invaders-No Training Needed. in *Viral Pathogenesis: From Basics to Systems Biology: Third Edition* 41–55 (Elsevier Inc., 2016). doi:10.1016/B978-0-12-800964-2.00004-5.

5. Marcus, A. *et al.* Recognition of tumors by the innate immune system and natural killer cells. in *Advances in Immunology* vol. 122 91–128 (Academic Press Inc., 2014).

6. Cerwenka, A. & Lanier, L. L. Natural killer cell memory in infection, inflammation and cancer. *Nature Reviews Immunology* vol. 16 112–123 (2016).

7. Prager, I. *et al.* NK cells switch from granzyme B to death receptor-mediated cytotoxicity during serial killing. *J. Exp. Med.* 216, 2113–2127 (2019).

8. Paul, S. & Lal, G. The molecular mechanism of natural killer cells function and its importance in cancer immunotherapy. *Frontiers in Immunology* vol. 8 1 (2017).

9. Abel, A. M., Yang, C., Thakar, M. S. & Malarkannan, S. Natural killer cells: Development, maturation, and clinical utilization. *Frontiers in Immunology* vol. 9 1869 (2018).

10. Lanier, L. L. Up on the tightrope: natural killer cell activation and inhibition. *Nat. Immunol. Vol.* 9, (2008).

11. Patente, T. A. *et al.* Human dendritic cells: Their heterogeneity and clinical application potential in cancer immunotherapy. *Front. Immunol.* 10, 3176 (2019).

12. Oh, J. & Shin, J.-S. The Role of Dendritic Cells in Central Tolerance. *Immune Netw.* 15, 111 (2015).

13. Howard, C. J., Charleston, B., Stephens, S. A., Sopp, P. & Hope, J. C. The role of dendritic cells in shaping the immune response. *Anim. Heal. Res. Rev.* 5, 191–195 (2020).

14. Sallusto, F. & Lanzavecchia, A. The instructive role of dendritic cells on T-cell responses. *Arthritis research* vol. 4 S127–S132 (2002).

15. LeBien, T. W. B Cell Development. in *Fetal and Neonatal Physiology* 1202–1207 (Elsevier, 2017). doi:10.1016/B978-0-323-35214-7.00124-4.

16. Budd, R. C. & Fortner, K. A. T-cell development. in *Clinical Immunology* 127–137 (Elsevier Ltd, 2008). doi:10.1016/B978-0-323-04404-2.10009-0.

17. Charles A Janeway, J., Travers, P., Walport, M. & Shlomchik, M. J. Principles of innate and adaptive immunity. *Immunobiol. Immune Syst. Heal. Dis. 5th Ed. New York Garl. Sci.* (2001)

18. Charles A Janeway, J., Travers, P., Walport, M. & Shlomchik, M. J. The Generation of Lymphocyte Antigen Receptors. *Immunobiol. Immune Syst. Heal. Dis. 5th Ed. New York Garl. Sci.* (2001).

19. Treanor, B. B-cell receptor: From resting state to activate. *Immunology* vol. 136 21–27 (2012).

20. Reth, M. & Wienands, J. Initiation and processing of signals from the B cell antigen receptor. *Annual Review of Immunology* vol. 15 453–479 (1997).

21. Lutz, J. *et al.* Reactivation of IgG-switched memory B cells by BCR-intrinsic signal amplification promotes IgG antibody production. *Nat. Commun.* 6, (2015).

22. Charles A Janeway, J., Travers, P., Walport, M. & Shlomchik, M. J. Antigen Recognition by B-cell and T-cell Receptors. *Immunobiol. Immune Syst. Heal. Dis. 5th Ed. New York Garl. Sci.* (2001).

23. Engels, N. *et al.* Recruitment of the cytoplasmic adaptor Grb2 to surface IgG and IgE provides antigen receptor-intrinsic costimulation to class-switched B cells. *Nat. Immunol.* 10, 1018–1025 (2009).

24. Wucherpfennig, K. W., Gagnon, E., Call, M. J., Huseby, E. S. & Call, M. E. Structural biology of the T-cell receptor: insights into receptor assembly, ligand recognition, and initiation of signaling. *Cold Spring Harbor perspectives in biology* vol. 2 5140–5141 (2010).

25. Wan, Y. Y. & Flavell, R. A. How Diverse-CD4 Effector T Cells and their Functions. *J. Mol. Cell Biol.* 1, 20 (2009).

26. Andersen, M. H., Schrama, D., Thor Straten, P. & Becker, J. C. Cytotoxic T cells. *Journal of Investigative Dermatology* vol. 126 32–41 (2006).

27. Germain, R. N. T-cell development and the CD4-CD8 lineage decision. *Nature Reviews Immunology* vol. 2 309–322 (2002).

28. Roth, D. B. V(D)J Recombination: Mechanism, Errors, and Fidelity. *Microbiol. Spectr.* 2, (2014).

29. Jung, D. & Alt, F. W. Unraveling V(D)J Recombination: Insights into Gene Regulation. *Cell* vol. 116 299–311 (2004).

30. Qi, Q. *et al.* Diversity and clonal selection in the human T-cell repertoire. *Proc. Natl. Acad. Sci. U. S. A.* 111, 13139–13144 (2014).

31. Dupic, T., Marcou, Q., Walczak, A. M. & Mora, T. Genesis of the αβ T-cell receptor. *PLoS Comput. Biol.* 15, e1006874 (2019).

32. Brodeur, J.-F., Li, S., Damlaj, O. & Dave, V. P. Expression of fully assembled TCR-CD3 complex on double positive thymocytes: synergistic role for the PRS and ER retention motifs in the intra-cytoplasmic tail of CD3e. *Int. Immunol.* 21, 1317–1327 (2009).

33. Freeman, J. D., Warren, R. L., Webb, J. R., Nelson, B. H. & Holt, R. A. Profiling the T-cell receptor beta-chain repertoire by massively parallel sequencing. *Genome Res. 10: 1817–1824 (2009)*

34. Mora, T. & Walczak, A. M. How many different clonotypes do immune repertoires contain? *Current Opinion in Systems Biology* vol. 18 104–110 (2019).

35. Langerak, A. W. *et al.* Molecular and flow cytometric analysis of the Vβ repertoire for clonality assessment in mature TCRαβ T-cell proliferations. *Blood* 98, 165–173 (2001).

36. Van Beemd, R. Den *et al.* Flow cytometric analysis of the Vβ repertoire in healthy controls. *Cytometry* 40, 336–345 (2000).

37. Rezvany, M. R., Jeddi-Tehrani, M., Wigzell, H., Österborg, A. & Mellstedt, H. Leukemia-associated monoclonal and oligoclonal TCR-BV use in patients with B-cell chronic lymphocytic leukemia. *Blood* 101, 1063–1070 (2003).

38. Wang, C. Y. *et al.* αβ T-cell receptor bias in disease and therapy (Review). *International Journal of Oncology* vol. 48 2247–2256 (2016).

39. Schrama, D., Ritter, C. & Becker, J. C. T cell receptor repertoire usage in cancer as a surrogate marker for immune responses. *Seminars in Immunopathology* vol. 39 255–268 (2017).

40. Goebels, N. Repertoire dynamics of autoreactive T cells in multiple sclerosis patients and healthy subjects: Epitope spreading versus clonal persistence. *Brain* 123, 508–518 (2000).

41. Shi, M. *et al.* Single Antibody Detection of T□Cell Receptor αβ Clonality by Flow Cytometry Rapidly Identifies Mature T□Cell Neoplasms and Monotypic Small CD8□Positive Subsets of Uncertain Significance. *Cytom. Part B Clin. Cytom.* 98, 99–107 (2020).

42. Li, Y. Leukemia Associated Clonal Expansion of TCR Vβ Subfamily T Cells Leukemia Associated Clonal Expansion of TCR Vb Subfamily T Cells. *Hematology,* 8:6, 375-384 (2003).

43. Wang, H.-W. & Raffeld, M. Molecular assessment of clonality in lymphoid neoplasms. *Semin. Hematol.* 56, 37–45 (2019).

44. Zheng, M. *et al.* TCR repertoire and CDR3 motif analyses depict the role of αβ T cells in Ankylosing spondylitis. *EBioMedicine* 47, 414–426 (2019).

45. Chang, C. M. *et al.* Characterization of T-Cell Receptor Repertoire in Patients with Rheumatoid Arthritis Receiving Biologic Therapies. *Dis. Markers* 2019, 2364943 (2019).

46. Naran, K., Nundalall, T., Chetty, S. & Barth, S. Principles of Immunotherapy: Implications for Treatment Strategies in Cancer and Infectious Diseases. *Front. Microbiol.* 9, 3158 (2018).

47. Li, X., Shao, C., Shi, Y. & Han, W. Lessons learned from the blockade of immune checkpoints in cancer immunotherapy Ahmed Tarhini; Timothy Burns; Rahul Parikh; Guarvel Goel; Annie im. *Journal of Hematology and Oncology* vol. 11 1–26 (2018).

48. Firor, A. E., Jares, A. & Ma, Y. From humble beginnings to success in the clinic: Chimeric antigen receptor-modified T-cells and implications for immunotherapy. *Exp. Biol. Med. (Maywood).* 240, 1087–98 (2015).

49. Guedan, S., Calderon, H., Posey, A. D. & Maus, M. V. Engineering and Design of Chimeric Antigen Receptors. *Molecular Therapy - Methods and Clinical Development* vol. 12 145–156 (2019).

50. Hartmann, J., Schüßler-Lenz, M., Bondanza, A. & Buchholz, C. J. Clinical development of CAR T cells—challenges and opportunities in translating innovative treatment concepts. *EMBO Mol. Med.* 9, 1183–1197 (2017).

51. Sadelain, M. Chimeric Antigen Receptors: A Paradigm Shift in Immunotherapy. *Annu. Rev. Cancer Biol.* 1, 447–466 (2017).

52. Torikai, H. & Cooper, L. J. N. Translational implications for off-the-shelf immune cells expressing chimeric antigen receptors. *Molecular Therapy* vol. 24 1178–1186 (2016).

53. Gross, G., Waks, T. & Eshhar, Z. Expression of immunoglobulin-T-cell receptor chimeric molecules as functional receptors with antibody-type specificity (chimeric genes/antibody variable region). *Immunology* vol. 86 (1989).

54. Eshhar, Z., Waks, T., Gross, G. & Schindler, D. G. Specific activation and targeting of cytotoxic lymphocytes through chimeric single chains consisting of antibody-binding domains and the γ or ζ subunits of the immunoglobulin and T-cell receptors. *Proc. Natl. Acad. Sci. U. S. A.* 90, 720–724 (1993).

55. Feins, S., Kong, W., Williams, E. F., Milone, M. C. & Fraietta, J. A. An introduction to chimeric antigen receptor (CAR) T-cell immunotherapy for human cancer. *Am. J. Hematol.* 94, S3–S9 (2019).

56. Schaefer, J. V & Plü Ckthun, A. Transfer of engineered biophysical properties between different antibody formats and expression systems. *Protein Eng. Des. Sel.* 25, 485–506 (2012).

57. Monnier, P., Vigouroux, R. & Tassew, N. In Vivo Applications of Single Chain Fv (Variable Domain) (scFv) Fragments. *Antibodies* 2, 193–208 (2013).

58. Gorovits, B. & Koren, E. Immunogenicity of Chimeric Antigen Receptor T-Cell Therapeutics. *BioDrugs* 33, 275–284 (2019).

59. Long, A., Haso, W., Shern, J.et al.4-1BB costimulation ameliorates T cell exhaustion induced by tonic signaling of chimeric antigen receptors. *Nat Med* 21, 581–590 (2015).

60. Whitlow, M., Filpula, D., Rollence, M. L., Feng, S.-L. & Wood, J. F. Multivalent Fvs: characterization of single-chain Fv oligomers and preparation of a bispecific Fv. Protein Engineering vol. 7, 1017-1026 (1994).

61. Dolezal, O. *et al.* ScFv multimers of the anti-neuraminidase antibody NC10: shortening of the linker in single-chain Fv fragment assembled in V L to V H orientation drives the formation of dimers, trimers, tetramers and higher molecular mass multimers. *Protein Engineering* vol. 13, 565–574 (2000).

62. Milone, M. C. *et al.* Chimeric receptors containing CD137 signal transduction domains mediate enhanced survival of T cells and increased antileukemic efficacy in vivo. *Mol. Ther.* 17, 1453–1464 (2009).

63. Kochenderfer, J. N. *et al.* Construction and preclinical evaluation of an anti-CD19 chimeric antigen receptor. *J. Immunother.* 32, 689–702 (2009).

64. Faitschuk, E., Nagy, V., Hombach, A. A. & Abken, H. A dual chain chimeric antigen receptor (CAR) in the native antibody format for targeting immune cells towards cancer cells without the need of an scFv. *Gene Ther.* 23, 718–726 (2016).

65. Eshhar, Z., Waks, T., Gross, G. & Schindler, D. G. Specific activation and targeting of cytotoxic lymphocytes through chimeric single chains consisting of antibody-binding domains and the γ or ζ subunits of the immunoglobulin and T-cell receptors. *Proc. Natl. Acad. Sci. U. S. A.* 90, 720–724 (1993).

66. Kershaw, M. H. *et al.* A phase I study on adoptive immunotherapy using gene-modified T cells for ovarian cancer. *Clin. Cancer Res.* 12, 6106–6115 (2006).

67. Lamers, C. H. J. *et al.* Treatment of metastatic renal cell carcinoma with autologous T-lymphocytes genetically retargeted against carbonic anhydrase IX: first clinical experience. *Journal of clinical oncology : official journal of the American Society of Clinical Oncology* vol. 24 (2006).

68. Till, B. G. *et al.* Adoptive immunotherapy for indolent non-hodgkin lymphoma and mantle cell lymphoma using genetically modified autologous CD20-specific T cells. *Blood* 112, 2261–2271 (2008).

69. Salter, A. I. *et al.* Phosphoproteomic analysis of chimeric antigen receptor signaling reveals kinetic and quantitative differences that affect cell function. *Sci. Signal.* 11, 6753 (2018).

70. Song, D.-G. *et al.* CD27 costimulation augments the survival and antitumor activity of redirected human T cells in vivo. *Blood* 119 (3), 696–706 (2012).

71. Guedan, S. *et al.* ICOS-based chimeric antigen receptors program bipolar TH17/ TH1 cells. *Blood* 124, 1070–1080 (2014).

72. Song, D. G. *et al.* A fully human chimeric antigen receptor with potent activity against cancer cells but reduced risk for off-tumor toxicity. *Oncotarget* 6, 21533–21546 (2015).

73. Hombach, A. A., Heiders, J., Foppe, M., Chmielewski, M. & Abken, H. OX40 costimulation by a chimeric antigen receptor abrogates CD28 and IL-2 induced IL-10 secretion by redirected CD4+ T cells. *Oncoimmunology* 1, 458–466 (2012).

74. Kintz, H., Nylen, E. & Barber, A. Inclusion of Dap10 or 4-1BB costimulation domains in the chPD1 receptor enhances anti-tumor efficacy of T cells in murine models of lymphoma and melanoma. *Cell. Immunol.* 351, 104069 (2020).

75. Lynch, A. *et al.* Adoptive transfer of murine T cells expressing a chimeric-PD1-Dap10 receptor as an immunotherapy for lymphoma. *Immunology* 152, 472–483 (2017).

76. Sievers, N. M., Dörrie, J. & Schaft, N. Cars: Beyond t cells and t cell-derived signaling domains. *Int. J. Mol. Sci.* 21, 1–30 (2020).

77. Chmielewski, M. & Abken, H. TRUCKS, the fourth-generation CAR T cells: Current developments and clinical translation. *Adv. CELL GENE Ther.* 3, e84 (2020).

78. Tokarew, N., Ogonek, J., Endres, S., von Bergwelt-Baildon, M. & Kobold, S. Teaching an old dog new tricks: next-generation CAR T cells. *British Journal of Cancer* vol. 120 26–37 (2019).

79. Di Stasi, A. *et al.* Inducible apoptosis as a safety switch for adoptive cell therapy. *N. Engl. J. Med.* 365, 1673–1683 (2011).

80. Cartellieri, M. *et al.* Switching CAR T cells on and off: a novel modular platform for retargeting of T cells to AML blasts. *Blood Cancer J.* 6, e458 (2016).

81. Burger, M. C. *et al.* CAR-Engineered NK Cells for the Treatment of Glioblastoma: Turning Innate Effectors Into Precision Tools for Cancer Immunotherapy. *Frontiers in Immunology* vol. 10 2683 (2019).

82. Habib, S., Tariq, S. M. & Tariq, M. Chimeric antigen receptor-natural killer cells: The future of cancer immunotherapy. *Ochsner Journal* vol. 19 186–187 (2019).

83. Wang, W., Jiang, J. & Wu, C. CAR-NK for tumor immunotherapy: Clinical transformation and future prospects. *Cancer Letters* vol. 472 175–180 (2020).

84. Suh, H. C., Pohl, K., Javier, A. P. L., Slamon, D. J. & Chute, J. P. Effect of dendritic cells (DC) transduced with chimeric antigen receptor (CAR) on CAR T-cell cytotoxicity. *J. Clin. Oncol.* 35, 144–144 (2017).

85. Gaud, G., Lesourne, R. & Love, P. E. Regulatory mechanisms in T cell receptor signalling. *Nature Reviews Immunology* vol. 18 485–497 (2018).

86. Salter, A. I. *et al.* Phosphoproteomic analysis of chimeric antigen receptor signaling reveals kinetic and quantitative differences that affect cell function. *Sci. Signal.* 11, 1–18 (2018).

87. Wu, L., Wei, Q., Brzostek, J. & Gascoigne, N. R. J. Signaling from T cell receptors (TCRs) and chimeric antigen receptors (CARs) on T cells. *Cellular and Molecular Immunology* vol. 17 600–612 (2020).

88. Engels, N., Engelke, M. & Wienands, J. Conformational Plasticity and Navigation of Signaling Proteins in Antigen-Activated B Lymphocytes. *Advances in Immunology* vol. 97 251–281 (2008).

89. Engelke, M., Engels, N., Dittmann, K., Stork, B. & Wienands, J. Ca2+ signaling in antigen receptor-activated B lymphocytes. *Immunological Reviews* vol. 218 235–246 (2007).

90. Riha, P. & Rudd, C. E. CD28 co-signaling in the adaptive immune response. *Self/Nonself - Immune Recognition and Signaling* vol. 1 231–240 (2010).

91. Engels, N. & Wienands, J. The signaling tool box for tyrosine-based costimulation of lymphocytes. *Curr. Opin. Immunol.* 23, 324–329 (2011).

92. Engels, N. *et al.* The immunoglobulin tail tyrosine motif upgrades memory-type BCRs by incorporating a Grb2-Btk signalling module. *Nat. Commun.* 5, (2014).

93. Patel, S. *et al.* Beyond CAR T cells: Other cell-based immunotherapeutic strategies against cancer. *Front. Oncol.* 9, 196 (2019).

94. Lindner, S. E., Johnson, S. M., Brown, C. E., Wang, L. D. & Wang, L. D. Chimeric antigen receptor signaling: Functional consequences and design implications. *Sci. Adv.* 6, 2–10 (2020).

95. Boomer, J. S. & Green, J. M. An enigmatic tail of CD28 signaling. *Cold Spring Harbor perspectives in biology* vol. 2 a002436. (2010).

96. Garrity, D., Call, M. E., Feng, J. & Wucherpfennig, K. W. *The activating NKG2D receptor assembles in the membrane with two signaling dimers into a hexameric structure*. 102 (21): 7641–7646 (2005).

97. Verneris, M. R., Karami, M., Baker, J., Jayaswal, A. & Negrin, R. S. Role of NKG2D signaling in the cytotoxicity of activated and expanded CD8 T cells. *Blood* 103 (8): 3065–3072 (2004).

98. Demoulin, B. *et al.* Exploiting natural killer group 2D receptors for CAR T-cell therapy. *Futur. Oncol.* 13, 1593–1605 (2017).

99. Wensveen, F. M., Jelenčić, V. & Polić, B. NKG2D: A master regulator of immune cell responsiveness. *Front. Immunol.* 9 441 (2018).

100. Billadeau, D. D., Upshaw, J. L., Schoon, R. A., Dick, C. J. & Leibson, P. J. NKG2D-DAP10 triggers human NK cell-mediated killing via a Syk-independent regulatory pathway. *Nat. Immunol.* 4, 557–564 (2003).

101. Prajapati, K., Perez, C., Rojas, L. B. P., Burke, B. & Guevara-Patino, J. A. Functions of NKG2D in CD8+ T cells: an opportunity for immunotherapy. *Cellular and Molecular Immunology* vol. 15 470–479 (2018).

102. Oberschmidt, O., Kloess, S. & Koehl, U. Redirected primary human chimeric antigen receptor natural killer cells as an 'off-the-shelf immunotherapy' for improvement in cancer treatment. *Frontiers in Immunology* vol. 8 654 (2017).

103. Zheng, L. *et al.* A Humanized Lym-1 CAR with Novel DAP10/DAP12 Signaling Domains Demonstrates Reduced Tonic Signaling and Increased Antitumor Activity in B-Cell Lymphoma Models. *Clin Cancer Res*. 26 (14) 3694-3706 (2020)

104. Agarwal, S. *et al.* In Vivo Generation of CAR T Cells Selectively in Human CD4+ Lymphocytes. *Mol. Ther.* 28, 1783–1794 (2020).

105. Stinchcombe, J. C. & Griffiths, G. M. Secretory Mechanisms in Cell-Mediated Cytotoxicity Cytotoxic T lymphocytes (CTLs): recognize and destroy virally infected and tumorogenic cells. *Annu Rev Cell Dev Biol.* 23, 495-517 (2007) doi:10.1146/annurev.cellbio.23.090506.123521.

106. Hassin, D., Garber, O. G., Meiraz, A., Schiffenbauer, Y. S. & Berke, G. Cytotoxic T lymphocyte perforin and Fas ligand working in concert even when Fas ligand lytic action is still not detectable. *Immunology* 133, 190–196 (2011).

107. Waterhouse, N. J. *et al.* Cytotoxic T lymphocyte-induced killing in the absence of granzymes A and B is unique and distinct from both apoptosis and perforin-dependent lysis. *J. Cell Biol.* 173, 133–144 (2006).

108. Chowdhury, D. & Lieberman, J. Death by a thousand cuts: Granzyme pathways of programmed cell death. *Annual Review of Immunology* vol. 26 389–420 (2008).

109. Tran, T. *et al.* Apoptosis Exocytosis-Independent Induction of Target Cells, Thereby Facilitating Cytotoxic T Cells Specifically Induce Fas on. *J Immunol Ref.* 165, 3663–3672 (2020).

110. Guicciardi, M. E. & Gores, G. J. Life and death by death receptors. *FASEB J.* 23, 1625–1637 (2009).

111. Sharma, S. *et al.* Apoptotic signalling targets the post-endocytic sorting machinery of the death receptor Fas/CD95. *Nat. Commun.* 10, 1–16 (2019).

112. Fu, Q. *et al.* Structural Basis and Functional Role of Intramembrane Trimerization of the Fas/CD95 Death Receptor. *Mol. Cell* 61, 602–613 (2016).

113. Porter, D. L., Levine, B. L., Kalos, M., Bagg, A. & June, C. H. Chimeric antigen receptor-modified T cells in chronic lymphoid leukemia. *N. Engl. J. Med.* 365, 725–733 (2011).

114. Grupp, S. A. *et al.* Chimeric antigen receptor-modified T cells for acute lymphoid leukemia. *N. Engl. J. Med.* 368, 1509–1518 (2013).

115. Maude, S. L. *et al.* Chimeric antigen receptor T cells for sustained remissions in leukemia. *N. Engl. J. Med.* 371, 1507–1517 (2014).

116. Porter, D. L., Levine, B. L., Kalos, M., Bagg, A. & June, C. H. Chimeric Antigen Receptor–Modified T Cells in Chronic Lymphoid Leukemia. *N. Engl. J. Med.* 365, 725–733 (2011).

117. Johnstone, R. W., Ruefli, A. A. & Lowe, S. W. Apoptosis: A link between cancer genetics and chemotherapy. *Cell* vol. 108 153–164 (2002).

118. Schmitz, N., Lenz, G. & Stelljes, M. Allogeneic hematopoietic stem cell transplantation for T-cell lymphomas. *Blood* vol. 132 245–253 (2018).

119. Martin, A., Tisch, R. M. & Getts, D. R. Manipulating T cell-mediated pathology: Targets and functions of monoclonal antibody immunotherapy. *Clinical Immunology* vol. 148 136–147 (2013).

120. Mamonkin, M., Rouce, R. H., Tashiro, H. & Brenner, M. K. A T-cell-directed chimeric antigen receptor for the selective treatment of T-cell malignancies. *Blood* 126, 983–992 (2015).

121. Gomes-Silva, D. *et al.* CD7-edited T cells expressing a CD7-specific CAR for the therapy of T-cell malignancies. *Blood* 130, 285–296 (2017).

122. Cooper, M. L. *et al.* An “off-the-shelf” fratricide-resistant CAR-T for the treatment of T cell hematologic malignancies. *Leukemia* 32, 1970–1983 (2018).

123. Png, Y. T. *et al.* Blockade of CD7 expression in T cells for effective chimeric antigen receptor targeting of T-cell malignancies. *Blood Adv.* 1, 2348–2360 (2017).

124. Chen, K. H. *et al.* Preclinical targeting of aggressive T-cell malignancies using anti-CD5 chimeric antigen receptor. *Leukemia* 31, 2151–2160 (2017).

125. Rasaiyaah, J., Georgiadis, C., Preece, R., Mock, U. & Qasim, W. TCRαβ/CD3 disruption enables CD3-specific antileukemic T cell immunotherapy. *JCI insight* 3, (13):e99442 (2018).

126. Scherer, L. D., Brenner, M. K. & Mamonkin, M. Chimeric Antigen Receptors for T-Cell Malignancies. *Front. Oncol.* 9, 126 (2019).

127. Maciocia, P. M. *et al.* Targeting the T cell receptor β-chain constant region for immunotherapy of T cell malignancies. *Nat. Med.* 23, 1416–1423 (2017).

128. Mullis, K., Faloona, F., Scharf, S., Saiki, R. & Horn, G. Specific Enzymatic Amplification of DNA In Vitro: The Polymerase Chain Reaction. *Cold Spring Harb Symp Quant Biol.* 51 Pt 1:263-73 (1986).

129. Bryksin, A. V. & Matsumura, I. Overlap extension PCR cloning: A simple and reliable way to create recombinant plasmids. *Biotechniques* 48, 463–465 (2010).

130. Letourneur, F. & Malissen, B. Derivation of a T cell hybridoma variant deprived of functional T cell receptor α and β chain transcripts reveals a nonfunctional α-mRNA of BW5147 origin. *Eur. J. Immunol.* 19, 2269–2274 (1989).

131. Schneider, U., Schwenk, H.-U. & Bornkamm, G. Characterization of EBV-genome negative “null” and “T” cell lines derived from children with acute lymphoblastic leukemia and leukemic transformed non-Hodgkin lymphoma. *Int. J. Cancer* 19, 621–626 (1977).

132. Morita, S., Kojima, T. & Kitamura, T. Plat-E: An efficient and stable system for transient packaging of retroviruses. *Gene Ther.* 7, 1063–1066 (2000).

133. Simmons, A. & Alberola-Ila, J. Retroviral transduction of T Cells and T cell precursors. in *T-Cell Development: Methods and Protocols* vol. 1323 99–108 (Springer New York, 2015).

134. Benjamin, D. *et al.* Immunoglobulin secretion by cell lines derived from African and American undifferentiated lymphomas of Burkitt’s and non-Burkitt’s type. *J. Immunol.* 129, 1336–1342 (1982).

135. Ben-bassats, H. *et al.* Establishment in continuous culture of a new type of lymphocyte from a “burkitt-like” malignant lymphoma (line d.g.-75). *Int. J. Cancer* 19, 27–33 (1977).

136. Pavlištová, D., Drbal, K., Hilgert, I. & Hořejší, V. A novel monoclonal reagent recognizing native and denatured V b5.3-related chains of human T cell receptor. *Immunology Letters* 88, 105-108. (2003).

137. Grynkiewicz, G., Poenie, M. & Tsien, R. Y. A new generation of Ca2+ indicators with greatly improved fluorescence properties. *Journal of Biological Chemistry* vol. 260 3440–3450 (1985).

138. Stinchcombe, J. C. & Griffiths, G. M. Secretory mechanisms in cell-mediated cytotoxicity. *Annual Review of Cell and Developmental Biology* vol. 23 495–517 (2007).

139. Pohlmann, R., Kruger, S., Hasilik, A. & Figura, K. Von. Effect of monensin on intracellular transport and receptor-mediated endocytosis of lysosomal enzymes. *Biochem. J* vol. 217 (1984).

140. O'Neil-Andersen, N. J. & Lawrence, D. A. Differential modulation of surface and intracellular protein expression by T cells after stimulation in the presence of monensin or brefeldin A. *Clin. Diagn. Lab. Immunol.* 9, 243–250 (2002).

141. Vanneste, M. *et al.* High content screening identifies monensin as an EMT-selective cytotoxic compound. *Sci. Rep.* 9, 1–15 (2019).

142. König, L. B Cell Antigen Receptor-intrinsic Costimulation of IgG and IgE Isotypes Isotype-specific Signaling Mechanisms of IgG- and IgE-B Cell Antigen Receptors. (2012).

143. Chen, K. H. *et al.* Novel anti-CD3 chimeric antigen receptor targeting of aggressive T cell malignancies. *Oncotarget* 7, 56219–56232 (2016).

144. Mamonkin, M., Rouce, R. H., Tashiro, H. & Brenner, M. K. A T-cell-directed chimeric antigen receptor for the selective treatment of T-cell malignancies. *Blood* 126, 983–992 (2015).

145. Langerak, A. W. *et al.* Molecular and flow cytometric analysis of the V repertoire for clonality assessment in mature TCR T-cell proliferations. *Blood* vol. 98, 1, 165-173 (2001).

146. Farmanbar, A., Kneller, R. & Firouzi, S. RNA sequencing identifies clonal structure of T-cell repertoires in patients with adult T-cell leukemia/lymphoma. *npj Genomic Med.* 4, 1–9 (2019).

147. Alatrakchi, N. *et al.* T-cell clonal expansion in patients with B-cell lymphoproliferative disorders. *J. Immunother.* 21, 363–370 (1998).

148. Zheng, M. *et al.* TCR repertoire and CDR3 motif analyses depict the role of αβ T cells in Ankylosing spondylitis. *EBioMedicine* 47, 414–426 (2019).

149. Wang, J. *et al.* A novel approach for the treatment of T cell malignancies: Targeting T cell receptor Vβ families. *Vaccines* 8, 1–13 (2020).

150. Hughes-Parry, H. E., Cross, R. S. & Jenkins, M. R. The evolving protein engineering in the design of chimeric antigen receptor T cells. *International Journal of Molecular Sciences* vol. 21, 204 (2020).

151. Zhao, L. & Cao, Y. J. Engineered T Cell Therapy for Cancer in the Clinic. *Front. Immunol.* 10 (2019).

152. Guedan, S., Calderon, H., Posey, A. D. & Maus, M. V. Engineering and Design of Chimeric Antigen Receptors. *Molecular Therapy - Methods and Clinical Development* vol. 12 145–156 (2019).

153. Kailayangiri, S., Altvater, B., Wiebel, M., Jamitzky, S. & Rossig, C. Overcoming heterogeneity of antigen expression for effective car t cell targeting of cancers. *Cancers (Basel).* 12, (2020).

154. Wang, Z., Guo, Y. & Han, W. REVIEW Current status and perspectives of chimeric antigen receptor modified T cells for cancer treatment. *Protein Cell* 8, 896–925 (2017).

155. Watanabe, N. *et al.* Fine-tuning the CAR spacer improves T-cell potency. *Oncoimmunology 5 (12): e1253656* (2016).

156. Moritz, D. & Groner, B. A spacer region between the single chain antibody-and the CDS ζ-chain domain of chimeric T cell receptor components is required for efficient ligand binding and signaling activity. *Gene Ther.* 2, 539–546 (1995).

157. Hombach, A., Hombach, A. A. & Abken, H. Adoptive immunotherapy with genetically engineered T cells: Modification of the IgG1 Fc spacer domain in the extracellular moiety of chimeric antigen receptors avoids off-target activation and unintended initiation of an innate immune response. *Gene Ther.* 17, 1206–1213 (2010).

158. Ewert, S., Honegger, A. & Plückthun, A. Structure-Based Improvement of the Biophysical Properties of Immunoglobulin V H Domains with a Generalizable Approach. *Biochemistry* 42, 1517-1528 (2003).

159. Ewert, S., Huber, T., Honegger, A. & Plückthun, A. Biophysical properties of human antibody variable domains. *J. Mol. Biol.* 325, 531–553 (2003).

160. Schaefer, J. V. & Plückthun, A. Transfer of engineered biophysical properties between different antibody formats and expression systems. *Protein Eng. Des. Sel.* 25, 485–505 (2012).

161. Clement, M. *et al.* Targeted suppression of autoreactive CD8+ T-cell activation using blocking anti-CD8 antibodies. *Sci. Rep.* 6, (2016).

162. Dornmair, K. *et al.* Polymyositis Lesion TCR Derived from a δ γ An Autoreactive. *J Immunol Ref.* 169, 515–521 (2002).

163. Almeida, C. F. *et al.* Distinct CD1d docking strategies exhibited by diverse Type II NKT cell receptors. *Nat. Commun.* 10, 1–14 (2019).

164. Maher, J., Brentjens, R. J., Gunset, G., Rivière, I. & Sadelain, M. Human T-lymphocyte cytotoxicity and proliferation directed by a single chimeric TCRζ/CD28 receptor. *Nat. Biotechnol.* 20, 70–75 (2002).

165. Davenport, A. J. *et al.* Chimeric antigen receptor T cells form nonclassical and potent immune synapses driving rapid cytotoxicity. *Proc. Natl. Acad. Sci. U. S. A.* 115, E2068–E2076 (2018).

166. Meiraz, A., Garber, O. G., Harari, S., Hassin, D. & Berke, G. Switch from perforin-expressing to perforin-deficient CD8+ T cells accounts for two distinct types of effector cytotoxic T lymphocytes in vivo. *Immunology* 128, 69–82 (2009).

167. Davenport, A. J. *et al.* CAR-T cells inflict sequential killing of multiple tumor target cells. *Cancer Immunol. Res.* 3, 483–494 (2015).

168. Tschumi, B. O. *et al.* CART cells are prone to Fas- and DR5-mediated cell death. *J. Immunother. Cancer* 6, 71 (2018).

169. Ramaswamy, M., Cleland, S. Y., Cruz, A. C. & Siegel, R. M. Many checkpoints on the road to cell death: regulation of Fas-FasL interactions and Fas signaling in peripheral immune responses. *Results Probl Cell Differ*. 49, 17–47 (2009).

170. Vonderheid, E. C. *et al.* Evidence for restricted Vβ usage in the leukemic phase of cutaneous T cell lymphoma. *J. Invest. Dermatol.* 124, 651–661 (2005).

171. Vanshylla, K. *et al.* Grb2 and GRAP connect the B cell antigen receptor to Erk MAP kinase activation in human B cells. *Sci. Rep.* 8, 1–18 (2018).

172. Zhao, R. *et al.* DNAX-activating protein 10 co-stimulation enhances the anti-tumor efficacy of chimeric antigen receptor T cells. *Oncoimmunology* 8, (2019).

173. Cho, H.-S. *et al.* CD8 + T Cells Require ITK-Mediated TCR Signaling for Migration to the Intestine . *ImmunoHorizons* 4, 57–71 (2020).

174. Berg, L. J., Finkelstein, L. D., Lucas, J. A. & Schwartzberg, P. L. Tec family kinases in T lymphocyte development and function. *Annual Review of Immunology* vol. 23 549–600 (2005).

8. Appendix

8.1 List of abbreviations

All units and prefixes are in conformity with the International system of Units (Système international d'unités, SI).

7-AAD	7-Aminoactinomycin D
AF647	Alexa Fluor 647
Ag	Antigen
APC	Allophycocyanin
ATG	Anti-thymocyte globulins
BCR	B cell receptor
BSL-2	Biosafety Level-2
BV421	Brilliant Violet 421
C	Constant domain
CAR	Chimeric antigen receptor
CD	Cluster of differentiation
CD3e	CD3 epsilon
CD3γ	CD3 gamma
CD3δ	CD3 delta
CD3ζ	CD3 zeta
cDNA	Copy DNA
CDR3	Complementarity-determination region 3
CH	Constant domain of heavy chain
CH	constant domains of heavy chain
CIP	Calf Intestine Phosphatase
CL	Constant domain of light chain
CL	constant domains of the light chain
CTLs	Cytotoxic T cells
D	Diversity
DAP10	DNAX-activating protein 10
dATPs	Deoxyribose adenine triphosphates
DC	Dendritic cells
dcCAR	Dual chain chimeric antigen receptor
ddH20	Double-distilled water
DNA	Deoxyribonucleic acid
dNTPs	Deoxyribonucleotide triphosphates
E.coli	Escherichia coli
E:T	Effector to target ratio
eGFP	Enhanced green fluorescent protein
env	Envelope, gene encoding glycoprotein 160

$F(ab´)_2$	Bivalent antigen-binding fragment
FACS	Fluorescent activated cell sorting
FasL	Fas ligand
FCS	Fetal Calf Serum
FII A	Filamin-A
Fwd	Forward
g	Gramm
gag	Gene encoding p55 (core protein)
Grb2	Growth factor receptor-bound 2
h	Hour
H	Heavy chain
i.e.	id est
IgH	Immunoglobulin heavy chains
IgL	Immunoglobulin light chains
Igα	Immunoglobulin-associated alpha
Igβ	Immunoglobulin-associated beta
INDO-1 AM	Indo-1 Acetoxymethyl ester
IPTG	Isopropyl-β-D-thiogalactopyranosid
IRES	Internal ribosomal entry site
IS	Immunological synapse
ITAM	Immunoreceptor tyrosine-based activation motif
ITT	Immunoglobulin tail tyrosine
J	Joining
K-R buffer	Kreb-Ringer Buffer
L	light chain
LAC operone	Lactose operon
LAT	Linker for activation of T cells
LB	Lysogeny broth
Lck	Lymphocyte-specific protein tyrosine kinase
MAPK	Mitogen-activated protein kinases
MHC	Major histocompatibility complex
mIg	Membrane-bound immunoglobulin
mIg	Membrane-bound immunoglobulin
MMLV	Moloney Murine Leukemia Virus
NF-AT	Nuclear factor of activated T cells
NF-κb	Nuclear factor of κb
NK	Natural killer cells
NKG2D	Natural killer (NK) group 2 member D
ON	Overnight
PAMPs	Pathogen-associated molecular patterns
pAPCs	Professional antigen-presenting cells
PBS	Phosphate buffered saline
PCR	Polymerase Chain Reaction

Pfu Polymerase	Pyrococcus furiosus strain derived Polymerase
PI3K	Phosphoinositide-3-kinase
PLAT E	Platinum E
PLCγ1	Phospholipase Cγ1
PMA	Phorbol myristate acetate
pol	Retroviral DNA polymerase
PS	Phosphatidylserine
R0	RPMI media without FCS
R10	RPMI media with 10% FCS
Rev	Reverse
RFP	Red fluorescent protein
RPMI	Roswell Park Institute Medium
RT	Room temperature
s	Seconds
sc	Single-chain
scCAR	Single-chain chimeric antigen receptor
scFv	Single-chain variable fragment
SD	Standard deviation
SLP76	SH2-domain-containing leukocyte protein of 76 kDa
SMAC	Supramolecular activating clusters
TCR	T cell receptor
Th	T helper cells
Tm	Melting temperature
TM domain	Transmembrane domain
TNF	Tumor necrosis factor
tNGFR	Truncated variant of the human nerve growth factor receptor
TCR VβC1	Constant domain 1 of TCR β chain
TCR VβC2	Constant domain 2 of TCR β chain
TRUCKs	T cells redirected for universal cytokine-mediated killing CARs
V	Variable domain
VH	Variable domain of the heavy chain
VL	Variable domain of the light chain
VSV-G	Vesicular stomatitis virus glycoprotein
Vα	Variable domain of alpha chain
Vβ	Variable domain of beta chain
X-Gal	5-Bromo-4-chloro-3-indolyl β-D-galactopyranoside
α	TCR alpha
β	TCR beta

Single letter Amino Acid Code

A	Alanine
C	Cysteine
D	Aspartic Acid
E	Glutamic-Acid
F	Phenylalanine
G	Glycine
H	Histidine
I	Isoleucine
K	Lysine
L	Leucine
M	Methionine
N	Asparagine
P	Proline
Q	Glutamine
R	Arginine
S	Serine
T	Threonine
V	Valine
W	Tryptophan
Y	Tyrosine

Deoxyribonucleotides

A	deoxyadenosine monophosphate
C	deoxycytidine monophosphate
G	deoxyguanosine monophosphate
T	deoxythymidine monophosphate

8.2 List of figures

Appendix

8.3 List of tables

Acknowledgements

First, I would like to express my sincere gratitude to Prof. Wienands for the opportunity to join the team of the Institute of Cellular and Molecular Immunology and to conduct my Ph.D. thesis on this exciting project. Prof. Wienands, thank you very much for your advice, support, and guidance in my growth as a scientist.

Furthermore, I would like to thank Prof. Alexander Flügel and Prof. Michael Schön for advising me on my Ph.D. project. I sincerely thank you for the fruitful scientific discussions and your valuable input during our thesis committee meetings.

Niklas, thank you so much for supervising me and for all your help and support. I am grateful for sharing your deep knowledge and experience with me and for always finding a time when I knock on your door on countless occasions with many questions. I sincerely thank you for your guidance and advice, but also for giving me the freedom to follow my ideas. Huge thank you for proof-reading my thesis and your valuable feedback. I enjoyed working together and I have learned so much from you. Vielen Dank für alles!

Ines, thank you so much for your invaluable technical assistance in the lab and for sharing your deep knowledge with me. It was a pleasure to work with you. Furthermore, I would like to thank Gabi Sonntag for advising me on technical questions, whenever I needed help. In addition, I would like to thank Anika Schindler and Ingrid Teuteberg, for all the support in organizational matters. Anika, a huge thank you for translating documents and forms for me in English and for helping me out to complete administrative tasks.

I would like to sincerely thank all members of the Institute. Many special thanks to my former and current colleagues Kanika, Vanessa, Jens, Matthias, Christina, Kristin, Jan, Jacob, Saed, Carolina, Florian for your invaluable support both professionally and personally. I enjoyed very much our scientific discussions, meetings outside, and your companion. I am happy that I could get to know you all and I hope we stay in touch long after our mutual professional journey. Kanika and Vanessa, many thanks for introducing me to the lab, your advice and the lovely coffee breaks. I would like to thank also my lab-rotation students Helen and Marcel for their contribution.

Last, but not least, I would like to express my enormous gratitude to my family for supporting me all the way and my dear friends who never left my side even at almost 2000 km distance. I would like to thank Asya, Natalia, Reni, Gergana, Metody, Radosveta, Georgi for the encouragement, all the support and the great times together. Thank you for your trust in me and for always being there in difficult times to cheer me up. Without your unconditional support, I wouldn´t have made it so far. You showed me that borders do not exist when you have such good and loving friends. I also would like to thank Matthias E. for inspiring me to follow my dreams and to go on this journey. Finally yet importantly, Dimitar thanks for being next to me in the very last stages of my Ph.D. and for all your support, advice and your trust in me.